AIMS ENERGY

VOLUME NO. 13
ISSUE NO. 3
SEPT - DEC 2025

ENRICHED PUBLICATIONS PVT. LTD

S-9, IInd FLOOR, MLU POCKET,
MANISH ABHINAV PLAZA-II, ABOVE FEDERAL BANK,
PLOT NO-5, SECTOR-5, DWARKA, NEW DELHI, INDIA-110075,
PHONE: - + (91)-(11)-47026006

AIMS ENERGY

AIM AND SCOPE

AIMS Energy is an international Open Access journal devoted to publishing peer-reviewed, high quality, original papers in the field of Energy technology and science. We publish the following article types: original research articles, reviews, editorials, letters, and conference reports.

AIMS Energy welcomes, but not limited to, the papers from the following topics:

- Alternative energy
- Bioenergy
- Biofuel
- Energy conversion
- Energy conservation
- Energy transformation
- Future energy development
- Green energy
- Power harvesting
- Renewable energy

Editor in Chief

Department of Industrial & Systems Engineering, Chung Yuan Christian Pekka Peura University, 200, Chung Pei Road, Chungli,Taiwan 32023, ROC Levón Institute, Vaasa Energy institute, University of Vaasa, Wolffintie 34,
65200 Vaasa, Finland May Wu
System Assessment Section, Energy System Division, Argonne National Daphiny Pottmaier Laboratory, 9700 S. Cass Avenue, Lemont, IL 60439, USA
Bin Yang
Department of Biological Systems Engineering, Washington State University, 2710 Crimson Way, Richland WA 99354, USA
Ahmad Zahedi
College of Science, Technology and Engineering, Division of Tropical Environments and Societies, James Cook University, Queensland, 4811, Australia
Zhiqiang (John) Zhai
Department of Civil, Environmental, and Architectural Engineering, University of Colorado@Boulder, UCB 428, ECCE 249, Boulder, CO 80309-0428, USA
Xiaowei Zhou
Department of Chemical & Biological Engineering, Northwestern University, Evanston, IL, USA

AIMS Energy

(Volume No. 13, Issue No. 3, Sept - Dec 2025)

Contents

Empirical assessment of drivers of electricity prices in East Africa: Panel data experience of Rwanda, Uganda, Tanzania, Burundi, and Kenya

Mburamatare Daniel1,*, William K. Gboney1, Hakizimana Jean de Dieu1, Akumuntu Joseph2,3 and Fidele Mutemberezi2

1 College of Science and Technology, African Centre of Excellence in Energy for Sustainable Development, University of Rwanda, KN 73 St, P.O.Box 3900, Kigali-Rwanda

2 College of Business and Economics, University of Rwanda, Kigali-Rwanda

3 Department of Business, Economics and Management, University of Kigali, Rwanda

ABSTRACT

Sustainable electricity supply plays a key role in economic development. Cost recovery, profitability and affordability of electricity through power tariff regulation, have become a subject of conflict between private providers and regulators. Consequently, regulators need to balance the interests of all stakeholders. The objective of this study, is to measure to which extent, Electricity Net Consumption (EC), Electricity Net Generation (EG), electricity transmission and distribution losses (Losses), International Average Crude oil prices (FP), Consumer Price Index (CPI), Industry Value Added (IVA) could influence the Average Electricity Prices (EP) in East Africa, especially in Rwanda, Uganda, Tanzania, Burundi, and Kenya. The data are from World Bank Indicators and cover the period from 2000 to 2019. This study adopts a three-stage approach, consisting of panel unit root tests, panel cointegration tests and estimating the long run cointegration relationship of the variables in a panel context. We applied four different panel unit root tests including ADF-Fisher Chi-square, Levin, Lin and Chu (LLC); PP-Fisher Chi-square, and Im, Pesaran, and Shin, (IPS). The results reveal that the variables are non-stationary at "level", stationary at first-differences and integrated with order one denoted as I(1). The Pedroni, Kao and Johansen Fisher co-integration tests were performed. This study uses full modified ordinary least squares (FMOLS) and dynamic ordinary least squares (DOLS) to estimate the long run relationship among the variables. We find that the increase in EG, FP, and CPI increase the Average Electricity Prices (EP); while the increase in Losses, EC, and IVA decreases EP. Therefore, we recommend the promotion of long-term investment policies in renewable sources and efficient policies to reduce technical and commercial losses. In addition, this study suggests that appropriate policies related to subsidized electricity prices would, however, prevent adverse effects related to inefficient over-consumption of electricity.

Keywords: *electricity prices; electricity consumption; electricity generation; cointegration; stationary; transmission losses; East Africa; Panel Data*

1. Introduction

Electricity supply plays a key role in the economy, both as an essential service to customers and as an intermediate input into other industries [1]. Before the first oil shock, the energy sector had a supply-oriented focus where the objective was to meet a given exogenous energy demand by expanding the

supply. Since the early 1970s, the energy sector has caught the attention of policymakers because of sudden price increases. Since then, energy research has grown significantly in size [2].

Energy models were however not developed for the same purpose. Some were concerned with better energy supply system design given a level of demand forecast, a better understanding of the present and future demand-supply interactions, energy and environment interactions, energy-economy interactions, and energy system planning [3]. The electricity industry has undergone significant changes in many countries since the 1990s and industrial operations and decision-making has changed from the state-dominated planned style to private-oriented decisions. Often the introduction of these structural changes made the decision-making more complex [3]. However, these changes happen generally in developed countries, and in developing countries, the electricity industry is generally still state-dominated.

In developing countries, the investments in the production and supply of electricity are almost done by the government budget where the private investments are still very low. Due to this situation, electricity markets behave as monopoly markets where there is one or very few sellers to many buyers. To meet the increasing demand, developing economies are more and more inviting private operators to invest in electricity production. This trend is likely to change their electricity market structure from monopoly markets to competitive markets. In a competitive market, the seller and the buyer are all price takers and the market forces influence the price. Electricity is now treated as a commodity worldwide, which can be bought, sold, and traded at market rates like any other commodity. Electricity as a commodity is probably the most important man-made commodity which is different from other commodities because it cannot be stored economically and has to be consumed whenever it is produced [4].

In a competitive market model, consumers maximize their utility subject to their budget constraints and producers maximize their profits subject to the constraints of production possibilities. In general, the demand for a good reduces as prices rise (i.e., inverse relationship with price) and vice versa. Similarly, producers face an upward sloping supply curve which implies that the higher the price, the more the supply, as at higher prices more producers become viable. In a competitive market, the interaction of supply and demand decides the market clearing price of the good and the quantity of goods that will be sold or purchased [3]. However, given the special characteristic of the non-storability of electricity, the supply of electricity is inelastic in short term. This implies that the supply of electricity could affect the change in electricity price in the short-term period, as well as in the long term, since the increase in electricity prices will attract new investors in the electricity sector and increase the production capacity, to increase the supply.

In developed countries, the electricity market deregulation has been implemented as an effective measure that addresses the energy supply and demand transactions in a commodity market platform. This has provided them with the competitive market model characteristics where the consumers have the autonomy to select their electricity provider. Still, the electricity market liberalization is a long- and

complex-term process requiring several market reforms, financial and human skills means which are not sufficient in developing countries [5]. This is a challenge to most of developing countries to undertake these reforms. Therefore, like most other commodity markets, electricity pricing in developed countries like USA and European countries is mainly driven by supply and demand [6]. This implies that the electricity market in developing countries behaves as a monopoly market while in developed countries, behaves as a competitive market. This difference in market structure affects the electricity pricing mechanisms in both blocks of countries. In addition, the difference in electricity generation technologies and sources plays also a key role in variations of drivers of electricity prices.

Despite ambitious targets to increase renewables penetration in electricity production, the natural gas and nuclear energy are still the leading source of electricity generation in developed countries while fossil fuels are still leading in developing countries [7–10]. In order to mitigate the negative impacts of fossil fuels on the environment, many countries have embraced the renewable energy agenda. In 2000, the German share of renewables was only 6%, while in 2021 it reached 41% [11]. The increasing share of renewables has been accompanied by decreasing day-ahead electricity prices. The prices dropped from 51 €/MWh in 2011–29 €/MWh in 2016 [12]. Besides that, given the high dependence of wind and solar power generation on weather factors, their intermittency tend to increase electricity spot price volatility in the absence of viable electricity storage [12]. However, as nuclear, coal, and oil-fired electricity generation slows, there is an increased reliance on natural gas-fired generators. At about 38.4%, natural gas was the largest source of US electricity generation in 2021 [13].

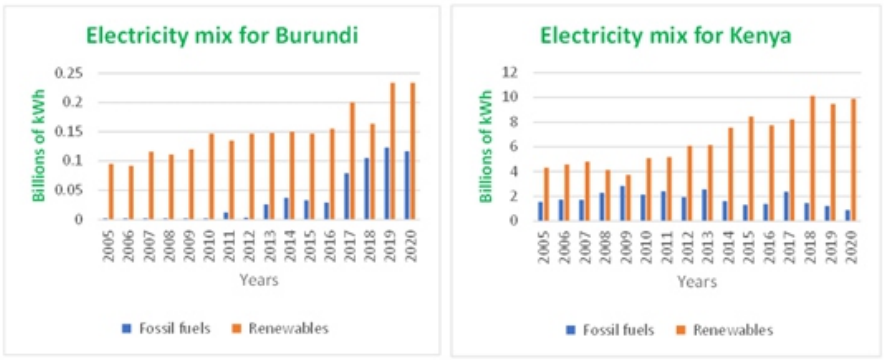

Figure 1. Electricity mix for Burundi and Kenya.

Concerning East African Countries under study, the electricity generation capacity has significantly increased as indicated by the Figures 1–4. In Burundi the electricity net generation increased from 97 million kWh in 2005 to 350 million kWh in 2020 while for Kenya, it increased from 5,862 million kWh in 2005 to 10,792 million kWh in 2020. For Rwanda, it increased from 113 million kWh in 2005 to 1,059 million kWh in 2019 while for Tanzania, it increased from 3,430 million kWh in 2005 to 7,176 million kWh in 2020 and Uganda, it increased from 1,953 million kWh in 2005 to 4,665 million kWh in 2020.

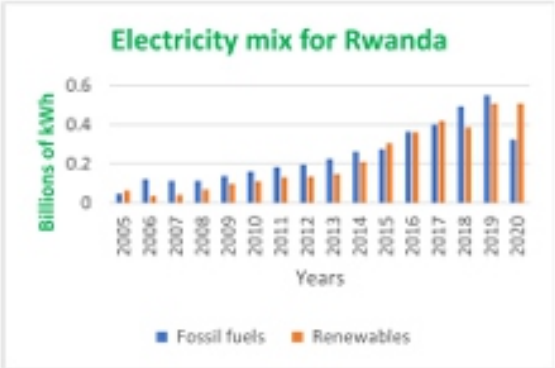

Figure 2. Electricity mix for Rwanda.

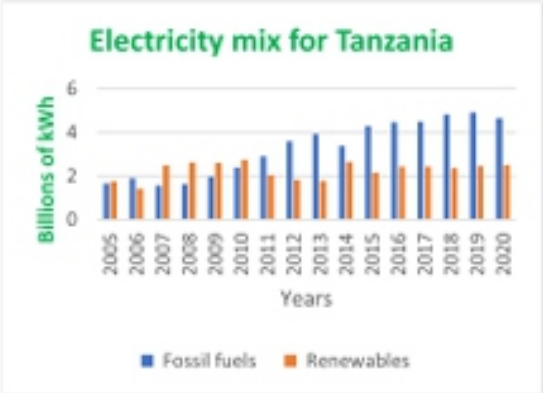

Figure 3. Electricity mix for Tanzania.

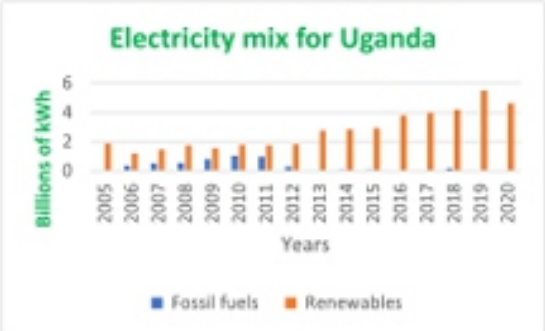

Figure 4. Electricity mix for Uganda.

Note: Authors' own elaboration with data retrieved from World Bank data, (2022): http://www.doingbusiness.org/methodology.

Despite the increase in electricity generation, as indicated by the Figure 5, the electricity prices slightly reduced in some countries like Rwanda, Uganda and Tanzania from 2016 and slightly increased for Kenya and Burundi for the same period. On one hand, a common characteristic of electricity generation in Kenya and Burundi where electricity prices have increased, is that their electricity mix sources were

mostly dominated by renewables under the period of the study. In Burundi renewable resources produced 97% in 2005 and 67% in 2020 of the total generated electricity while in Kenya, it was 74% in 2005 and 92% in 2020. On the other hand, concerning Rwanda and Tanzania, it was 58% and 48% for Rwanda and 51% and 35% for Tanzania respectively in 2005 and 2020. While the increase in electricity prices in Kenya and Burundi follows the increase in electricity generation from renewable sources, in Uganda, the reduction in electricity prices follows, the increase in renewable sources for electricity generation.

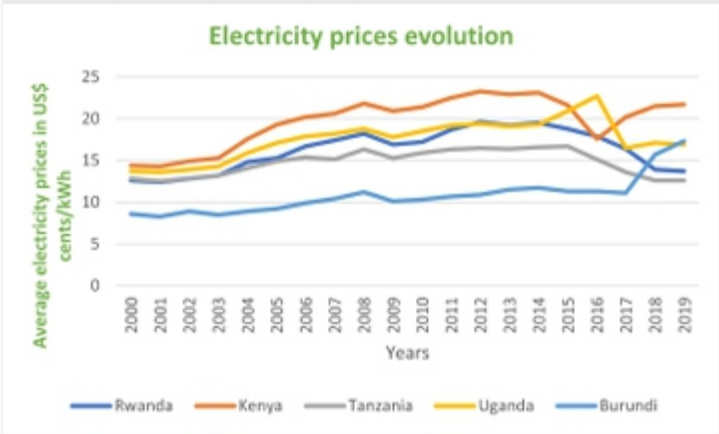

Figure 5. Evolution of average electricity prices.

Note: Authors' own elaboration with data retrieved from World Bank data, (2022): http://www.doingbusiness.org/methodology.

In developing countries, electricity prices are not volatile as it is in liberalized market of developed countries. These prices could be fixed in the short term, but in long term, prices could change following the change in the cost of supplying electricity. Natural, technological, market, and regulatory factors affect the cost of supplying electricity [1]. These include operating environment, production economies, energy losses as well as government interventions and regulatory decisions, which all affect the total environment in which each power utility operates. However, given the key role of electricity in the socio-economic development of any country, governments have established regulatory authorities to control electricity prices and monitor the operations of the utilities. The mission of regulatory authorities includes among others, protecting the rights of consumers, balancing the interests of all stakeholders, ensure cost reflective but affordable prices and delivery of quality services to all.

Electricity production, transmission and distribution involve huge long-term investments. Therefore, economic operators in the electricity sector need to ensure that they are able to recover their investment cost plus a reasonable rate of return, as approved by the regulator. While developing economies, especially East African countries are inviting private operators to invest in the electricity sector, the market is generally still behaving as a monopoly type. It is in this context that, cost recovery and

affordability of electricity through electricity tariff setting, have become a subject of conflict between electricity providers and regulators. On one hand, electricity providers expect a tariff that covers all costs related to electricity production, transmission and distribution as well as earn a positive return on their investments. On the other hand, regulatory authorities seek to balance positive returns on investments and the socio-economic well-being of the population through tariff signals [14]. Therefore, in the context of balancing the interests of all stakeholders and transparency, policymakers, regulatory authorities, as well as investors should be aware of the main macroeconomic, investment, operational, and demographic factors that affect electricity prices.

1.1. Research objective

The objective of this study, is to conduct a panel data analysis of five East African countries to measure to which extent, Electricity Net Consumption (EC), Electricity Net Generation (EG), electricity transmission and distribution losses (Losses), International Average Crude oil prices (FP), Consumer Price Index (CPI), Industry value added (IVA) could influence the electricity prices (EP). In addition, a comparative analysis will be conducted between Rwanda, Kenya, Uganda, Burundi, and Tanzania. This study was particularly motivated by the fact that no similar research has been conducted in this area for the electricity-regulated markets in East Africa, based on the literature review. The novelty of the study resides in the macroeconomic and operational variables considered, location of the study, and the applied panel data model. The remainder of the study is organized as follows: section 2 presents the literature review, section 3 explores Econometric model, data, and methods, section 4 shows and discusses the results, and section 6 provides conclusions and policy recommendations.

2. Literature review

Most of the studies related to "drivers of electricity prices" have been conducted in developed countries with liberalized or deregulated electricity markets. Most of these countries produce more electricity than they consume from advanced technologies such as nuclear. For environment purposes, developed countries are slowing nuclear, coal, and oil-fired electricity generation. However, there is an increased reliance on natural gas-fired generators in developed countries. In addition, there are several electricity producers in these countries at low cost due to their advanced technologies and advanced human skills. This implies that the main drives of electricity prices in developed countries are the interaction between supply and demand for electricity as well as the natural gas market [12,15]. As indicated in the Figures 1–4, developing countries like East African countries are still abundantly using oil-fired electricity generation and hydropower and the cost of electricity supply is still very high. The electricity market structure in both block of countries is practically different. Therefore, the fundamental drivers of electricity prices in developed countries are different from those of developing countries especially East

Africa without such potentials.

The literature agrees that the price of electricity depends on fundamental factors, demand and supply of electricity, power systems, and strategic factors. Girish [4] argues that in a competitive electricity market, factors influencing electricity prices can be the price of fuel, weather conditions, time indices, and the cost of production of electricity per unit. Ruksans et al. [16], in the analysis of factors that affect electricity prices in Baltic Countries, used an econometric model where the dependent variable is the price of electricity. They point out that, Fuel prices (coal, gas, oil); political decisions (for example shutdown of German nuclear), Natural disasters (for example tsunami in Japan), power plant operation, transmission capacity restriction, and flood time for countries depending on hydropower plants like Norway and Sweden, have a great influence on the amount of produced electricity and therefore on electricity price. This implies that weather conditions affect electricity net consumption and generation which in turn affect electricity prices.

Uribe et al. [7] investigated the transmission of natural gas shocks to electricity prices under different scenarios of electricity generation for 21 European markets. They found that the level of market integration is the main factor underlying national differentiation. Denmark, Finland, Sweden, and Germany were showed to be the most vulnerable markets to natural gas price shocks under distress. Moreover, Spain, Italy, Portugal, and Norway presented the lowest vulnerability indicators. However, Mosquera-López & Nursimulu [12] assessed the drivers of electricity price dynamics in German electricity market. They found that short-run and medium/long-run price drivers differ and, more importantly, that they vary over time. In the case of the spot market, the determinants of prices are renewable infeed and electricity demand, while in the futures market the main drivers are natural gas, coal and carbon prices. This is in line with the study of Gil-Alana et al. [15] that found a close relation between energy consumption and energy prices in Spain and Portugal. In addition, they highlighted that against the backdrop of numerous evidence the variable renewable generation decreases electricity prices and increases price volatility. This result related to the influence of renewables, corroborate with many recent findings such as of Sirin and Yilmaz [17]. They assessed the effects of the variable renewable energy technologies (wind and run-of-river hydro) on Turkish balancing market prices. Their model results show that system marginal price declines as variable renewable energy generation increases. Moreover, there is a higher probability of positive imbalance as the positive difference between real-time and projected variable renewable energy generation increases. They conclude that, an increase in variable renewable energy generation implies lower prices, but higher positive imbalances for the system.

Contrary to developing countries, in most developed countries the electricity is traded on electric power exchange spot market like other commodities. Saad Suliman & Farzaneh [5] conducted a study on pricing and energy policy regulations in Japan electric power exchange spot market. From their results, a

one GWh addition from nuclear, hydroelectric, geothermal, biomass, solar, or wind power production technologies decreases spot prices. Contrarily, adding one GWh from thermal, hydroelectric storage, or regional interconnections raises the spot prices. While most studies related to drivers of electricity prices in developed countries ignore macroeconomic variables, Foroni et al. [18] included them in their empirical study, to analyze the importance of macroeconomic information, for forecasting daily electricity prices in two of the main European markets, Germany and Italy. They reach on the conclusion that industrial production index and oil price are more important for short horizons than for longer horizons pricing. The fundamental drivers of electricity price in competitive markets were also assessed by Afanasyev et al. [10]. Their obtained results show that the influence of electricity demand is most prominent both in the short and long terms for Europe-Ural price area (ATSEU) market and APX power spot exchange in the UK. However, for the Siberia price area (ATS SI), its impact is significant only in the long term. Finally, for all the electricity exchanges under their study, the influence of fuel markets was absent in the short term and became prominent only in the medium or long terms.

Based on the literature, it is clear that in competitive markets, the price of electricity is mostly set by the interaction of supply and demand for electricity, renewable energy technologies as well as natural gas market. In developing countries however, there is a limited competition in the electricity market, the price of electricity is generally determined by operational, demographic and macroeconomic factors. Luis et al. [19] conducted a fractional integration and cointegration study of several Kenyan electricity price series. After examining which factors that might be behind the electricity price movements in Kenya, they noted that the Consumer Price Index (inflation), oil prices, and interest rate all have positive and significant effects on the electricity prices. Even though, they noted that both demand and supply side shocks have historically influenced electricity prices in Kenya. Demand side shocks arise from high demand for electricity in years of higher production associated with higher growth rates of critical sectors such as manufacturing that rely heavily on electricity as an input into the production process. They also arise from higher consumer demand associated with an increasing population.

Most developing countries, use mainly off-grid electricity such as solar or biogas in rural areas and on-grid electricity in urban areas. Therefore, it seems that it is the increase in population and access to electricity in urban zones which could significantly affect electricity consumption and hence its prices. However, Kwakwa and Aboagye [20] investigated the impact of growth, industrialization, urbanization, and trade openness on the energy consumption in Ghana, and they found that in the short run the increase in urbanization (measured as the annual growth rate of the urban population) did not significantly affect the consumption of electricity, while in long run, the urbanization increased energy consumption. Li et al. [21] in their study explores the intrinsic relationship among urbanization, industrialization, and energy security, as well as the influencing mechanisms of urbanization and industrialization on energy efficiency using a fixed effect model. They conclude that, while energy security level decreases

considerably with the rise of energy consumption and population growth, the increase in urbanization and industrialization levels can increase energy security through energy efficiency improvements. This can be explained by the fact that urbanization can reduce electricity distribution and transmission losses and hereafter the cost of electricity supply. In addition, regional industrialization creates a competitive spirit among industries, and to reduce the industrial cost of production, they tend to use new technology which requires less energy and with a high-power factor which implies lower line losses.

Some of the literature suggests that high economic growth rates (GDP) increase the demand for electricity and in turn have an impact on electricity prices. Mabea [22] investigates the relationship between Kenya's electricity consumption, real disposable income, and residential electricity prices. In his research, he employed the Engle and Granger two-step procedure and error correction model for a time series from the period 1980 to 2009 to analyze electricity demand. The results of the analysis show that as Kenya achieves higher GDP growth rates, electricity requirements rise and conclude that this has a potential implication for electricity prices. This positive relationship between economic growth and electricity demand has been evidenced by many other scholars [23–30].

Mumo et al. [31], combine operational factors and macroeconomic factors in their model when seeking to determine the best tariff model that can be used in Kenya to improve electricity consumption.

Their study explored all the factors, which affect the cost of electrical energy. They find that the price of electricity (tariff) is mainly determined by fuel prices, economic factors such as inflation and the purchasing power of the consumers, capital cost as well as operational costs. Besides that, the Kenya Institute for Public Policy Research and Analysis (KIPPRA) [32] in their comprehensive study and analysis of energy consumption patterns in Kenya concludes that the fuel and exchange rate costs affect the electricity prices in Kenya and highlighted that the Tariff Adjustment Factor applicable in each quarter comprises of the Fuel Adjustment Factor, Exchange Rate Adjustment Factor as well as Inflation Rate Adjustment Factor. This is because, in most developing countries, thermal energy plays an important role in the production of electricity. This implies that the price of fuel on the international market, the exchange rate, and the country's inflation rate could affect the cost of production and hence the electricity prices in the national currency.

Electricity Regulatory Authority of Uganda (ERA) [33], in their electricity tariff quarterly adjustment methodology of January 2018, pointed out that, the price of electricity depends on the base tariff which is set taking into account the power utilities' Revenue Requirements, which is the amount of revenue that a company requires to meet its regulated costs. They indicated that the annual Base Tariff should be adjusted at the beginning of each calendar year to take into account changes in other tariff parameters such as electricity losses, collection rates, operations and maintenance costs, and investment costs. In setting the base tariff, they also took into account macroeconomic factors such as the Exchange rate, CPI (Inflation), US producer price index, and international price of fuel (US$ per barrel). Although the Base

Tariffs are expected to remain constant throughout the calendar year, the macroeconomic parameters used in the determination of the Base Tariffs are not kept constant necessitating a need for applying the adjustment Factors.

Donna and Poudineh [34] also pointed out that in Tanzania, the Energy and Water Utility Regulatory Authority (EWURA) determines the electricity price (Tariff) based on TANESCO's (the power utility's) operating expenses, financial costs, and other operating income (including government subsidy), depreciation and TANESCO's Capital Investment Plan (CIP). Besides that, TANESCO has requested that a tariff indexation mechanism have to be used to adjust changes in costs that are outside of TANESCO's control so that the tariff revenue is kept at pace with rising costs during periods between formal reviews. Local inflation and foreign exchange rate fluctuation adjustments based on Bank of Tanzania data are also proposed, along with the indexation of fuel costs. Dragasevic et al. [35] in their analysis of the factors influencing the formation of the price of

electricity in the deregulated markets of developing countries, found that network capacity utilization and losses in the transmission system, do not have a significant impact on the price of electricity because the loss was only 2%. They also pointed out that the increase in the number of consumers in the system leads to an increase in the cost of distribution capacity utilization and has a greater impact on the price of electricity. In addition, they noted that an increase in the generated amount of electricity, and a small increase in the price of electricity occurs because there is still one large electricity producer in the market, which, despite the deregulation of the market, has a significant monopoly and consequently power. In fact, the electricity supply cost and prices are influenced by internal and external factors. Internal factors such as productive efficiency are under the control of management and external factors are those that the industry has no control such as the price of fuel or inflation. As reliable supply and efficient pricing contribute to overall economic performance, in delivering electricity many factors must be taken into account, including those that are out of the control of the service providers [1]. This study combines external and internal factors considered in the panel data model for five countries in the East African region. From the literature review, no such empirical work has yet been conducted for East African countries using panel data.

3. Econometric model, data, and methods

3.1. Definition of econometric variables

This research used econometric panel data from five East African Countries, Rwanda, Uganda, Kenya, Tanzania, and Burundi. The dataset is based on yearly observations from 2000 to 2019. The data on Average Electricity Prices (EP), Electricity Net Generation (EG), and Electricity Generation mix was downloaded on 16 June 2022 from http://www.doingbusiness.org/methodology (World Bank). The data

on Industry value added (IVA) and Consumer Price Index (CPI) was downloaded on July 20, 2022 from World Bank Development Indicators of World Bank (WDI). Moreover, the data on International Average Crude oil prices (FP) was downloaded on July 05, 2022 from World Bank Commodity Price Data (The Pink Sheet). Finally, the data on Electricity Transmission and Distribution losses (Losses) and Electricity Net Consumption (EC) was downloaded on 16 June 2022 from World Bank portal https://www.worldbank.org/en/programs/business-enabling-environment. The used software for estimations is E-views 12.

3.1.1. Dependent variable

3.1.1.1. Average end-user electricity prices (EP)

Electricity as an essential service to customers and as an intermediate input into other industries, it plays a vital role in the development of any country. This is the reason why most countries have established regulatory authorities to monitor the performance of power utilities and undertake price regulation. Contrarily to developed countries where the electricity market is liberalized and the electricity price is set by the market forces[10,12,36], in developing countries electricity tariff is set by utility regulatory authorities. The electricity tariff design must meet two main objectives including, to generate the needed money to cover the efficient costs of the activities of the utility [37] as well as sending the right economic signals to each customer to ensure optimal socio-economic use of electricity [38]. The literature on electricity pricing [25–33] suggests different factors that can be taken into account when determining electricity prices. These include internal factors that are under the control of the power utility on one hand, and on the other hand, there are external factors that are beyond the control of the utility company. However, most of the literature agrees that the level of electricity generation, consumption, electricity generation mix technologies, transmission, and distribution losses, macroeconomic factors as well as fuel prices have a great impact on electricity prices. In electricity tariff design, customers are categorized and each category experience different tariff based on time of use and other factors such as load factor, consumer uptake voltage level and level of consumption. Therefore, this research uses average electricity prices as computed by the World Bank through doing business project and take into account only commercial and industrial customers' electricity tariffs. Figure 5 shows the graphical representation of the evolution average electricity prices in countries and period under study.

Table 1. Variables, data measurement, and source.

Variable	Abbreviation	Measurement	Data source
Average electricity prices	EP	US cents per kilowatt-hour (kWh)	http://www.doingbusiness.org/methodology (World Bank) and country regulatory authorities report.
Electricity net generation	EG	kWh	http://www.doingbusiness.org/methodology (World Bank)
Electricity transmission and distribution losses	Losses	kWh	https://www.worldbank.org/en/programs/business-enabling-environment (World Bank)
Electricity net consumption	EC	kWh	https://www.worldbank.org/en/programs/business-enabling-environment (World Bank)
International average crude oil prices	FP	US$/Barrel	World Bank Commodity Price Data (The Pink Sheet)
Industry value added	IVA	US$	World Bank Development Indicators, 2022
Consumer price index	CPI	-	World Bank Development Indicators, 2022

3.1.2. Independent variables

3.1.2.1. Electricity net generation (EG)

Generation data consist of both utility and non-utility sources from electricity, combined heat and power plants. Electricity net generation excludes the energy consumed by the generating units. There are economies of scale in electricity generation. This is attributed to lesser leakages and power losses obtained in larger generating units as well as operating and maintenance costs that increase less than proportionally with power plant unit size [1]. Due to the insufficiency of financial and human resource means, most developing countries develop electricity generating units that are not large enough to benefit from the economies of scale of generating units. This could affect the electricity cost of production and price. However, developed and developing countries mostly experience two different scenarios. Based on the non-storable and continuous consumption characteristics of electricity, generators are required to match supply to demand in real-time. To handle short-term peak loads, generally developed countries use the excess capacity of their baseload generators with low supply costs while developing countries use quick-start generators with high supply costs. Consequently, the increase in electricity demand could affect electricity prices in developed and developing countries in different ways. Figure 6 describes the evolution of the variable Electricity Net Generation.

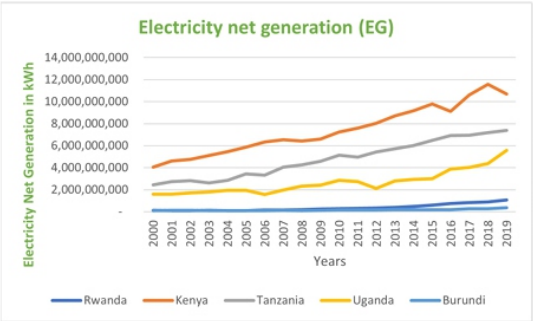

Figure 6. Evolution of electricity net generation.

3.1.2.2. Electricity net consumption (EC)

Total electric power consumption consists of total net electricity generation combined with electricity imports subtracting electricity exports and electricity transmission and distribution losses. However, some countries in East Africa, consume more electricity than they generate due to electricity imports. Figure 7 describes the evolution of the variable Electricity Net Consumption.

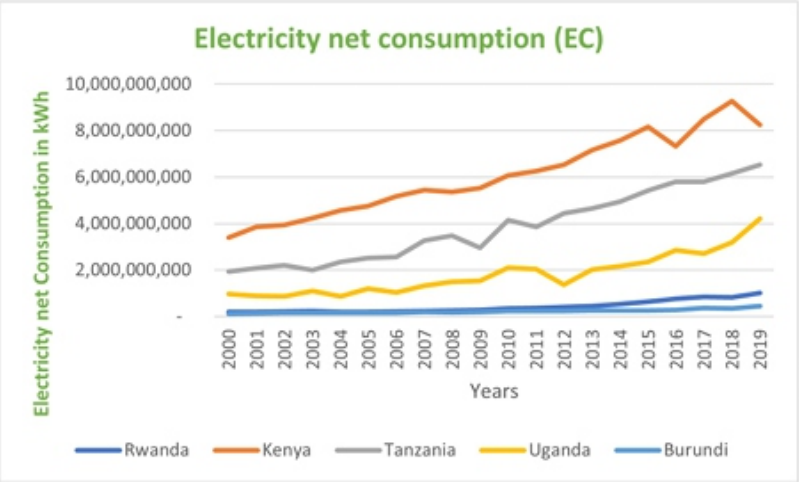

Figure 7. Evolution of electricity net consumption.

3.1.2.3. Electricity transmission and distribution losses (Losses)

Transmission and distribution losses are fundamentally linked to the electricity supply network configuration, with their size depending upon voltage delivered and line or network resistance encountered in delivery. The number of customers, length of distribution line, locational, and physical factors all contribute to resistance in delivering electricity to final customers [1]. Low customer densities can increase losses because longer lengths of distribution lines that must be used. Therefore, losses are at lower levels in the predominantly urban networks. This is because urban networks have lower levels of resistance in delivering electricity over shorter distances. Dragasevic et al. [35] like most of the literature [1,10] agree that electricity transmission and distribution losses affect electricity production cost and hereafter prices. Figure 8 describes the evolution of the variable Electricity Transmission and Distribution losses.

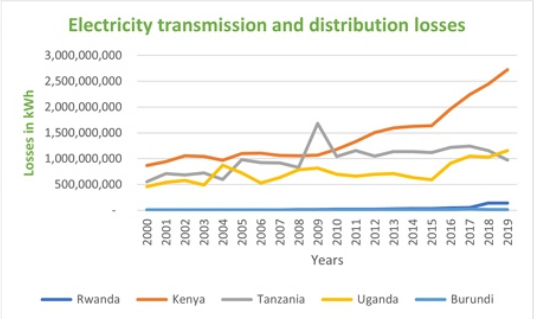

Figure 8. Evolution of transmission and distribution losses.

3.1.2.4. International average crude oil prices (FP)

Data on International Average Crude oil prices are expressed in real and nominal terms. The nominal value of any economic statistic is measured in terms of actual prices that exist at the time. The real value refers to the same statistic after it has been adjusted for inflation. For this study, we used oil prices in real terms. The price is expressed in $/bbl. where the abbreviation bbl. refers to a barrel of crude oil. The data has been extracted from World Bank Commodity Price Data (The Pink Sheet) (2022) and Energy Intelligence Group (EIG). Figure 9 describes the evolution of the variable international average crude oil prices.

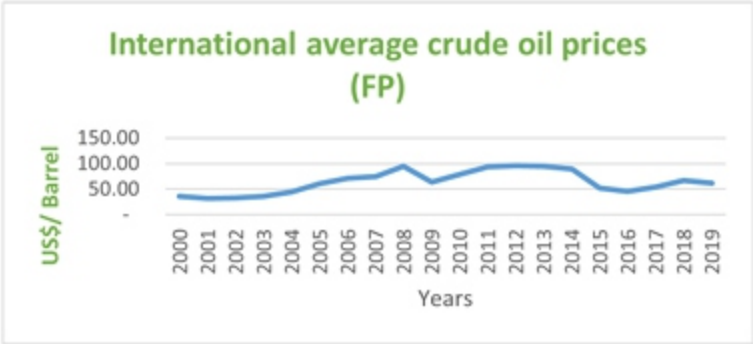

Figure 9. Evolution of international average crude oil prices.

3.1.2.5. Industry value added (IVA)

According to World Development Indicators, Industry value added (IVA) comprises value added in mining, manufacturing, construction, electricity, water, and gas. This is the net output of a sector after adding up all outputs and subtracting intermediate inputs. Data are in constant 2015 prices, expressed in U.S. dollars. One of the economic characteristics of the electricity supply is its capital intensiveness. Therefore, the investments if not well-planned can result in stranded assets and with a very high proportion of fixed assets. Due to this reason, economies of density and output in distribution can affect electricity cost of production. This implies that the average cost of servicing a particular area declines as the number of customers in that area using existing assets increases, or as the average load drawn by those customers increases [1].

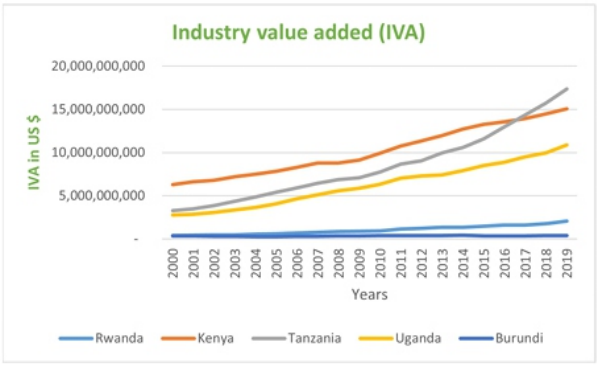

Figure 10. Evolution of Industry value added.

It is also obvious to note that the industrialization of any country requires more and more electricity as an input in the production process. However, Dan [47] notes that there has been a gradual decline in energy consumption in China since 1978 despite increasing industrial growth and attributed this to energy efficiency. After the oil price shocks in 1973/74 and 1979/80, average productivity in energy use increased due partly to the replacement of energy-inefficient capital with efficient ones [48]. This indicates that industrial growth in developed countries following the replacement of energyinefficient capital with efficient ones could reduce the consumption of electricity. However, in developing countries that are on the starting phase of industrialization, their industrial growth could increase the consumption of electricity as this form the accumulation of new electricity consumption devices. Most of the literature used the Industrial Value Added as a proxy for industrialization[49–52]. Figure 10 describes the evolution of the variable Industry value added.

3.1.2.6. Consumer price index (CPI)

The Consumer Price Index (CPI) is strongly linked to the inflation rate. Thus, inflation is the annual rate of change of CPI. As highlighted by the literature, inflation positively affects electricity prices [4,16,34]. Therefore, most regulatory authorities in setting the base tariff, they take into account macroeconomic factors among which national inflation[33,34,53]. However, as inflation rate is the annual rate of change of CPI, the variable inflation is considered as the first difference of CPI. This implies that the variable inflation is stationary at level or integrated with order zero I(0) as indicated in Table 3. For co-integration tests between variables, they should be non-stationary at level and integrated with the same order. Therefore, we consider CPI which is non stationary at level and integrated with order one as other variables instead of Inflation. Figure 11 describes the evolution of the variable Consumer Price Index.

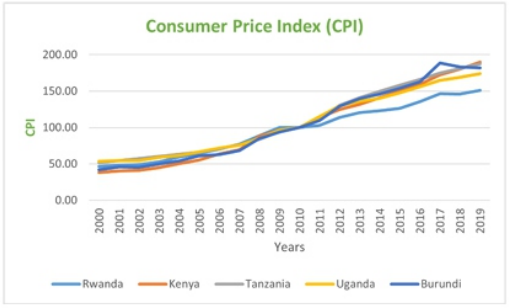

Figure 11. Evolution of consumer price index.

3.2. Panel data and econometric model

Table 2. Econometric model abbreviations.

N°	Abbreviation	Explanation
1.	ADF	Augmented dicky fuller
2.	BLUE	Best linear unbiased estimator
3.	DOLS	Dynamic ordinary least squares
4.	FEM	Fixed effect model
5.	FMOLS	Fully modified ordinary least squares
6.	GLS	Generalized least squares
7.	i.i.d.	Independent and identically distributed
8.	IPS	Im, Pesaran, and Shin
9.	LLC	Levin, Lin & Chu
10.	OLS	Ordinary least squares

The use of panel cointegration techniques to test for the presence of long-run relationships among integrated variables has been appreciated by an increasing number of researchers [54]. The use of panel data which comprises data observed for N entities (countries, regions, cities, firms, and so on) over T periods gives the researcher a large number of observations, increasing the number of degrees of freedom and reducing the collinearity among explanatory variables. Besides that, it is well known that panel data models are better able to deal, in a more natural way with the effects of missing or unobserved variables [55]. The literature describes different characteristics of panel datasets and models. Hill et al. [56] clearly note that the panel data set can be balanced or unbalanced. As missing data are very common in panel data sets, panels in which group sizes differ across groups are called "unbalanced" while when T periods data are all available for all N entities, the panel data sets are called "balanced panels" [57].

Most of the literature agrees on three-panel data regression models that are mostly used in the econometric analysis [56–61]. The first consist of Pooled Model, the second is the Fixed Effect Model as well as the Random Effect Model. In Pooled Model, the data on different individuals are simply pooled together with no provision for individual differences that might lead to different coefficients. However, this model presents some drawbacks related to the fact that it does not include unobserved heterogeneity. This implies that this model does not take into account the specificities of the various countries of the sample. A pooled model with two explanatory variables can be written as:

$$Y_{it} = \beta_0 + \beta_1 X_{1it} + \beta_2 X_{2it} + \mu_{it} \quad (1)$$

where "i" denotes the ith country and "t" denotes the tth period. Thus, "Yit" represents the tth observation on the dependent variable for the ith country, while "Xit" represents the tth observation on the independent variable for the ith country.

The coefficients in Eq (1) are assumed to be constant for all "i" countries in all time periods, and do not allow for possible individual heterogeneity. It is this characteristic that leads it to be called a pooled model. An alternative way to use panel data is to view the unobserved factors affecting the dependent variable as consisting of two types: those that are constant and those that vary over time. Letting i denote the cross-sectional unit and "t" the time period, we can write a model as:

$$Y_{it} = \beta_{1i} X_{1it} + \beta_{2i} X_{2it} + \cdots + \beta_{ki} X_{kit} + \alpha_i + \mu_{it} \quad (2)$$

The variable ai captures all unobserved time-constant factors that affect yit. Generically, ai is called an unobserved effect. It is also common in applied work to find ai referred to as a fixed effect, which helps us to remember that ai is fixed over time [58].

It is generally admitted that it is necessary to introduce a minimum of heterogeneity into the model to take account of the specificities of the various countries of the sample. The simplest method for introducing parameter heterogeneity consists of assuming that the constants of the model vary from country to country. This is precisely the specification of the well-known individual or fixed effect model

(FEM). Ignoring such parameter heterogeneity could lead to inconsistent or meaningless estimates of interesting parameters. The individual effects can be fixed or random. When individual effects are assumed to be fixed, the simple Ordinary Least Squares (OLS) estimator is the BLUE (Best Linear Unbiased Estimator) and is commonly called a Within estimator. When individual effects are specified as random variables, they are assumed to be independent and identically distributed (i.i.d.). In this case, the BLUE is a Generalized Least Squares (GLS) estimator [62].

However, various scholars like Chen et al. [63] studied the proprieties of the OLS estimator and suggest that alternatives estimators, such as the Fully Modified Ordinary Least Squares (FMOLS) or the Dynamic Ordinary Least Squares (DOLS) estimators, maybe more promising in cointegrated panel regressions. In addition, Daniel [54] cites Ouedraogo [64] in his article to point out that in the cointegrated panels, using the ordinary least squares (OLS) method to estimate the long-run equation leads to a biased estimator of the parameters unless the regressors are strictly exogenous and conclude that the OLS estimators cannot generally be used for valid inference. Therefore, this study uses FMOLS and DOLS to estimate the coefficients of the long-run relationship between EP, EG, Losses, EC, FP, CPI, and IVA for Rwanda, Tanzania, Uganda, Burundi, and Kenya. The FMOLS and DOLS estimators are generated from the following equation:

$$Y_{it} = \alpha_i + X'_{it}\beta + \sum_{j=-q_1}^{j=q_2} c_{ij}\Delta X_{i,t+j} + \mu_{it} \quad (3)$$

where:

Y_{it}: represents the log of the dependent variable,

X: is the log of explanatory variables,

β: denotes the coefficients of explanatory variables,

c_{ij}: represents the coefficients of lag differenced variables,

α_i: Individual Effects and μ_{it} denotes the error term.

The variables used in panel data analysis should be stationary to avoid causing possible spurious relationships among the variables. To assess the stationarity properties of the variables used, this study utilizes four different panel unit root tests including ADF-Fisher Chi-square, PP-Fisher Chi-square, Levin, Lin, and Chu, hereafter referred to as LLC [65]; Im, Pesaran, and Shin, hereafter referred to as IPS [62], this test is less restrictive and more powerful compared to others like LLC which do not allow for heterogeneity in the autoregressive coefficient. The test proposed by IPS solves Levin and Lin's serial correlation problem by assuming heterogeneity between units in a dynamic panel framework [66]. The basic equation for the panel unit root test for IPS is as follows:

$$\Delta y_{it} = \alpha_i + \rho_i y_{i,t-1} + \sum_{j=1}^{p} \phi_{ij}\Delta y_{i,t-j} + \varepsilon_{i,t}; \quad i = 1,2,\dots,N; \quad t = 1,2,\dots,T, \quad (4)$$

where y_{it} stands for each variable under consideration in our model, α_i is the individual fixed effect, $\varepsilon_{i,t}$ is the error term, ϕ_{ij} represents the coefficients of lag differenced of variables and ρ_i is selected to make the residuals uncorrelated over time.

Once the variables considered are stationary and before the estimation of the unbiased coefficients, we use Kao and Johansen Fisher co-integration tests to determine whether there is a long-run relationship between EP, EG, Losses, EC, FP, CPI, and IVA. In addition, this study will also apply cointegration tests advanced by Pedroni [67], despite that these tests have been criticized for the common factor restriction condition to hold and their failure can cause a significant loss of power for residual-based cointegration tests.

The functional econometric log-log model is used. The main advantage of using the log-log model, is that the estimated coefficients are expressed as elasticities. The econometric model describes the relationship between Average end-user Electricity Prices (EP), Electricity Net Generation (EG), Electricity Transmission and Distribution losses (Losses), Electricity Net Consumption (EC), International Average Crude oil prices (FP), Consumer Price Index (CPI) and Industry value added (IVA) for Rwanda, Tanzania, Uganda, Burundi, and Kenya is as follows:

$$logEP_{it} = \beta_0 + \beta_1 logEG_{it} + \beta_2 logLosses_{it} + \beta_3 logEC_{it} + \beta_4 logFP_{it} + \beta_5 logCPI_{it} + \beta_6 logIVA_{it} + \alpha_i + \mu_{it} \quad (5)$$

where:

Log (EP_{it}) = The natural logarithm of the Average Electricity Prices of the country "i" at the time "t" in US$/kWh

Log (EG_{it}) = The natural logarithm of the Electricity Net Generation of the country "i" at the time "t" in kWh

Log ($Losses_{it}$) = The natural logarithm of Total System Losses (Transmission and Distribution) of the country "i" at the time "t" in kWh.

Log (EC_{it}) = The natural logarithm of the Electricity Net Consumption of the country "i" at the time "t" in kWh

Log (FP_{it}) = The natural logarithm of International Average Crude oil prices in the country "i" at the time "t" in US$/gallon (This price is the same for all countries)

Log (CPI_{it}) = The natural logarithm of the Consumer Price Index of the country "i" at time "t"

Log (IVA_{it}) = The natural logarithm of the industry value added of the country "i" at the time "t" in US$

α_i = Individual Effects

μ_{it} = Error Term

β = Coefficients to be estimate

4. Results and discussions

This paper adopts a three-stage approach as follows:

i. panel unit root tests,
ii. panel cointegration tests,
iii. panel coefficients estimation to study and evaluate to which extent EG, Losses, EC, FP, CPI, and IVA affect the electricity prices (EP) for Rwanda, Tanzania, Uganda, Burundi, and Kenya.

4.1. Panel unit root test results

The unit root tests have been carried out to establish whether the variables are stationary or non-stationary at "level" and in "first-differences". Unit root tests are tests for stationarity in a time series. A time series has stationarity if a shift in time doesn't cause a change in the shape of the distribution; unit roots are one cause for non-stationarity. Four different tests have been used, these include the Levin, Lin & Chu (LLC), the Im, Pesaran, and Shin (IPS), the ADF-Fisher Chi-square, and the PP-Fisher Chi-square. The unit root statistics are reported in Tables 3 and 4.

The statistics in Table 3 presents the results from unit root test at level. In statistics, a unit root test tests whether a time series variable is non-stationary and possesses a unit root. The null hypothesis is defined as the presence of a unit root or non-stationary and the alternative hypothesis is either stationarity or trend stationarity. If the probability is greater than 5% or 0.05, the null hypothesis cannot be rejected and implies that the variable is non-stationary. Based on the results in Table 3, all probabilities are greater than 5% or 0.05, and we can conclude that the null hypothesis of the presence of a unit root cannot be rejected for all tests. This implies that they are non-stationary at level.

Table 3. Panel unit root tests results of the variables at level.

Null Hypothesis: Has Unit Root →non-Stationary Alternate Hypothesis: Does not have Unit Root →Stationary									
Methods		Levin, Lin & Chu (LLC)		Im, Pesaran and Shin (IPS) W-stat		ADF-Fisher Chi-square		PP-Fisher Chi-square	
		Constant	Constant & trend	Constant	Constant & trend	Constant	Constant & trend	Constant	Constant & trend
Variables									
Level	Log (EP)	–1.14477	2.08900	–0.19504	2.53937	11.1786	2.84759	7.02668	1.14364
	Prob	(0.1262)	(0.9816)	(0.4227)	(0.9944)	(0.3438)	(0.9848)	(0.7229)	(0.9997)
	Log (EG)	0.72249	–1.96002	3.79067	0.14513	1.07888	9.00057	7.50197	37.2936
	Prob	(0.7650)	(0.0250)	(0.9999)	(0.5577)	(0.9998)	(0.5320)	(0.6774)	(0.0001)
	Log (Losses)	2.86129	0.96983	3.27317	0.99494	3.77754	7.01685	7.43760	11.4109
	Prob	(0.9979)	(0.1661)	(0.9995)	(0.8401)	(0.9568)	(0.7239)	(0.6836)	(0.3264)
	Log (EC)	1.47598	–0.90628	3.89270	–0.85769	1.18627	13.6224	5.38390	28.7571
	Prob	(0.9300)	(0.1824)	(1.0000)	(0.1955)	(0.9996)	(0.1909)	(0.8641)	(0.0014)
	Log (FP)	–2.52756	0.07141	–1.64365	1.03623	15.9106	3.64899	8.7373	1.63924
	Prob	(0.0057)	(0.5285)	(0.0501)	(0.8500)	(0.1022)	(0.9618)	(0.5572)	(0.9984)
	Log (CPI)	–2.86046	–2.54488	–2.74800	–1.19721	25.6143	16.7217	31.0123	25.0948
	Prob	(0.0921)	(0.0855)	(0.2930)	(0.1156)	(0.0843)	(0.0808)	(0.4566)	(0.3452)
	Log (IVA)	–1.62393	–0.43331	1.29044	21.290	4.06528	6.91779	4.84217	4.31595
	Prob	(0.0522)	(0.3324)	(0.9016)	(0.5843)	(0.9444)	(0.7332)	(0.9015)	(0.9320)

The results in Table 4 show that after taking the first difference of the variables, LLC, IPS, ADF-Fisher Chi-square, and PP-Fisher Chi-square panel unit root tests reject the null hypothesis at a 1% significance level for EG, EC, FP, CPI, Losses, and IVA variables. Concerning EP, the statistics reject the null hypothesis with constant and trend at less than 1% with PP-Fisher Chi-square test, at less than 5% with IPS and the ADF - Fisher Chi-square panel unit root tests, and at 6% with LLC test. Therefore, we can conclude that all variables are stationary and integrated with order one, I (1). As all variables are stationary at first difference and integrated with the same order which is one, implies that we can proceed with co-integration tests to determine whether there is a long-run relationship or equilibrium among the variables under variables.

Table 4. Panel unit root tests results of the variables at first difference.

Null Hypothesis: Has Unit Root →non-Stationary Alternate Hypothesis: Does not have Unit Root →Stationary									
Methods		Levin, Lin & Chu (LLC)		Im, Pesaran and Shin (IPS) W-stat		ADF-Fisher Chi-quare		PP-Fisher Chi-square	
		Constant	Constant & trend	Constant	Constant & trend	Constant	Constant & trend	Constant	Constant & trend
Variables									
First difference	ΔLog (EP)	–1.12435	–1.52796	–1.41846	–1.98680	16.0131	20.1155	40.2887	56.4666
	Prob	(0.1304)	(0.0633)	(0.0780)	(0.0235)	(0.0993)	(0.0282)	(0.0000)	(0.0000)
	ΔLog (EG)	–5.76548	–6.44348	–5.66003	–5.71215	48.4942	46.1986	90.9441	110.107
	Prob	(0.0000)	(0.0000)	(0.0000)	(0.0000)	(0.0000)	(0.0000)	(0.0000)	(0.0000)
	ΔLog (Losses)	–4.57520	–5.30875	–5.01663	–5.60254	43.2696	45.3499	113.617	88.8381
	Prob	(0.0000)	(0.0000)	(0.0000)	(0.0000)	(0.0000)	(0.0000)	(0.0000)	(0.0000)
	ΔLog (EC)	–5.64146	–6.52383	–6.50226	–6.34644	56.0913	51.0100	343.615	79.7705
	Prob	(0.0000)	(0.0000)	(0.0000)	(0.0000)	(0.0000)	(0.0000)	(0.0000)	(0.0000)
	ΔLog (FP)	–4.46724	–4.69960	–2.77599	–2.31841	24.1772	20.8984	40.6758	35.1141
	Prob	(0.0000)	(0.0000)	(0.0028)	(0.0102)	(0.0071)	(0.0218)	(0.0000)	(0.0001)
	ΔLog (CPI)	–3.54003	–4.47617	–3.03765	–2.42538	27.0679	23.6062	30.4908	24.8252
	Prob	(0.0002)	(0.0000)	(0.0012)	(0.0076)	(0.0025)	(0.0087)	(0.0007)	(0.0057)
	Prob	(0.0000)	(0.0000)	(0.0000)	(0.0000)	(0.0000)	(0.0000)	(0.0000)	(0.0000)
	ΔLog (IVA)	–3.74434	–3.14605	–2.98534	–1.80649	26.3404	18.4526	38.6912	28.2769
	Prob	(0.0001)	(0.0008)	(0.0014)	(0.0354)	(0.0033)	(0.0478)	(0.0000)	(0.0016)

4.2. Panel cointegration test results

Having established that all variables are integrated with the same order, we apply Pedroni, Kao and Johansen Fisher co-integration tests to determine whether there is a long-run relationship or equilibrium among the variables: EP, EG, Losses, EC, FP, CPI, and IVA. If the variables are cointegrated, implies that the equation 5 can be estimated and provide unbiased coefficients. Pedroni [67] suggested some tests which allow heterogeneity in the co-integration analysis. This test does not allow only dynamic and fixed effects to be different among the cross sections of the panel, but also allows the co-integrated vector to be different among the cross sections under the alternative hypothesis allowing multiple regressors, varying of co-integration vector in different parts of the panel and allowing heterogeneity of errors through cross-sectional units constitute good sides of Pedroni's tests [30]. Pedroni tests use four within-group tests which are panel statistics based on estimators that pool the autoregressive coefficient across different countries for the unit root tests on the estimated residual and three between-group tests that are group statistics based on estimators that average individually estimated coefficients for each country.

Table 5. Pedroni panel cointegration test.

Pedroni residual cointegration test					
Methods	Within dimension (Panel statistics)			Between dimension (Individuals statistics)	
	Test	Statistics	Prob.	Statistics	Prob.
Pedroni	Panel v-statistic	0.472062	0.3184	-	-
	Panel rho-statistic	1.404765	0.9200	1.747855	0.9598
	Panel PP-statistic	–3.024805	0.0012	–4.411635	0.0000
	Panel ADF-statistic	–3.840508	0.0001	–5.051929	0.0000
Pedroni	Panel v-statistic	0.750266	0.2265	-	-
(Weighted statistic)	Panel rho-statistic	1.111894	0.8669	-	-
	Panel PP-statistic	–3.593525	0.0002	-	-
	Panel ADF-statistic	–4.578828	0.0000	-	-

Table 5 reports the within and between dimension results of the panel cointegration tests. These results suggest that the null hypothesis of no cointegration cannot be rejected for five tests out of eleven. However, six tests out of eleven suggest that the null hypothesis of no cointegration can be rejected at a 1% significance level. This implies that, as more than half of the tests propose the rejection of the null hypothesis, we may conclude that the variables of the model are cointegrated and therefore exhibit long-run relationship. To check the robustness of the Pedroni's test results, the Kao and Johansen Fisher co-integration tests are performed to confirm these first results. Table 6 provides the results of the Kao residual panel cointegration test, which reject the null of no cointegration of the variables of the model at the 1% level of significance. In addition, the Johansen Fisher Panel Cointegration Test results reported in Table 7, provide also strong evidence of the cointegration relationship between all variables, indicating that there are at most 3 cointegrating equations. Based on the above results, we can conclude that all variables are cointegrated and have a long-run equilibrium relationship between EP, EG, Losses, EC, FP, CPI, and IVA in East African countries.

Table 6. Kao residual cointegration test.

Kao residual cointegration test Null hypothesis: No cointegration		
ADF	t-Statistic	Prob.
	–3.369657	0.0004
Residual variance	0.004641	
HAC variance	0.003789	

Table 7. Johansen fisher panel cointegration test.

Unrestricted cointegration rank test (Trace and maximum eigenvalue)				
Hypothesized No. of CE(s)	Fisher Stat.* (from trace test)	Prob.	Fisher Stat.* (from max-eigen test)	Prob.
None	124.4	0.0000	129.5	0.0000
At most 1	47.66	0.0000	28.97	0.0013
At most 2	24.17	0.0072	13.20	0.2126
At most 3	14.61	0.1470	8.555	0.5748
At most 4	10.63	0.3870	5.269	0.8725
At most 5	11.87	0.2941	11.21	0,3410
At most 6	11.52	0.3182	11.52	0.3138

4.3. Coefficients estimation results with FMOLS and DOLS

As highlighted in the literature, this study uses two techniques to estimate and test the consistency of the unbiased coefficients of the long-run relationship between the variables. This relationship has been estimated by using the FMOLS and the DOLS methods. FMOLS method corrects the biases of estimators with standard fixed effects which could arise from problems such as autocorrelation and heteroscedasticity, while the DOLS method can correct biases of static regression which could result from endogeneity problems by including dynamic considerations in the model [30]. Tables 8 and 9 show the results and given that the variables are expressed in a natural logarithm, the coefficients can be expressed and interpreted as elasticities.

The overall outcomes of this study show that there is a strong long-run relationship between the dependent and independent variables. The independent variables explain the variations in electricity prices at 91% for both DOLS and FMOLS as shown by the R-squared. It is interesting to note that the regression results for both methods are quite similar in negative or positive signs, magnitude, and significance level of coefficients. The panel regression results indicate that the overall considered variables are statistically significant at a 1% level, except EC which is statistically significant at 2% for DOLS only.

The variable Electricity Generation (EG) has a positive estimated coefficient, showing that a 1% increase in EG, causes an increase of 0.5% in the electricity prices (EP). This is in line with the findings of Shields and Chris Sayers [1] in their research related the electricity prices and cost factors. They point out that the lack of economies of scale in electricity generation could cause the increase in electricity prices as the electricity generation increases. This could be attributed to lesser leakages and power losses obtained in larger generating units as well as operating and maintenance costs that increase less than proportionally with power plant unit size. Due to the insufficiency of financial and human resource means, most developing countries develop electricity generating units that are not large enough to benefit from the economies of scale of generating units. This could affect the electricity cost of

production and price. Even if most of the literature agrees that the increase of renewable sources in electricity generation reduces the electricity prices [10,12,17,36], the results of this study show that the increase in renewables for Kenya and Burundi have not reduced the electricity prices. This can be explained by the fact that hydropower generation requires huge investments and the private investors in the sector for developing countries require short payback period. Therefore, this can increase the prices in short term and expect to reduce prices in long term.

Moreover, the positive relationship between electricity generation and electricity prices in countries under study, can be attributed to the structure of the electricity generation mix in the East African countries in the research sample. Most of the countries are still more dependent on fossil fuels for electricity generation. It is significant to note that for example in 2020, fossil fuels in electricity generation mix were 33% in Burundi, 39% in Rwanda, and 65% in Tanzania and this was the same pattern in the previous years. As this source of electricity is one of the most expensive, this could explain why the cost of electricity production increases results in the average electricity price also increasing. This in some respects corroborates the results of the positive sign on the Fuel Price (FP) variable, which shows that a 1% increase in FP, also causes a 0.2% increase in the electricity price, this is in line with the findings of various scholars [7,10,12] . Moreover, in the framework of increasing their electricity generation capacity, East African Countries in general, have started to invite foreign investors with the required human and financial resources means. Projected returns would have to be attractive enough to encourage investment, therefore, country utility regulators should have to set electricity prices that cover all costs related to electricity generation, transmission and distribution as well as earn a positive return on their investments. This could also explain why the increase in electricity generation results in an increase the electricity prices.

Table 8. Panel FMOLS long-run estimation results.

Dependent variable: LEP				
Method: Panel fully modified least squares (FMOLS)				
Sample (adjusted): 2001 2019				
Periods included: 19				
Cross-sections included: 5				
Total panel (balanced) observations: 95				
Variable	Coefficient	Std. Error	t-Statistic	Prob.
LEG	0.505354	0.070970	7.120692	0.0000
LLOSSES	–0.222519	0.036648	–6.071736	0.0000
LEC	–0.239851	0.072683	–3.299935	0.0014
LFP	0.248166	0.021433	11.57863	0.0000
LCPI	0.238064	0.028054	8.485913	0.0000
LIVA	–0.299632	0.044162	–6.784775	0.0000
R-squared	0.913429			
S.E. of regression	0.079267			

Concerning the Electricity Transmission and Distribution losses (Losses), the regression outcomes show that the increase in 1% of losses, decreases the average electricity price by 0.2%, while for Electricity Consumption (EC) an increase of 1% reduces the average electricity prices of 0.2%. This result supports the findings of various scholars who found a close relationship between electricity consumption or demand with electricity prices [5,12,18]. However, developing countries tend to use oil fired electricity generation in hours or days of peak demand, and this require higher cost of production than renewables. Thus, the increase in electricity demand or consumption could increase the electricity prices. One of the economic characteristics of the electricity supply is its capital intensiveness. Therefore, the investments if not well-planned can result in stranded assets and with a very high proportion of fixed assets. Due to this reason, economies of density and output in distribution can affect electricity cost of production and prices. This implies that the average cost of servicing a particular area decline as the number of customers in that area using existing assets increases, or as the average load drawn by those customers increases [1].

Table 9. Panel DOLS long-run estimation results.

Dependent variable: LEP				
Method: Panel dynamic least squares (DOLS)				
Sample: 2001 2019				
Periods included: 20				
Cross-sections included: 5				
Total panel (balanced) observations: 100				
Variable	Coefficient	Std. Error	t-Statistic	Prob.
LEG	0.525211	0.126392	4.155405	0.0001
LLOSSES	–0.241122	0.064613	–3.731795	0.0003
LEC	–0.264953	0.112249	–2.360409	0.0204
LFP	0.228005	0.034616	6.586598	0.0000
LCPI	0.227116	0.053747	4.225647	0.0001
LIVA	–0.225842	0.064731	–3.488947	0.0008
R-squared	0.912995			
S.E. of regression	0.079910			

Consumer Price Index (CPI) has a positive effect on electricity prices. More specifically, the increase of 1% in CPI, increases the average electricity prices increase by 0.2%. This result is in line with the findings of several studies whether in developed or developing countries. As highlighted in the literature, inflation or the increase in CPI positively affects electricity prices [4,16,34]. In addition, most regulatory authorities in setting the base tariff, they take into account macroeconomic factors among which national inflation or CPI [33,34,53]. Lastly, the variable Industry Value Added (IVA) has a negative effect on electricity prices such that increase of 1% in IVA, decreases electricity prices by 0.29%. Most of the literature used the Industrial Value Added as a proxy for industrialization [49–52]

and have found a significant relationship between IVA and EP. In addition, for developed countries, Foroni et al. [18], to analyze the importance of macroeconomic information, for forecasting daily electricity prices in two of the main European markets, Germany and Italy. They also reach on the conclusion that industrial production index and oil price are more important for short horizons than for longer horizons pricing.

Moreover, the negative relationship between IVA and EP can be attributed to the efficient use of electricity by industries, which is one a key factor of production. This support the findings of Dan [47] who clearly noted that there has been a gradual decline in energy consumption in China since 1978 despite increasing industrial growth and attributed this to energy efficiency. The results of this study imply that an increase in industrialization through efficient use of electricity or any other factors such as energy efficiency practices that affect electricity consumption, can reduce average end-user electricity prices to the consumer. It is important to note that the behaviors of the drivers of EP could also change depending on the economic structure, energy policy of governments and price regulation policies of the countries.

5. Conclusion, regulatory implications, and policy recommendations

The objective of this study, is to measure to which extent, Electricity Net Consumption (EC), Electricity Net Generation (EG), electricity transmission and distribution losses (Losses), International Average Crude oil prices (FP), Consumer Price Index (CPI), Industry Value Added (IVA) could influence the Average Electricity Prices (EP) in five countries of East Africa for a period of 2000 to 2019. This study adopts a three-stage approach, consisting of panel unit root, panel cointegration tests and estimating the long run cointegration relationship of the variables in a panel context. We applied four different panel unit root tests including ADF-Fisher Chi-square, Levin, Lin and Chu (hereafter referred to as LLC); PP-Fisher Chi-square, and Im, Pesaran, and Shin, (hereafter referred to as IPS). The results of the tests reveal that the variables are non-stationary at “level”, stationary at first-differences integrated with order one denoted as I(1). For cointegration analysis, the Pedroni, Kao and Johansen Fisher co-integration tests were performed. The results of the tests reject the null hypothesis of no cointegration of the variables at 1% level of significance. Therefore, we can conclude that there is a long-run relationship between all variables.

FMOLS and DOLS coefficients estimation results, demonstrated that the independent variables explain the variations in electricity prices at 91% as shown by the R-squared. In addition, the overall considered variables are statistically significant at a 1% level, except EC which is statistically significant at 2% for DOLS only. The panel coefficients estimation indicates that 1% increase in EG, leads to 0.5% increase in the electricity prices (EP); 1% increase in FP, causes a 0.2% increase in the electricity price; 1% increase in losses, decreases the average electricity price by 0.2%; an increase of 1% in EC reduces the average

electricity prices of 0.2%; an increase of 1% in CPI, increases the average electricity prices increase by 0.2%, and an increase of 1% in IVA, decreases electricity prices by 0.29%. The results revealed the existence of a negative long run relationship from electricity generation and fuel prices to electricity prices. This study recommends that governments should develop policies to support development of renewable sources which are also environmentally friendly, to increase the share of renewables in the overall energy mix in East African countries. They should renegotiate some of the terms and conditions of the agreement with the investment firms that were entrusted with the generation of hydroelectricity especially in terms of payback periods. They could also utilize equity financing arrangements, which are cheaper to reduce the electricity cost of production. This could reduce in long term the electricity prices. In addition, appropriate policies related to subsidized electricity prices need to be reformulated, to prevent adverse effects related to inefficient overconsumption of electricity. Furthermore, despite that subsidized electricity prices offset the negative effects of losses on electricity prices, the regulatory policies should adopt a performance-based regulation to cope the utilities to reduce the technical and commercial losses which can increase enduser electricity prices.

This study is a first attempt to determine the drivers of electricity price in East African countries. The current study provides good insight into the behaviors of the key drivers of electricity prices in the East Africa region that could shape policy and regulatory decisions that will make the electricity sector financially viable and sustainable. Going forward, the authors have however identified some areas which can be improved upon in future studies. For instance, since investment affects electricity prices and is driven largely by peak capacity needs, it will be appropriate to have in the econometric model, Peak Demand (MW) as one of the independent variables. Also, for robust results in future studies, it will be important to disaggregate the total loss variable into Distribution System Losses (technical and commercial losses) and Transmission System Losses.

Acknowledgments

I acknowledge African Centre of Excellence in Energy for Sustainable Development (ACEESD) for the support towards this research.

Conflict of interest

The authors declare no conflicts of interest.

Authors' contributions

Mr. Mburamatare Daniel: Conception, design of the study, interpretation of data and drafting the article; Dr. Akumuntu Joseph: Acquisition of data, analysis and interpretation of data; Dr. William K. Gboney: Critically revising its important intellectual content; Dr. Hakizimana Jean de Dieu: Final approval of the

version submitted; Dr. Fidele Mutemberezi: Support in the analysis and interpretation of data.

References

1. Sayers C, Shields D (2001) Electricity prices and cost factors. Productivity Commission Staff Research Paper, Melbourne Available .from: https://www.pc.gov.au/research/supporting/electricity-prices.

2. Robert S, Pindyck S (1979) The structure of world energy demand. 2nd ed. Cambridge: MIT Press. Available from: https://mitpress.mit.edu/9780262661775/the-structure-of-world-energy-demand/.

3. Bhattacharyya S (2011) Energy Economics Concepts, Issues, Markets and Governance. 1st ed. London: Springer-Verlag London LimitedAvailable from: https://link.springer.com/book/10.1007/978-0-85729-268-1.

4. Girish GP, Vijayalakshmi S (2013) Determinants of electricity price in competitive power market. Int J Bus Manage 8: 70–75. https://doi.org/10.5539/ijbm.v8n21p70

5. Suliman MS, Farzaneh H (2022) Econometric analysis of pricing and energy policy regulations in Japan power exchange spot market. Clean Eng Technol 9: 100523. https://doi.org/10.1016/j.clet.2022.100523.

6. Watchwire (2018) Electricity market drivers. Energy Watch, 1–6. Available from: https://watchwire.ai/electricity-pricing-market-drivers/.

7. Uribe JM, Mosquera-López S, Arenas OJ (2022) Assessing the relationship between electricity and natural gas prices in European markets in times of distress. Energy Policy 166: 113018. https://doi.org/10.1016/j.enpol.2022.113018

8. Akay EC, Uyar SGK (2016) Determining the functional form of relationships between oil prices and macroeconomic variables: The case of Mexico, Indonesia, South Korea, Turkey countries. Int J Econ Financ Issues 6: 880–891. Available from:https://dergipark.org.tr/en/pub/ijefi/issue/32012/353753.

9. Kojima M, Han JJ (2017) Electricity tariffs for nonresidential customers in sub-saharan Africa. Electr Tarif Nonresidential Cust Sub-Saharan Africa, https://doi.org/10.1596/26571

10. Afanasyev DO, Fedorova EA, Gilenko EV (2021) The fundamental drivers of electricity price: a multi-scale adaptive regression analysis.Empir Econ 60: 1913–1938. https://doi.org/10.1007/s00181-020-01825-3

11. Alves B (2022) Distribution of energy sources used for gross electricity generation in Germany. Available from: https://www.statista.com/statistics/736640/energy-mix-germany/.

12. Mosquera-López S, Nursimulu A (2019) Drivers of electricity price dynamics: comparative analysis spot and futures https://doi.org/10.1016/j.enpol.2018.11.020 markets. Energy Policy 126: 76–87.

13. EIA (2022) What is U.S. electricity generation by energy source? Available from: https://www.eia.gov/tools/faqs/faq.php?id=427&t=3.

14. Briceño-Garmendia C, Shkaratan M (2011) Power tariffs: caught between cost recovery and affordability. Policy research working paper, World Bank Group, Washington, D.C. [Online]. Available from: http://elibrary.worldbank.org/doi/book/10.1596/1813-9450-5904.

15. Gil-Alana LA, Martin-Valmayor M, Wanke P (2020) The relationship between energy consumption and prices: Evidence from futures and spot markets in Spain and Portugal. Energy Strateg Rev 31: 100522. https://doi.org/10.1016/j.esr.2020.100522

16. Ruksans O, Oleinikova I (2014) Analysis of factors that are affecting electricity prices in Baltic Countries. In IEEE, 55th Int. Sc. Conf. on Power and Elec. Eng Riga Tech Un (RTUCON), 232237. https://doi.org/10.1109/RTUCON.2014.6998197

17. Sirin SM, Yilmaz BN (2021) The impact of variable renewable energy technologies on electricity markets: An analysis of the Turkish balancing market. Energy Policy 151: 112093. https://doi.org/10.1016/j.enpol.2020.112093

18. Foroni C, Ravazzolo F, Rossini L (2019) Forecasting daily electricity prices with monthly macroeconomic variables. SSRN Electron J, 2250. https://doi.org/10.2139/ssrn.3357361

19. Gil-Alana LA, Mudida R, Carcel H (2017) Shocks affecting electricity prices in Kenya, a fractional integration study. Energy 124: 521–530, https://doi.org/10.1016/j.energy.2017.02.092

20. Adjei P, Solomon K (2014) Energy consumption in Ghana and the story of economic growth , industrialization, trade openness and urbanization. Asian Bull Energy Econ Technol 1: 1–6. Available from: http://asianonlinejournals.com/index.php/ABEE/article/view/713/739.

21. Li M, Li L, Strielkowski W (2019) The impact of urbanization and industrialization on energy Security: A case study of China. Energies 12: 2194. https://doi.org/10.3390/en12112194

22. Mabea GA (2014) Modelling residential electricity demand for Kenya. J Econ Sustainable Dev 5: 145–153. Available from: https://core.ac.uk/reader/234646280.

23. Odhiambo MN (2010) Energy consumption, prices and economic growth in three SSA countries: A comparative study. Energy Policy 38: 2463–2469. https://doi.org/10.1016/j.enpol.2009.12.040

24. Asafu-Adjaye J (2000) The relationship between energy consumption, energy prices and economic growth: Time series evidence from Asian developing countries. Energy Econ 22: 615–625. https://doi.org/10.1016/S0140-9883(00)00050-5

25. Odhiambo MN (2009) Energy consumption and economic growth nexus in Tanzania: An ARDL bounds testing approach. Energy Policy 37: 617–622. https://doi.org/10.1016/j.enpol.2008.09.077

26. Sari R, Soytas U (2007) The growth of income and energy consumption in six developing countries. Energy Policy 35: 889–898. https://doi.org/10.1016/j.enpol.2006.01.021

27. Shao Z (2017) On electricity consumption and economic growth in China. Renewable Sustainable Energy Rev 76: 353–368. https://doi.org/10.1016/j.rser.2017.03.071

28. Jumbe CBL (2004) Cointegration and causality between electricity consumption and GDP:

Empirical evidence from Malawi. Energy Econ 26: 61–68. https://doi.org/10.1016/S01409883(03)00058-6

29. Fatai BO (2014) Energy consumption and economic growth nexus: Panel co-integration and causality tests for Sub-Saharan Africa. J Energy South Africa 25: 93–100. https://doi.org/10.17159/2413-3051/2014/v25i4a2242

30. Bayar Y, Özel H (2014) Electricity consumption and economic growth in emerging economies. J Knowl Manage Econ Inf Technol 4: 15–15. Available from: http://www.scientificpapers.org/download/351/.

31. Mumo M, Saulo M, Kibaara S (2015) Integrated electricity tarrif model for Kenya. Int J Energy Power Eng 4: 95–98. https://doi.org/10.11648/j.ijepe.s.2015040201.19

32. KIPPRA (2010) A comprehensive study and analysis on energy consumption patterns in Kenya. The Energy Regulatory Commission (ERC), Nairobi, Kenya. Available from: https://www.cofek.africa/wp-content/uploads/2013/05/ERCStudy_ExecSummary_02082010.pdf.

33. Uganda Electricity Regulatory Authority (2018) Quarterly tariff adjustment methodology. Kampala, Uganda. Available from: https://www.era.go.ug/index.php/tariffs/tariff-adjustmentmethodology.

34. Peng D, Poudineh R (2016) Sustainable electricity pricing for Tanzania. International Growth Centre (IGC), Dar es Salaam, Tanzania. [Online]. Available from: http://www.theigc.org/wpcontent/uploads/2016/08/Peng-Poudineh-2016-Working-Paper.pdf.

35. Dragasevic Z, Milovic N, Djurisic V, et al. (2021) Analyzing the factors influencing the formation of the price of electricity in the deregulated markets of developing countries. Energy Rep 7: 937949 https://doi.org/10.1016/j.egyr.2021.07.046

36. Oosthuizen AM, Inglesi-Lotz R, Thopil GA (2022) The relationship between renewable energy and retail electricity prices: Panel evidence from OECD countries. Energy 238: 121790. https://doi.org/10.1016/j.energy.2021.121790

37. Apolinário I, Felizardo N, Garcia AL, et al. (2006) Additive tariffs in the electricity sector. IEEE Power Eng Soc Gen Meet PES, 1–8. https://doi.org/10.1109/pes.2006.1709499

38. Pérez-Arriaga IJ (2013) Regulation of the power sector. New York: Springer-Verlag London Limited. https://doi.org/ 10.1007/978-1-4471-5034-3

39. Campbell A (2018) Price and income elasticities of electricity demand: Evidence from Jamaica. Energy Econ 69: 19–32, https://doi.org/10.1016/j.eneco.2017.10.040

40. Braithwait S, Hansen D, O'Sheasy M (2007) Retail electricity pricing and rate design in evolving markets. Edison Electr Inst, 1–45. Available from: http://www.madrionline.org/wpcontent/uploads/2017/02/eei_retail_elec_pricing.pdf. nuclear

41. Thoenes S (2014) Understanding the determinants of electricity prices and the impact of the German

moratorium https://doi.org/10.5547/01956574.35.4.3 in 2011. Energy J 35: 61–78,

42. Dutta G, Mitra K (2016) A literature review on dynamic pricing of electricity. J Oper Res Soc https://doi.org/10.1057/s41274-016-0149-4

43. Murthy GGP, Sedidi V, Panda AK, et al. (2014) Forecasting electricity prices in deregulated wholesale spot electricity market: A review. Int J Energy Econ Policy 4: 32–42. Available from: https://www.econjournals.com/index.php/ijeep/article/view/621.

44. Munasinghe M, Warford JJ (1982) Electricity pricing: Theory and case studies. The International Bank for Reconstruction and Development & The World Bank, Available from: https://prdrse4all.spc.int/node/4/content/electricity-pricing-theory-and-case-studies.

45. Zweifel P, Praktiknjo A, Erdmann G (2017) Energy Economics. Berlin, Germany: Springer International Publishing AG 2017. https://doi.org/10.1007/978-3-662-53022-1

46. Bhattacharyya SC (2019) Energy economics: Concepts, issues, markets and governance, 2nd ed. 2019, 2nd ed. Springer-Verlag London.Available from: https://link.springer.com/book/10.1007/978-1-4471-7468-4.

47. Shi D (2002) The improvement of energy consumption efficiency in China's economic growth. Econ Res J 9: 49–56.

48. Berndt ER (1990) Energy use, technical progress and productivity growth: A survey of economic issues. J Product Anal 2: 67–83. https://doi.org/10.1007/BF00158709

49. Abid M, Mraihi R (2015) Energy consumption and industrial production: Evidence from Tunisia at aggregated and disaggregated levels. J Knowl Econ 6: 1123–1137. https://doi.org/10.1007/s13132-014-0190-y

50. Tapsın G (2017) The link between industry value added and electricity consumption. Eur Sci J ESJ 13: 41. https://doi.org/10.19044/esj.2017.v13n13p41

51. Shahbaz M, Salah GU, Rehman IU, et al. (2014) Industrialization, electricity consumption and CO2 emissions in Bangladesh. Renewable Sustainable Energy Rev 31: 575–586. https://doi.org/10.1016/j.rser.2013.12.028

52. Olufemi OJ (2015) The effects of electricity consumption on industrial growth in Nigeria. J Econ Sustainable Dev 6: 54–60. https://www.iiste.org/Journals/index.php/JEDS/article/view/24275.

53. Management Consulting (2012) Manual for the ERA tariff model in Uganda. Available from: https://www.ogel.org/legal-and-regulatory-detail.asp?key=17590.

54. Mburamatare D, Gboney WK, Hakizimana JDDK, et al. (2022) Effects of industrialization, technology and labor efficiency on electricity consumption : Panel data experience of Rwanda, Tanzania and Kenya. Int J Energy Econ Policy 12: 349–359. https://doi.org/10.32479/ijeep.12551

55. Keppler JH, Bourbonnais R, Girod J (2006) The econometrics of energy systems. Econom Energy Syst,1–266, https://doi.org/10.1057/9780230626317

6. Carter RH, Griffiths EW, Guay CL (2011) Principles of econometrics. Fourth Edi. USA/Danvers: John Wiley Sons, Inc. Available from: http://zalamsyah.staff.unja.ac.id/wp content/uploads/sites/286/2019/11/7-Principles-of-Econometrics-4th-Ed.-R.Carter-Hill-et.al_.-1.pdf.

57. Greene WH (2002) Econometrics analysis. Fifth Ed. New Jersey: Printice Hall. Available from: https://spu.fem.uniag.sk/cvicenia/ksov/obtulovic/Mana%C5%BE.%20%C5%A1tatistika%20a%20ekonometria/EconometricsGREENE.pdf.

58. Wooldridge JM (2016) Introductory econometrics, a modern approach. Sixth Ed. USA, Boston: Cengage Learning. Available from: https://economics.ut.ac.ir/documents/3030266/14100645/Jeffrey_M._Wooldridge_Introductory_Econometrics_A_Modern_Approach__2012.pdf.

59. Gujarati DN (2004) Basic econometrics. Fourth Ed. The McGraw-Hill Companies. Available from: https://www.nust.na/sites/default/files/documents/Basic%20Econometrics%20%2CGujarati%204e.pdf.

60. Johnston J, Dinardo J. Econometric methods. Fourth Ed. MacGraw-Hill. Available from: https://economics.ut.ac.ir/documents/3030266/14100645/econometric%20methods-johnston.pdf. 61. Stock JH, Watson MW. Introduction to econometrics. Boston: PEARSON/ Addison Wiesley. Available from: https://www.ssc.wisc.edu/~mchinn/stock-watson-econometrics-3e-lowres.pdf.

62. Pesaran MH, Im KS, Shin Y (2003) Testing for unit roots in heterogeneous panels. J Econom 115: 53–74. https://doi.org/10.1016/S0304-4076(03)00092-7 data:

63. Chen B, Mc Coskey SK, Kao C (1999) Estimation and inference of a cointegrated regression in panel A monte carlo study. Am J Math Manage Sci 19: 75–114. https://doi.org/10.1080/01966324.1999.10737475

64. Ouedraogo NS (2013) Energy consumption and economic growth: Evidence from the economic community of West African States (ECOWAS). Energy Econ 36: 637–647. https://doi.org/10.1016/j.eneco.2012.11.011

65. Levin A, Lin CF, Chu CJ (2002) Unit root tests in panel data: Asymptotic and finite-sample properties. J Econom 108: 1–24, https://doi.org/10.1016/S0304-4076(01)00098-7

66. Eggoh JC, Bangake C, Rault C (2011) Energy consumption and economic growth revisited in African countries. Energy Policy 39: 7408–7421 https://doi.org/ 10.1016/j.enpol.2011.09.007

67. Pedroni P (2004) Panel cointegration: Asymptotic and finite sample properties of pooled time series tests with an application to the PPP hypothesis. Econom Theory 20: 597–625. https://doi.org/10.1017/S0266466604203073

Bioenergy potential of agricultural crop residues and municipal solid waste in Cameroon

Robinson J. Tanyi1 and Muyiwa S Adaramola2,*
1 Department of Mechanical Engineering, Kwame Nkrumah University of Science and Technology, Kumasi Ghana
2 Faculty of Environmental Sciences and Natural Resource Management, Norwegian University of Life Sciences (NMBU), P.O. Box 5003, NO-1432 Ås, Norway

ABSTRACT

Biomass has emerged as an important and promising energy source, particularly in developing countries, owing to continuous research for sustainable energy sources that do not interfere with food, water or land needs. This study introduces the surplus availability factor (SAF), minimum, average and maximum biogas production technique in the assessment of crop production data in 2020 to provide a more precise and current estimate of Cameroon's crop residue and municipal solid waste (MSW) bioenergy potential. Crop residues contributed roughly 96% while MSW contributed the remaining 4% of the total bioenergy potential of 606 PJ per year. The bioenergy potential was calculated using crop production statistics derived from the FAOSTAT database of the Food and Agriculture Organization, while the residue-to-product ratio (RPR) and surplus availability factors (SAF) were found from related studies. The study concludes that crop residues and MSW have significant energy potential capable of meeting the country's electricity, transport fuel and biogas demand while simultaneously mitigating climate change through the capture of about 1.6 billion kg of CO2 through biogas recovery. It also highlights the lack of accurate and up-to-date data on the country's biomass potential and recommends ground data collection and geospatial mapping of areas with enormous potential for these resources to guide policymakers and investment plans.

Keywords: *Sub-Saharan Africa; energy access; crop residues; surplus availability factor; waste generated per capita*

1. Introduction

Agricultural crop residues and municipal solid waste (MSW) are highly neglected and underutilized energy sources, as they are generally regarded as waste in most parts of the world, especially in developing countries like Cameroon. Cameroon is a Central African nation with the third largest biomass potential in Sub-Saharan Africa [1], owing to its vast tropical rainforest in the Congo Basin (Figure 1). This biomass potential is thought to equal about 6.3 billion tons [2]. Biomass and waste make up between 75–80% of the country's total energy supply, contributing about 290 PJ in 2020 [3]. When these wastes are collected and disposed of in landfills, they undergo decomposition usually anaerobically. In the process, they emit biogas (composition of carbon dioxide and methane) which, if properly captured and processed, can provide many times over the world's energy needs. The criticisms which have come with the clearing of land for the production of energy crops have encouraged research for biofuels from nonedible sources such as plant material, typically crop residues, and waste from other economic sectors [4]. Furthermore, the need to address major health and environmental concerns (such as indoor air pollution, deforestation, global warming, environmental pollution and climate change)

associated with improper MSW management, widespread use of fossil fuels and cooking with traditional biomass necessitates the research of waste-to-energy ventures [5].

Cameroon's economy is dominated by the agricultural sector, which produces nearly 60 million tonnes of different crops annually [6]. This presents a huge market of agricultural residues from which bioenergy could be tapped to address the country's energy challenges. Crop residues can be categorized into primary and secondary residues, depending on whether they are primarily from the farm or industrial processing, respectively. Primary residues usually consist of shells, leaves and peelings that are left in fields or plowed back for organic manure or used as feed for animals. Meanwhile, secondary residues like bagasse and husks are derived during crop processing into more useful products [5]. Usually, the process residues have a higher residue recovery rate, of almost 100%, as compared to the lower residue recovery of field residues, where most are either used as animal feed or reused for cultivation [7]. Most of the crops used in this study are available throughout the year in Cameroon and as such can be regarded as renewable biomass feedstock. However, most residues are used for non-energy purposes, such as animal feed, reuse for cultivation and organic manure. The energy applications of these residues are usually done traditionally as cooking fuels, causing health and environmental concerns. Many business and public sector actors have taken steps to harness the energy potential of these crops' residues in order to reduce the use of fossil fuels, meet climate change targets and avoid the use of food crops for energy reasons. So far, most of these initiatives have been directed towards the production of cleaner cooking fuels (biogas and biochar) for the population in rural areas who mostly burn these residues directly for their energy needs. This does not only contribute to increasing the amount of greenhouse gas (GHG) in the atmosphere but also deteriorates the health of vulnerable women and children who stay more at home and are thereby more exposed.

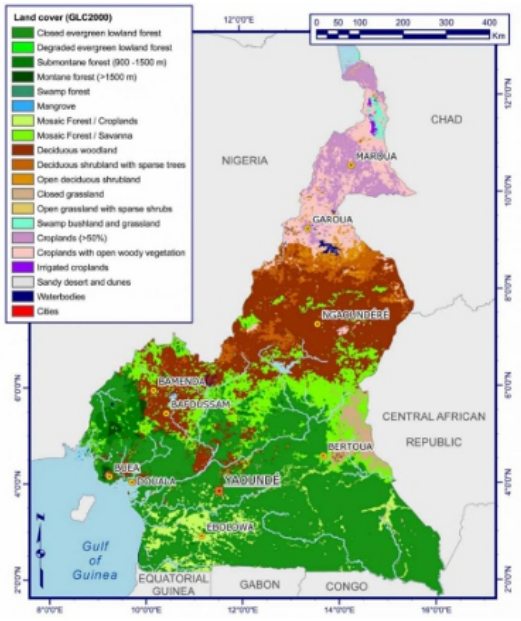

Figure 1. Vegetation cover in Cameroon (Source: https://www.wri.org/data/cameroon-vegetation-cover).

On the MSW management side, about 2.01 billion tonnes of waste is generated globally per annum, with at least 33% of it not managed in an environmentally friendly manner [8] These figures are relatively higher in developing countries like Cameroon, where most municipal waste is left uncollected and untreated due to irregular and insufficient waste collection and treatment facilities. Ref. [7] add that the component diversity of MSW, which is usually composed of organic waste, paper waste, plastic waste, glass, textiles, electrical appliances, etc., makes it difficult to manage. Moreover, the GHGs such as CO2, N2O and CH4 emitted from improper waste management are responsible for about 5% of total GHGs in the atmosphere, while its leachate can cause significant environmental pollution in air and groundwater and gives rise to odor [9].

The drive for bioenergy in Cameroon can be attributed to many factors, including energy security, revenue additions from agricultural and forestry sectors, socio-economic benefits and the expensive cost of importation of refined oil [2]. Also, due to Cameroon's enormous biomass potential, many researchers have sought ways to exploit this enormous potential for energy purposes. As such, there are several published reviews, studies and technical works on techniques, prospects and economic feasibility of waste-to-energy using crop residues and MSW in Cameroon. Ref. [5] assessed the forest, crop, animal and MSW biomass resources in Cameroon, their bioenergy potential and potential contribution to the sustainable development of the country. They found out that the electricity production potential of these biomass sources for the year 2012 was about 67.5 TWh.y-1 which amounted to more than twelve times Cameroon's total electricity production for the year 2010. Based on this, they concluded that biomass resources can significantly contribute to the country's energy supply. Ref. [2] also assessed the biomass resource potential in Cameroon from sustainably extracted agricultural and forest residues. They concluded that this potential could help spread electricity throughout the country, especially in farming communities where the residues are enormous. Ref. [10] examined the ground biomass assessment mapping in Cameroon's savanna ecosystem using ALOS PALSAR data and produced a biomass map of Cameroon, though they did not do an assessment of its bioenergy potential. Similar studies by [11] sought to evaluate the energy potential of crop residues (maize and sorghum stalk) for use in biomass power plants to produce electricity and thermal energy in the Northern region of Cameroon and the economic feasibility of it. Their techno-economic analysis of some 6 communities in this region gave an estimated total investment cost of about 874.5 million USD to produce a 270 MW installation, with levelized cost of electricity (LCOE) values between 6.81 USDcent/kWh to 12.9 USDcent/kWh. They however found that this project was only realizable with a Carbon bonus incentive of 5.16 USDcent/kWh for the biomass power plant, without which losses in the municipalities of Bouki and Tchollere were to the tune of 72.778 GWh/year and 137.331 GWh/year, respectively. They recommended that the biomass cost can be reduced by creating a biomass market for electricity generation and a biomass supply chain including the private company. Ref. [12] studied the potential of

converting the lignocellulosic biomass wastes from banana plantations in Cameroon into bioethanol, biomethane and wood pellets. They found that about 4.5 million tons of fresh banana plant when bone-dried can produce approximately 93800, 92133, 447500 tons of bioethanol, biomethane and pellets, respectively.

Most studies on MSW in Cameroon dwell mostly on the composition, sources, management and environmental impacts with little or no assessment of its energy potential. Other studies like [13] provide a broad description of the energy potential of MSW for African cities, including Cameroon. This study showed that Cameroon's MSW in 2012 had a potential of about 290 million Nm3 and is expected to almost double in 2025 to about 524 million Nm3. In terms of potential energy recovery from waste incineration and landfill gas, recovery values were approximately 31,034 TJ/year and 7799 TJ/year, respectively, from the total waste generated in 2012. Correspondingly, this translates to 1724 Gwh and 758 GWh of electricity potential.

Nonetheless, from the reviewed literature, there is limited data and an information gap on the energy potential of the country's crop residues and MSW, and this served as the impetus for this study. There is very little country-specific data on the moisture content, residue-to-product (RPR) and surplus availability factor (SAF) of crop residues. Most of the values utilized in this study are derived from similar studies in countries with identical weather patterns as Cameroon. Also, the geographical scope of many studies is limited to specific cities and does not give a comprehensive review of the energy potential of these resources nationally. Research around MSW is usually focused on its composition, generation, collection and disposal, with little or no characterization of its energy potential. There is also no GIS mapping of MSW hotspots and regions with high crop production to ease identification for further research or development. Most importantly, most studies do not depict a realistic picture of the total energy potential of crop residues, as they do not consider the surplus availability factor (SAF) of each crop residue. This introduces inaccuracies in the energy potential assessment, as it is assumed all residues are used for energy generation purposes while some are used for animal feeding and organic manure. The lack of updated information leaves policymakers flying blind and could deter investors who may be unable to conduct feasibility studies due to limited or outdated data.

This study aims to bridge some of these gaps by

1. providing a more accurate and recent assessment of the energy potential of crop residues and MSW in Cameroon through the introduction of the SAF as used in similar studies by [14,15];
2. introducing the minimum, average and maximum biogas production methodology used by [16,17] to observe uncertainties in results;
3. assessing the electricity generation potential of these sources, the amount of CO2 emissions saved with their use and the quantity of biofuels that could be produced from crop residues.

The bioenergy assessment in this study is however limited to data collected from recommendable sites

and related literature. No ground data collection for crop residues and MSW was done. Also, the most up-to-date data consulted was for 2020, as it was the most recent in the FAOSTAT database available at the time of this study.

2. Methods and materials

The statistics of human population and annual crop production of different kinds of crops for 2021 were obtained from the Food and Agricultural Organization statistics database [6]. To estimate the number of residues generated from each crop, the residue-to-product ratio (RPR) of each crop was used. The RPR values of several crops, as well as their respective heating values, were found in various published studies. Similarly, the heating values of biomass residues and MSW-derived biogas were sought from published documents.

2.1. Determining the bioenergy potential of agricultural crop residues

Procedures and methods for estimating bioenergy from agricultural residues were adapted from [18,19]. The crop residues can be primary residues generated during crop harvesting and primary processing in farms or secondary residues generated during secondary processing in industries [14]. The amount of residue recovered from these crops is unknown, but for this study, it is assumed at 100% to enable the determination of the maximum energy potential of crop residues generated in Cameroon. The crop residues can be further divided into gross residue and surplus residue, which is the part of the gross residue used for energy production. The gross residue as given in formula (1) is a function of the area covered by the crop, the crop yield and the residue-to-product (RPR) ratio of the crops.

$$R_{g(l)} = \sum_{i=1}^{n} A(il) * Y(il) * RPR(il) \quad (1)$$

where Rg(l) is the gross residue potential at the lth location from n number of crops in t y-1, A(il) is the area of the area ith crop at the lth location in ha, Y(il) is the yield of the ith crop at the lth location in t ha-1, and RPR(il) is the residue to product ratio of the ith crop at the lth location. The value of total crops produced (A(il)* Y(il)) was sourced from the FAOSTAT 2022 database [6], while the RPR values given in Table 1 were obtained from already published studies conducted in other countries, such as Ghana, Uganda, Zambia and China.

Table 1. The RPR, SAF and LHV for studied crops.

Crop	Residue Type	RPR	SAF	LHV (MJ/kg)	Sources
Maize	Stalk	2	0.8	16.3	a,b,j
	Cob	0.273	1	16.63	
	Husk	0.2	1	15.56	
Rice	Straw	1.757	0.684	8.83	b,d,e
	Husk	0.23	0.83	12.9	c,e,f
Sorghum	Straw	1.25	0.8	12.38	a,b
	Husk	1.4	1	13	c,j
Millet	Straw	1.4	1	13	c,j
	Stalk	1.75	0.8	15.51	a,b,f
Wheat	Straw	1.2	0.29	15.6	b,j
	Husk	0.23	0.29	12.9	b,f
Cassava	Stalk	0.062	0.407	16.99	a,d,e
	Peelings	3	0.2	10.61	a,i
Cocoyam	Peelings	0.2	0.8	10.61	i,j
Sweet potato	Peelings	0.6	0.8	10.61	b,j
Yam	Peelings	0.2	0.8	10.61	i,j
Potatoes	Peelings	0.75	0.8	10.61	i,j
Groundnuts	Shells/husks	0.477	1	15.56	a,i,c
	Straw	2.3	1	17.58	a
Palm oil	Fiber	0.147	1	19.94	a,i
	Shells	0.049	1	21.1	a,i
	Fronds	2.604	1	7.97	i
	Empty bunches	0.428	1	19.41	a,i
	Male bunches	0.233	1	14.86	i,j
Coconuts	Shell	0.6	1	10.61	i,j
	Husk	1.03	1	18.6	i,j
	Coir dust	0.62	1	13.4	j
Beans	Straw	2.5	1	12.38	j
Soybean	Straw	2.66	0.8	18	b,f
	pods	1	0.8	18	a,b,f
Banana	leaves	0.35	1	11.37	g
	stem	5.6	1	11.66	a,j
	peels	0.25	1	17	h,j
Plantain	leaves	0.35	0.8	12.12	g,i
	stem	3.91	0.8	10.9	g,i
	peels	0.25	1	12.56	a,h
Sugar Cane	baggase	0.25	1	6.43	b,c
	tops/leaves	0.32	0.8	15.8	b,c
Coffee	husk	1	1	12.8	b,c
Cocoa	pods/husks	1	1	15.48	j
Cotton	stalk	2.1	1	15.9	c,i

Data sources:

a = Ref. [20]; b = Ref. [15]; c = Ref. [14]; d = Ref. [21] ; e = Ref. [22]; f = Ref. [23] ; g = Ref. [24] ; h = Ref. [25] ; i = Ref. [4] ; j = Ref. [5]

It should be noted that some parts of the generated gross residue from crops were used for other purposes like feeding livestock or for soil amendment. The unused part is the surplus, and this surplus (referred to as surplus residue potential (SRP)) is considered to be available for bioenergy purposes. The SRP is

estimated using the surplus availability factor (SAF) or recoverability factor of the crop residues. The SAF is defined as the ratio of residues available for energy purposes compared to the total residue amount. The SAF values used in this study were taken from similar published work (such as Ref. [15]), and where SAF for a particular crop (or crop residue) is not available, a SAF value of 1 was assumed. The surplus residue potential at location l is estimated using formula (2) according to Ref. [18].

$$R_{sl} = \sum_{i=1}^{n} (Rg(il) * SAF(il)) \quad (2)$$

where Rsl is the surplus residue potential at location l in tonnes per year, and SAF is the surplus availability factor or surplus residue fraction of the ith crop at lth location.

The bioenergy crop residue potential is then calculated from the available surplus residue using Eq (3).

$$E_l = \sum_{i=1}^{n} (R(sl) * LHV(il)) \quad (3)$$

where El is the estimated bioenergy potential at the lth location in PJ y-1, and LHV(il) is the lower heating value of the ith crop at lth location in MJ kg-1. The lower heating values were obtained in similar studies in Ghana and Nigeria with similar climate patterns as Cameroon. Though the moisture content of the residues was not directly used in computing the bioenergy potential, it should be known as it varies with location, harvest and storage periods and substantially affects the heating value of the crop [26].

The energy potential of crop residues can be realized through their heat, electricity and biofuels production potential. In this study, the electricity potential and the bioethanol and biodiesel potential were analyzed using methodologies proposed and used by [2,27]in their studies. The average moisture content of 22.7% for all crop residues was used in calculating the total bone-dry mass, which was subsequently used in the calculation of the bioethanol and biodiesel production potential. In the bioethanol production, a low conversion factor of 110 litres per bone dry tonne was applied, and 300 liters per bone dry tonne was utilized for high limit biochemical enzymatic hydrolysis and fermentation ethanol. Meanwhile, for Fischer Tropsch biodiesel production, a lower conversion factor of 75 liters per bone dry tonne was used, and 200 liters per bone dry tonne was utilized as the higher conversion factor.

2.2. Bioenergy potential of Municipal Solid Wastes (MSW)

Municipal Solid Waste includes waste generated from households, commerce, trade, small businesses, office buildings and institutions (such as schools, hospitals and government buildings). It also includes bulky waste (e.g., old furniture, mattresses) and wastes from selected municipal services, e.g., waste from park and garden maintenance, waste from street cleaning services (street sweepings, the content of litter containers, market cleansing waste), if managed as waste. These sources exclude waste from municipal sewage network and treatment, municipal construction and demolition waste [28]. The economic status, season, food habit, age and gender of household members all affect the per capita generation from house to house [5]. Usually, larger per capita MSW generation amounts are seen in countries with higher socio-economic indicators like Gross Domestic Product (GDP) per capita, Gross

National Income (GNI) and Human Development Index (HDI) [29]. According to [5], MSW in Cameroon can broadly be classified into three main groups (see Figure (2)), which are as follows:

• The directly and rapidly biodegradable fraction (69.50%) consists of organic matter, paper/cardboard and herbs.

• The combustible and slowly biodegradable fraction (5.20%) includes solid organic matter such as wood chips, leather and plastics.

• The inert and non-valorizable fraction (5.80%) is composed of pebbles, stones, ceramics, sand and metals.

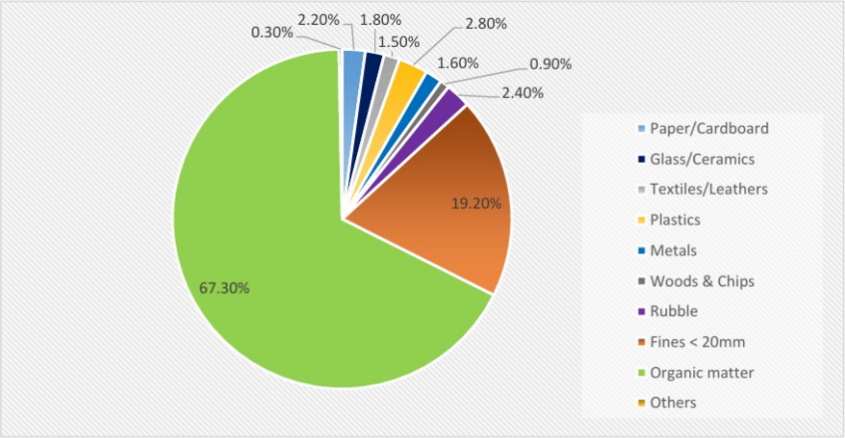

Figure 2. Average composition of MSW in Cameroon (Source: Ref. [5]).

As per the 2020 World Bank World Development Indicators, Cameroon's total population stood at 26545864 people with an urban population of 57.56%. The country's per capita MSW generation as of 2018 stood at 0.42 kg/person/day [30]. According to Cameroon's main waste collection company, HYSACAM, it collects about 5000 tons of waste per day for over 15 million people [31]. This is about 45.5% of the estimated 11000 tons generated daily throughout the country as per the daily generation rate of 0.42 kg/day*person. Assuming that the national per capita waste generation level remained fairly the same between 2018 and 2020 and using 18.47 MJ/kg as LHV of MSW, the energy potential of MSW generated in Cameroon for 2020 can be calculated using Eq (4):

$$MSW_{SE(i)} = 365\ [(N*Q*\mathcal{E})\ *\ (Q_{OR}*LHV)] \quad (4)$$

where MSWSE(i) is the gross municipal solid waste solid energy potential in MJ/year, N is the total population, Q is the quantity of waste generated per capita per day for a household, QOR is the fraction of the rapidly and slowly degradable organic waste content, Ɛ is the waste collection efficiency, LHV is the lower heating value of the MSW, and product N*Q*E is the quantity of organic waste collected.

The energy potential of landfills can be exploited through the capture of the biogas produced for cooking fuels, combustion engines and electricity generation. It is important to predict the rate and volume of biogas production for the feasibility of energy generation projects [17]. As such, the amount of waste collected and its level of biodegradability are very important. As seen in Figure 2, the rapidly degradable

(organic matter and paper/cardboard) and slowly degradable (textiles/leathers, plastics, wood and chips) portions of Cameroon's MSW are 69.5% and 5.2%, respectively.

To calculate the methane production potential and rate in this study, it is assumed that the landfills are engineered for biogas recovery. The Ref. [17] methodology was used with slight modifications, while the Ref. [16] approach (which estimates the potential for 3 scenarios: minimum, average and maximum) was applied to account for result uncertainty. The minimum, maximum and average biogas production factors (Table 2) were generated from [32] for moderate and rapidly degradable organic waste.

Table 2. Suggested values for methane production potential*.

MSW type	CH4 production factor (m^3/t of waste)		
	Minimum value	Average value	Maximum value
Relatively inert	5	15	25
Moderately degradable	140	170	200
Highly degradable	225	262.5	300

*Source: Ref. (17,32].

For the landfill collection efficiency, the arithmetic mean of 55.5% used by [17] was considered. The gross methane production was computed using Eq (5) below:

$$Q_{CH4} = \frac{fL * fLF * MMSW * \mathcal{E}gas}{1000} \quad (5)$$

where QCH4 is the methane production potential as m3 per year, fL is the biogas production factor (m3/tonne) of MSW, fLF is the fraction of MSW sent to landfills, Ɛ gas is the landfill gas collection efficiency, MMSW is the organic fraction (rapidly degradable and moderately degradable), and 1000 = factor for unit adjustment.

The energy potential of the generated methane can be calculated using Eq (6):

$$E_{CH4} = Q_{CH4} * LHV_{CH4} \quad (6)$$

where LHV_{CH4} is the lower heating value of methane = 35.5 MJ/m^3 [33].

The captured methane can be purified for various energy uses like electricity production, which can be calculated using the following equation [33]:

$$E_{M(i)} = \frac{M_{T(i)} * P_{eff} * LHV_{CH4} * CF}{3.6 \times 10^6} \quad (7)$$

where $E_{M(i)}$ is the annual electrical energy production potential (GWh/year), $M_{T(i)}$ is the total methane to be produced annually in the landfills (m^3/year), P_{eff} is the efficiency of the internal combustion engines (typically 35% for such systems [33], LHVCH4 is the lower heating value for methane, 35.5 MJ/m3, CF capacity factor of the plant is 0.8 [17], and 3.6 × 106 is the factor unit conversion. Given the need to meet carbon emission reduction targets, it will be of interest to many countries and investors to know how much carbon dioxide emissions are avoided using any renewable energy source. Avoidable equivalent CO2 refers to the amount of methane that could have been released into the atmosphere in CO2 equivalents, if the gas had not been captured [33]. This amount can be calculated for methane using its global warming potential (GWP) with respect to CO2. Methane being 25 times more potent than CO2 as a greenhouse gas implies the ratio can be given as 25 kgCO2/kgCH4 [34] was used and with a density

of 0.716 kg/m3 [35], the mass of methane can be computed.

3. Results and discussion

3.1. Energy potential of agricultural crop residues in Cameroon

Table 3 shows the estimated quantities of selected crop residues produced in Cameroon in 2020 and their corresponding energy potentials. The selected crops are the country's main subsistence and cash crops in terms of production quantities and can be generally found throughout the country. Also, the availability of data for these crops made them suitable for this study. From this table, it can be seen that the annual estimated bioenergy potential of agricultural residues available for energy purposes is about 580 PJ/y. Furthermore, this table shows that the crop residues with the highest energy potential are plantains, palm oil, maize, sorghum and cassava with estimated energy potentials of 183 PJ/y,80 PJ/y, 71 PJ/y, 37 PJ/y and 32 PJ/y, respectively. The high energy contents of these crops can be attributed to their high production quantities, residue-to-product ratios and heating values of their residues.

Table 3. Energy potential of agricultural crop residues.

Crop	Surplus Residue (tonnes)	Energy Potential (PJ/year)
Maize	4335188.20	70.540
Rice	457502.19	4.300
Sorghum	2916904.80	37.170
Millet	273264.30	3.900
Wheat	181.22	0.002
Cassava	3037592.47	33.010
Cocoyam	290439.36	3.080
Sweet potato	249483.84	2.650
Yam	113212.16	1.200
Potatoes	212642.40	2.260
Groundnuts	1388500.00	23.930
Palm oil	8532832.46	89.970
Coconuts	8687.25	0.130
Beans	1066192.50	13.200
Soybean	70842.96	1.280
Banana	7500450.00	88.940

Crop	Surplus Residue (tonnes)	Energy Potential (PJ/year)
Plantain	16556360.40	183.890
Sugar Cane	632022.34	7.060
Coffee	36207.00	0.460
Cocoa	290000.00	4.490
Cotton	516600.00	8.210
Total	48485105.853	579.672

3.2. Energy potential of MSW resources in Cameroon.

Deducing from Eq (4), approximately 4.07 million tonnes of MSW were generated in Cameroon in 2020 with about 1.85 million tonnes collected. The energy potential of the collected waste amounts to about 25.5 PJ. On the other hand, the methane production potential of MSW collected and landfilled computed from Eq (5) gives an average yield of about 88.64 million m3 of methane per year, corresponding to 3.15 PJ worth of energy for just over 45% of MSW collected (see Table 4). This is a significant amount of energy potential which could be used to feed the country's demand for clean electricity, heating or cooking energy sources.

Table 4. Methane and energy potential of MSW in Cameroon.

MSW type	Biogas production potential (million m^3/t/y)			Energy Potential (PJ/y)		
	Minimum value	Average value	Maximum value	Minimum value	Average value	Maximum value
Moderately degradable	3.0	4.10	4.82	0.12	0.15	0.17
Highly degradable	70.0	84.54	96.61	2.57	3.0	3.43
Total	73.0	88.64	101.43	2.69	3.15	3.6

Deducing from Eq (7) the methane generated from landfills in Cameroon has an electricity generation potential of 0.24 GWh/year, which could add significantly to the country's electricity generation potential from biofuels, which stood at 41.0 GWh in 2019 [3]. Using the proposed methodology above to determine the amount of avoided carbon dioxide emissions, it can be estimated that the captured methane in Cameroon's landfills can save up to about 1.6 billion kgs of CO2 from entering the atmosphere, hence mitigating its global warming and consequent climate change effects.

3.3. General discussions

From the calculations, the total annual energy potential of both crop residues and collected MSW is about 606 PJ y-1. The approximately 580 PJ energy potential of crop residues is significantly greater than the 251.3 TJ energy potential in 2012 of Ref. [5]. This can be attributed to the increase in crop productivity of the selected crops over the years, which stood at about 18 million tons in 2012 compared to 57 million tons in 2020 [6]. Furthermore, the energy potential of major food and cash crops like maize, sorghum, rice, millet, wheat, sugarcane, cocoa, coconut and coffee considered in [2] gives a significantly lower energy potential of about 2.46 PJ as compared to the 128 PJ in this study.

This significant difference is also due to increased productivity over time and because their analysis was based on the energy potential of the bone-dry residue.

From Table 5, about 37 million tons of bone-dry crop residues were available for biofuel or electricity production in 2020. These residues had the potential of producing between 4.13–11.23 billion liters of

bioethanol which could be used to offset gasoline consumption in Cameroon. Using the estimation methodology used by [2], this quantity of bioethanol is more than 5 times Cameroon's total gasoline consumption of 8.74 thousand barrels per day in 2018 [36]. Alternatively, it could also yield between 2.81 to 7.51 billion liters per year of biodiesel which could be used in reducing the demand for petroleum diesel consumption. On the electricity generation side, crop residues could generate between 24.35 and 64.92 TWh of electricity, which is 3.67 to 9.83 times the entire country's electricity consumption, of 6.6 TWh in 2019 [3].

Table 5. Electricity, bioethanol and biodiesel production potential from crop residues.

Average Moisture Content (%)	Surplus residue (Bone-dry tons)	Total Energy Potential (GJ)	Electricity potential (GJ *0.28* Efficiency)		Bioethanol potential		Biodiesel potential	
			15% efficiency TWh (Low)	40% efficiency TWh (High)	(Low) liters	(High) liters	(Low) liters	(High) liters
22.6	37.53E+06	579.66E+06	24.35	64.92	4.13E+09	11.23E+09	2.81E+09	7.51E+09

At an annual population growth rate of 2.6% [37], Cameroon could have a population of around 33 million people by 2030, with a 62 percent urbanization rate [38]. Economic expansion and rapid urbanization are expected to follow this population increase marked by increased energy demand for biomass and an equivalent increase in MSW generation. The 1.6 billion kgs of CO_2 that could potentially be captured in landfills through biogas recovery shows that uncontrolled disposal sites can be a major source of Greenhouse Gases (GHG) in Cameroon. The Ref. [39] report predicts that about 8–10% of global anthropogenic GHG emissions by 2025 will come from the waste sector, particularly food waste. This may present a major challenge to governments if this growth is not matched with adequate planning of energy security projects and proper waste management. In contrast, this presents a huge market for resource recovery and cheap energy generation. The development and integration of renewable energy from crop residues and MSW can provide sustainable solutions to the energy demands which could double in the next decade. Energy from these sources will not only satisfy energy needs but also help in clearing the streets from unwanted garbage and contribute to the waste management efforts of the government and, in general, foster its transition into a circular economy. Also, energy generation from crop residues and MSW takes away the question of food-vs-fuel that usually comes with the generation of bioenergy using edible food crops. The crop residues of plantain, palm oil, maize, sorghum and cassava are the most energy-intensive crops in Cameroon and should be priority crops for energy generation investments.

Despite all these advantages, there are challenges to the wide-scale development of bioenergy

technology in Cameroon. Ref. [5] raise concern over the sustainability of supply, environmental impacts and difficulties with the collection, transportation and storage. In addition, most of these wastes are not sorted at the source, and there is a social stigma around MSW waste collection and sorting. Not up to half of MSW generated is collected and landfilled, with the rest being emptied into waterways and streams. There is also a lack of spatial geographical information system (GIS) data on the crop production level per region of Cameroon, and this makes it challenging to situate areas for potential research and investment. If proper waste-to-energy techniques are set up, the integration of biomass energy in the country's energy mix will be accelerated.

4. Conclusions

In this study, the energy potentials of agricultural residues and MSW in Cameroon are calculated and estimated at roughly 580 PJ and 26 PJ, respectively, in 2020. This is an enormous amount of energy potential which is not sufficiently utilized and, in most cases, utilized traditionally and unsustainably. These crop and MSW resources could be harnessed to provide electricity for off-grid communities and also used to replace fossil-based transportation fuels and cooking gas through bioethanol and biodiesel production.

However, there are not sufficient policies to create the demand or promote technological development for modern biofuels in order to reduce the country's dependence on expensive fossil fuel options. This has slowed the integration of alternative energy sources and consequently its climate change mitigation and adaptation efforts. These policies cannot be put in place without the availability of sufficient and accurate data on national energy demand and supply potential. In that light, there is a need for ground research and geospatial analysis of the country's crop residue potential and waste generation hotspots so that concrete policies and plans can be drawn from realistic estimates and not guesstimates. Furthermore, Cameroon's waste management needs to be improved holistically, with biogas recovery at landfill sites developed, with sorting at source encouraged, and waste collection coverage expanded to vulnerable and remote communities. There is also a lack of accurate and updated data on the quantity of landfilled waste and the per capita waste generation in various cities and nationally.

In all, biomass and MSW are key resources which, if developed sustainably, will enable the country to be energy secure and self-sufficient, while achieving its emission reduction targets without compromising on its socio-economic development goals and fight against poverty.

Acknowledgments

The authors appreciate the support from the Faculty of Environmental Sciences and Natural Resources Management, Norwegian University of Life Sciences, Ås, Norway.

Conflict of interest

The authors declare no conflict of interest.

References

1. Kidmo DK, Deli K, Bogno B (2021) Status of renewable energy in Cameroon. Renewable Energy Environ Sustainability 6: 2. https://doi.org/10.1051/rees/2021001

2.Ackom EK, Alemagi D, Ackom NB, et al. (2013) Modern bioenergy from agricultural and forestry residues in Cameroon: Potential, challenges and the way forward. Energy Policy 63: 101113. https://doi.org/10.1016/j.enpol.2013.09.006

3.IEA—Cameroon Key energy statistics, 2019. https://www.iea.org/countries/cameroon (Accessed: 22 April 2022).

5.Kemausuor F, Kamp A, Thomsen ST, et al. (2014) Assessment of biomass residue availability and bioenergy yields in Ghana. Resou Conser Recycl 86: 28–37. https://doi.org/10.1016/j.resconrec.2014.01.007

5.Mboumboue E, Njomo D (2018) Biomass resources assessment and bioenergy generation for a clean and sustainable development in Cameroon. Biomass Bioenergy 118: 16–23. https://doi.org/10.1016/j.biombioe.2018.08.002

6.FAO (2022) FAOSTAT, 2020. Available from: https://www.fao.org/faostat/en/#data/QCL (Accessed: 22 April 2022).

7.Islam MK, Khatun MS, Arefin MA, et al. (2021) Waste to energy: An experimental study of utilizing the agricultural residue, MSW, and e-waste available in Bangladesh for pyrolysis conversion. Heliyon 7: e08530. https://doi.org/10.1016/j.heliyon.2021.e08530

8.World Bank World Bank (2022) Trends in Solid Waste Management. Available from: https://datatopics.worldbank.org/what-a-waste/trends_in_solid_waste_management.html (Accessed on 06. May 2022).

9.IEA (2003) Municipal Solid Waste and its Role in Sustainability A Position Paper Prepared by IEA Bioenergy.

10. Mermoz S, Le Toan T, Villard L, et al. (2014) Biomass assessment in the Cameroon savanna using ALOS PALSAR data. Remote Sen Environ 155: 109–119. https://doi.org/10.1016/j.rse.2014.01.029

11. Alain Christian B, Yılancı A (2019) Feasibility study of Biomass power plant fired with maize and sorghum stalk in the Sub-Saharan region: the case of the northern part of Cameroon. Eur Mech Sci 3: 102–111. https://doi.org/10.26701/ems.493188

12. Kamdem I, Tomekpe K, Thonart P (2011) B A Production potentielle de bioéthanol, de biométhane et de pellets à partir des déchets de biomasse lignocellulosique du bananier (Musa spp.) au Cameroun.

Biotechnol Agron Soc Environ 15: 471–483. Available from: https://www.cia.gov/library/publications/the-world-ctbook/geos/CM.html (Accessed: December 2022).

13. Scarlat N, Motola V, Dallemand JF, et al. (2015) Evaluation of energy potential of Municipal Solid Waste from African urban areas. Renewable Sustainable Energy Rev 50: 1269–1286. https://doi.org/10.1016/j.rser.2015.05.067

14. Okello C, Pindozzi S, Faugno S, et al. (2013) Bioenergy potential of agricultural and forest residues Uganda. Biomass Bioenergy 56: 515–525. https://doi.org/10.1016/j.biombioe.2013.06.003

15. Gabisa EW, Gheewala SH (2018) Potential of bio-energy production in Ethiopia based on available biomass residues. Biomass https://doi.org/10.1016/j.biombioe.2018.02.009 Bioenergy 111: 77–87.

16. Moreda IL (2016) The potential of biogas production in Uruguay. Renewable Sustainable Energy Rev 54: 1580–1591. https://doi.org/10.1016/j.rser.2015.10.099

17. Silva dos Santos IF, Vieira NDB, de Nóbrega LGB, et al. (2018) Assessment of potential biogas production from multiple organic wastes in Brazil: Impact on energy generation, use, and emissions abatement. Resour Conserv Recycl https://doi.org/10.1016/j.resconrec.2017.12.012 131: 54–63.

18. Hiloidhar M, Das D, Baruah DC (2014) Bioenergy potential from crop residue biomass in India. Renewable Sustainable Energy Rev 32: 504–512. https://doi.org/10.1016/j.rser.2014.01.025

19. Shane A, Gheewala SH, Fungtammasan B, et al. (2016) Bioenergy resource assessment for Zambia. Renewable Sustainable https://doi.org/10.1016/j.rser.2015.08.045 Energy Rev 53: 93–104.

20. Jekayinfa SO, Scholz V (2009) Potential availability of energetically usable crop residues in Nigeria. Energy Sources, Part A: Recovery, Util, Environ Effects 31: 687–697. https://doi.org/10.1080/15567030701750549

21. Koopmans A, Koppenjan J (1998) The Resource Base. Reg Consult Mod Appl Biomass Energy, 6–10.

22. San V, Ly D, Check NI (2013) Assessment of sustainable energy potential on non-plantation biomass resources in Sameakki Meanchey district in Kampong Chhnan pronice, Cambonia. Int J Environ Rural Dev 4: 173–178.

23. Yang J, Wang X, Ma H, et al. (2014) Potential usage, vertical value chain and challenge of biomass resource: Evidence from China's crop residues. Appl Energy 114: 717–723. https://doi.org/10.1016/j.apenergy.2013.10.019

24. Patiño FGB, Araque JA, Kafarov DV (2016) Assessment of the energy potential of agricultural residues in non-interconnected zones of Colombia: Case study of Chocó and Putumayo katherine Rodríguez cáceres. Chem Eng Trans 50: 349–354. https://doi.org/10.3303/CET1650059

25. Milbrandt A (2011) Assessment of biomass resources in Liberia. Liberia: Dev Resour, 117–166.

26. Pradhan D (2018) Environment and rural development. Bibechana 2: 17–20. https://doi.org/10.3126/bibechana.v2i0.19230

27. Mendu V, Shearin T, Campbell JE, et al. (2012) Global bioenergy potential from high-lignin agricultural residue. PNAS 109: 4014–4019. https://doi.org/10.1073/pnas.1112757109

28. UN Habitat (2021) Waste Wise Cities Tool (WaCT), 78. Available from: https://unhabitat.org/wwc-tool.

29. Kawai K, Tasaki T (2015) Revisiting estimates of municipal solid waste generation per capita and their reliability. J Material Cycles Waste Manage 18: 1–13. https://doi.org/10.1007/S10163-0150355-1

30. Kaza S, et al. (2018) What a waste 2.0: A Global snapshot of solid waste management to 2050. [Preprint]. https://doi.org/10.1596/978-1-4648-1329-0

31. HYSACAM (no date) Chiffres clés|Hysacam. Available from: https://www.hysacamproprete.com/fr/node/17 (Accessed: 3 May 2022).

32. The World Bank (2004) Handbook for the Preparation of Landfill Gas to Energy Projects in Latin America the Caribbean, 236. Available from: https://www.esmap.org/sites/esmap.org/files/Handbook_Preparation_LandfillGas_to_EnergyProjects_LAC_Resized.pdf.

33. Arthur R, Baidoo MF, Osei G, et al. (2020) Evaluation of potential feedstocks for sustainable biogas production in Ghana: Quantification, energy generation, and CO2 abatement. Cogent Environ Sci 6. https://doi.org/10.1080/23311843.2020.1868162

34. Ryu C (2010) Potential of municipal solid waste for renewable energy production and reduction of greenhouse gas emissions in South Korea. J Air Waste Manage Assoc 60: 176–183. https://doi.org/10.3155/1047-3289.60.2.176

35. UNFCCC (2003) Methane density. Gautam Dutt, MGM International, 2003, 7157.

36. Cameroon Gasoline consumption—data, chart|TheGlobalEconomy.com (no date). Available from: https://www.theglobaleconomy.com/Cameroon/gasoline_consumption/ (Accessed: 13 June 2022).

37. World Bank (2020) Trends in Solid Waste Management. The World Bank, 1. Available from: https://datatopics.worldbank.org/what-a-waste/trends_in_solid_waste_management.html (Accessed: 22 April 2022).

38. UNECA (2018) Urbanization and National Development Planning in Africa. 39. UN Habitat (2021) Waste Wise Cities Tool (WaCT), 78. Available from: https://unhabitat.org/wwc-tool.

Performance evaluation of solar still integrated with thermoelectric heat pump system

Fouad Alkilani*, Ouassini Nemraoui and Fareed Ismail
Mechanical Engineering Department, Cape Peninsula University of Technology (CPUT), Cape Town, South Africa

ABSTRACT

This research presents a method for improving a conventional solar still to produce potable water during adverse conditions where there is low or no solar radiation. Summer and winter conditions in the Western Cape province of South Africa were considered. A comparative experimental study was conducted between a conventional solar still and the developed solar still. The developed solar still incorporated a photovoltaic powered thermoelectric heat pump. The purpose of the thermoelectric (TE) heat pump was to accelerate convection inside the developed solar still assembly. The coefficient of performance (COP) of the thermoelectric heat pump installed in the developed solar still ranged from 0.4 to 1.9 at an input current of 5 A. The results indicated that the developed solar still was able to produce 2300 mL per day of drinkable water during a good day in the winter, but the conventional solar still was only able to produce 650 mL per day. The developed solar still produced 2180 mL per day, whereas the ordinary solar still produced 1050 mL per day, during a mild summer day. The developed still had an accumulated water production of 1180 mL during a night with mild temperatures. This significant improvement in yield of the developed solar still system is due to the change in temperature difference between the glazing and the water surface within the developed solar still. This is a significant contribution to the technology of solar water purification.

Keywords: *solar distillation; solar still; thermoelectric heat pump*

1. Introduction

Water treatment refers to the processing of water to achieve a water quality that meets specified standards set by consumers, communities and organizations through regulatory agencies [1]. Water treatment can be classified into three main methods: chemical, physical and energy-intensive methods [2]. Desalination is the most used approach to produce clean water for drinking, irrigation and industrial purposes. Desalination technologies can be classified into two main categories based on the phase change of the treated water: mechanical and thermal desalination [3]. The first category is desalination without phase change (membrane-based), including reverse osmosis (RO), Nanofiltration (NF) and Electro-dialysis (ED). The second category is desalination that utilizes thermal energy to produce fresh water by evaporation and condensation, including multi-stage flash (MSF), multi effect distillation (MED), vapor compression distillation (VCD), vacuum distillation (VD) and solar distillation (SD) [4,5]. Desalination technologies have become a viable solution for water supply in many coastal countries that have limited natural freshwater resources [6]. A new survey shows that more than 15,900 desalination plants are currently operational, most of them located in the Middle East and North Africa [7]. One of the disadvantages of centralized desalination plants is the intensive energy required to

operate the large scale units and to transport the water to the consumers [8]. Moreover, there are negative environmental impacts due to burning fossil fuels, brine disposal and the capital investment cost [9].

Solar distillation is categorized into two main categories: direct solar distillation and indirect solar distillation. In the first category, solar energy is used directly to carry out the evaporation process via devices called solar stills. Meanwhile, in the second category, a solar collector (thermal/photovoltaic) is used as an auxiliary device to provide thermal energy or generate electrical energy to run the distillation unit [10,11]. Direct solar water distillation is similar to the natural hydrological phenomenon of the water cycle; the difference is that solar water distillation is a controlled process (closed-loop system) while the natural water cycle is an open-loop system [12]. Solar distillation technologies are considered a promising alternative over the conventional desalination processes. They have many advantages, such as cost-effectiveness, environmental friendliness and suitability for remote areas where a large-scale desalination facility is not appropriate [13]. However, solar distillation technologies have not been widely used due to the low productivity of potable water. There are two reasons for the low productivity of solar distillation processes. First, the solar still has considerable thermal inertia because of the high specific heat capacity of the contaminated water; and second, there is difficulty in latent heat rejection of the condensation to the ambient [14].

Therefore, several research studies have been conducted to improve the performance of solar stills. Mohamed et al. [15] investigated the performance of a single-effect solar still equipped with fine stones as a porous absorber with different particle sizes. The results showed that the daily water yield of the solar still increased by 19.8, 27.8 and 33.3% when they used fine stones size of 1 cm, 1.5 cm and 2 cm, respectively. Bataineh and Abo Abbas [16] examined the effect of using both internal reflectors and fins on the performance of a single-slope solar still. They found that the effectiveness of solar stills is improved by installing internal reflectors on three of their sides. The efficiency increased by 36 and 47% in January and December, respectively. Porta-Gándara et al. [17] investigated the increase in water output of a 1.7 m2 single-slope solar still equipped with a perturbation device. Through this apparatus, air bubbles are injected into the water basin, which results in ripples on the water's surface. This results in an increase in the overall evaporative surface area and stimulates the mass transfer coefficient. The results showed that on a sunny day, the daily distillation production was 6.1 kg in a semi-desert region of La Paz, Mexico. Jani and Modi [18] examined the impact of cavity fins on the performance of a double slope solar still. The results indicated that the optimal water depth for desalination was 1 cm and that circular fins performed better than fins with a rectangular cross-section. The maximum water yield produced from the circular finned solar still was 1.49 kg/m2-day, while the square finned solar still produced 0.96 kg/m2-day. Kabeel and Abdelgaied [19] studied the performance of pyramidal solar still equipped with graphite absorber plate that had a high thermal conductivity as well as cooling of the condensation surface. The results indicated that combining the two methods could increase distillation

efficiency by 97.2–98.9% compared with a conventional pyramid still. Esfe et al. [20] presented a mathematical model to study the effect of the dimensions of a solar still equipped with thermoelectric system. The obtained results showed that the water yield improved by 6.8% compared to the conventional solar still. Esfe and Toghraie [21] introduced a numerical method to investigate the performance of a solar still with thermoelectric cooling system. The results showed that the use of the thermoelectric cooling system improved the daily water yield by 62% under the weather of Semnan province of Iran. Sheikholeslami et al. [22] introduced numerical simulation for thermal analysis of a parabolic solar collector with wavy absorber pipe and nanofluid. The results showed a 180% improvement in heat transfer coefficient. In addition, the performance and categorization of solar stills based on design guidelines, efficiencies and productivity were investigated by [14,23–28].

As noted in the literature review, most of these related studies on solar still performance enhancement focused on the productivity improvement by changing the design, structure or operation parameters. These kinds of improvements may work on ideal days (sunny, warm days). Note that, however, solar still systems still show poor performance on cloudy and partly cloudy days. Moreover, during hot days, the pure water yield decreases due to the low water-cover temperature difference. With this research gap identified, this work has therefore been undertaken to effectively improve the efficiency of a conventional solar still by employing a thermal energy backup system. A solar photovoltaic powered thermoelectric heat pump system is designed and integrated with the conventional solar still. Seasonal performance of the advanced solar still is reported in the research work herein with respect to the overall energy efficiency. The article is organized as follows: A literature review with focus on the water crisis and the attempted solutions is presented. Then, the principle of a solar still with emphasis on the developed solar still is presented, followed by practical designs and implementations of the developed and conventional solar stills. The experimental results are analyzed and compared, with the conventional solar still as the reference. Important findings are noted, concluding remarks are made, and recommendations are made for further studies.

2. Overview of the thermoelectric heat pump system

The thermoelectric phenomenon is the conversion of thermal energy into electrical energy or vice versa [29]. The conversion of electric energy into a temperature gradient is called the Peltier effect, while the reverse phenomenon is called the Seebeck effect [30]. Since the advent of semiconductor materials, thermoelectric devices (TEC/TEG) have become widely used in many fields, such as building ventilation and air conditioning [31], the automotive industry [32], waste heat recovery [33] electronic equipment cooling [34].

As a solid state heat pump, thermoelectric devices have many advantages over conventional heat pump systems, such as compact size, no moving parts, environmental friendliness due to the lack of use of

refrigerants and fast convenient heating and cooling sustainability. The coefficient of performance of thermoelectric heat pumps is relatively low compared with conventional systems. The trend of low performance is mainly caused by the poor heat conversion efficiency of the semiconductor materials, which is reflected by the figure of merit (ZT) value [35]. The value of figure of merit can be derived from Eq (1).

$$ZT = \frac{\alpha^2 \sigma}{k} T \quad (1)$$

where α is the Seebeck coefficient (VK^{-1}), σ is the electrical conductivity (S/m), k is the thermal conductivity (W/K), and T is the absolute temperature. The coefficient of performance (COP) of the thermoelectric heat pump can be defined as in Eq (2).

$$COP = Q_h/(Q_h - Q_c) \quad (2)$$

$$Q_h = \alpha_m I T_h - K_m(T_h - T_c) + \frac{1}{2} R_m I^2 \quad (3)$$

$$Q_c = \alpha_m I T_c - K_m(T_h - T_c) - \frac{1}{2} R_m I^2 \quad (4)$$

where Q_h is the flow of heat to the heat sink (heating capacity), Q_c is the flow of heat from the heat source (cooling capacity), I is the applied current, T_h is the temperature of the hot side of the module, T_c is the temperature of the cold side of the module, and R_m is the electric resistance. The properties α, σ and k are essential to determine the performance of thermoelectric materials. The specifications of the modules used in this research are listed in Table 1.

Table 1. TEC1-12706 specifications.

Type	I_{max}	V_{max}	Couples *(N)*	QC_{max} (W)	DT_{max} (°C)	*R* (Ω)	*K* (W/K)	P_{max} (kg/cm^2)	Dimensions (mm)
TEC1-12706	6	15	127	65	70–80	1.53	0.5	10.8	40*40*4

3. Materials and methods

Figure 1 shows a photograph of the experimental apparatus of the developed solar still proposed in this research, which basically consists of a single-effect basin type solar still integrated with a thermoelectric heat pump system. The basin section is made of 0.5 m2 aluminum sheet. A polystyrene board with a thickness of 15 mm was used as a thermal insulator. It is sandwiched between the aluminum sheets of each side of the solar still. The basin liner was coated in black using waterproof and high heat resistant paint to maximize solar energy absorptivity. A polycarbonate sheet with a thickness of 1 mm was used to cover the basin. Thermal silicon was used to seal the edges. The thermoelectric heat pump system section consists of six TEC modules, two water-cooled heat sinks, two 10 W DC water pumps, circuit controls and a plumbing system. The heat sinks are made of aluminum tanks. Thermal grease was applied to attach the thermoelectric modules to the heat sinks. Insulation cotton washers designed specifically for THC application were used to prevent moisture formation around and inside the TE module. Typical

fasteners were used to mount the arrangement, and 15 kg/cm2 is the recommended tension to maintain proper contact with the TE heat sinks assembly. The cold side of the heat pump was connected to the cold water inlet of the condensation surface, while the hot side was connected to the heat exchanger routed inside the basin. A PV system consisting of a 270 W PV panel, circuit breaker, 20 A pulse width modulation (PWM) charge controller and 200 Ah deep cycle battery was used to power the thermoelectric heat pump system.

Figure 1. Pictorial view of the experiment apparatus.

The experiment was conducted outdoors to evaluate the system performance under different weather conditions. Its site is located at 33.92° S, 18.4° E. Elevation was about 68.5 m above sea level. The selected tilt angle of both collectors (PV & still cover) was about 35.5°. In addition, an identical conventional solar still was used for comparison with the developed one. A set of thermocouples was used to measure the temperature of the water inside the basin, the condensation surface and other components of the TE heat pump system. Figure 2 shows a schematic diagram of the developed solar still and the positions of the thermocouples. A data logger meteorological station equipped with two pyranometers and an anemometer was used to record the incident solar radiation and wind velocity.

The basins in both stills were filled with 10 L of seawater. The desirable water depth is about 20–30 mm [36]. For the developed solar still, it is crucial to keep the heat exchanger always submerged.

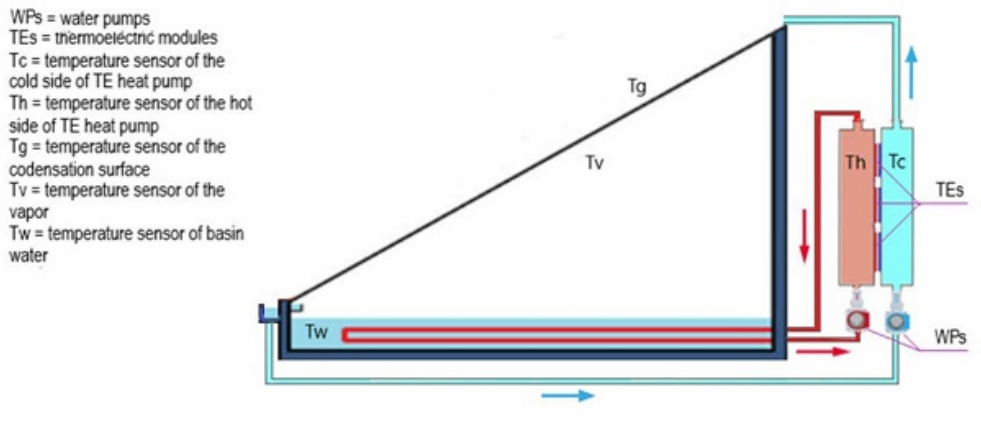

Figure 2. Schematic diagram of the developed solar still.

4. Results and discussion

This section presents and discusses the experimental results of the outdoor experimental test conducted to evaluate the performance of the conventional single-effect solar still integrated with thermoelectric heat pump system. A comparison between the conventional solar still and the developed solar still is discussed from a thermodynamic point of view.

4.1. The meteorological conditions of the test location

During the experimentation period, the weather conditions of the location of the experiment were monitored using a weather station mounted at the top of the university's mechanical engineering building. Samples of the weather conditions over the course of the testing period are illustrated in Figures 3,4. During a typical summer day, the ambient temperature can reach up to 35 °C, while on a winter day, the ambient temperature average is around 15 °C. The wind speed has seasonal dependence, and it ranges between 0.5 and 14.7 m/s.

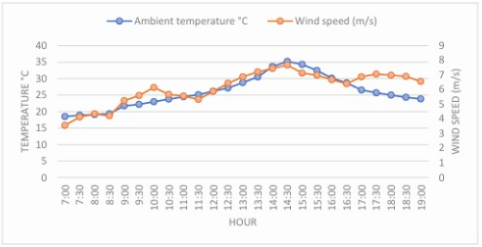

Figure 3. The variation of wind speed and ambient temperature during a typical summer day (2021).

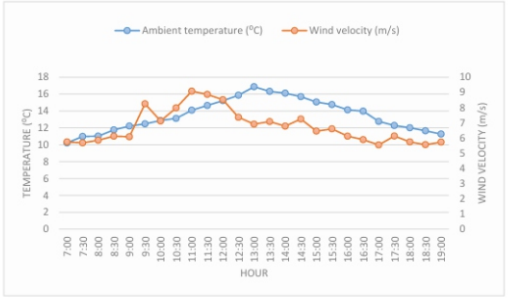

Figure 4. The variation of wind speed and ambient temperature during a typical winter day (2021).

Figure 5 shows the variation of the computed incident solar radiation on the solar collectors (PV and solar still). The value of the solar radiation on the tilted surface was calculated by using the Perez formula (Eq 5).

$$I_T = I_b R_b + I_d \left[(1 - f_1)\left(\frac{1+\cos\beta}{2}\right) + F_1 \frac{a}{b} + F_2 \sin\beta\right] + I_h \rho_g \left(\frac{1-\cos\beta}{2}\right) \quad (5)$$

As shown in the graphs, the maximum solar radiation recorded during a week of the experimental test in May 2021 was 827 W/m^2. Day 5 shows a fluctuation in incident solar radiation due to a partly cloudy sky.

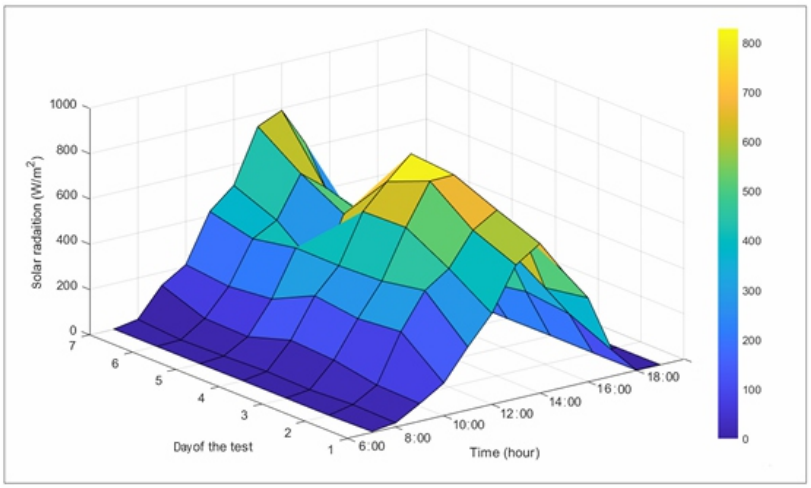

Figure 5. The variation of incident solar radiation in May 2021.

Figure 6 shows the trend of the incident solar radiation in the early days of September 2021, and the maximum value of the computed solar radiation during six experimental days was 680 W/m2. On a mostly cloudy day, the maximum value was 135 W/m2.

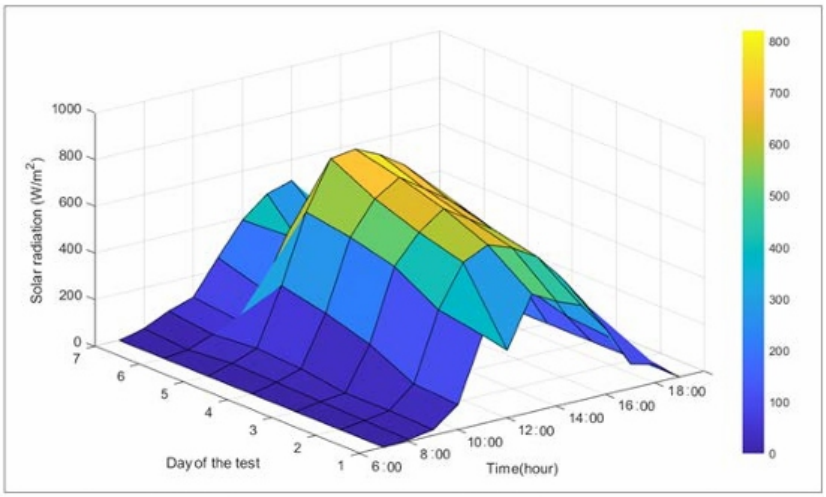

Figure 6. The variation of incident solar radiation in September 2021.

4.2. The developed and conventional solar stills' performances

The water to water thermoelectric heat pump consists of 6 TEC-12706 modules integrated into a single-effect solar still to enhance the daily potable water productivity. An identical conventional solar still was used as a reference to evaluate the performance. The stills were operated simultaneously side by side. The temperatures of both solar stills' components were monitored. Herein, Tw represents basin water temperature, Tv represents vapor temperature, Tg represents condensation surface temperature, and Ta represents ambient temperature.

The distillate yields of both stills were recorded. Also, the effect of the temperature difference between the cold and hot sides of the module on the coefficient of performance (COP) of the thermoelectric heat pump system was investigated.

Figure 7 presents the temperature trend of the developed solar still's components. The ambient temperature recorded at the start of the experiment was 17 °C, and it then increased to 26 °C at midday. The initial temperature of the water basin was 16 °C, and it then increased to 45 °C within 4 hours. At midday, the basin water temperature reached 60 °C. It stayed above 50 °C till 17:00 and then decreased to 49 °C at the end of the experiment. The sharp increase in basin water temperature was due to the input heat delivered from the TE heat pump system. The vapor temperature had the same trend as the basin water temperature. It reached 54 °C at midday. The temperature difference between the water basin and the condensation surfaces is the key aspect of the solar still. It stayed above 20 °C. The highest value recorded was 32 °C.

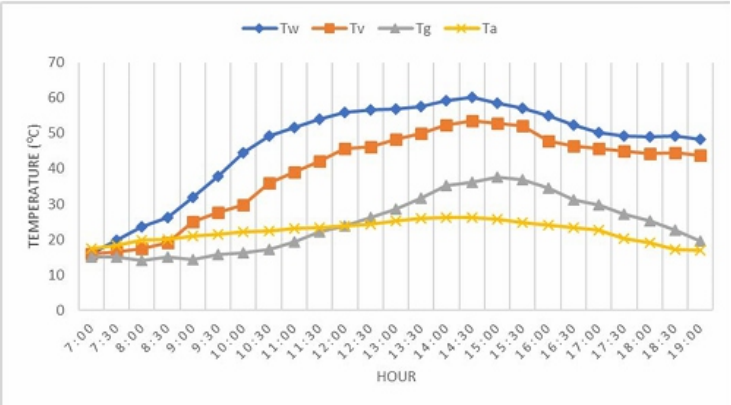

Figure 7. The temperature trend of the developed solar still.

Figure 8 presents the temperature trend of the conventional solar still. The ambient temperature recorded at the start of the experiment was 17 °C, and then increased to 26 °C at midday. At the end of the experiment, the ambient temperature decreased to 18 °C. The initial temperature of the water basin was 16 °C, and within 3.5 hours, it reached 26 °C. There was a linear increase in the water basin temperature until midday, after which a linear decreasing tendency was noticed. The maximum basin temperature recorded was 53 °C. The vapor temperature had similar behavior as the water basin temperature. It

reached 49 °C at midday. The condensation surface temperature increased with the increase of the vapor temperature. The maximum value recorded was 41 °C at midday. The temperature difference between the water basin and the condensation surfaces varied between 4 and 14 °C.

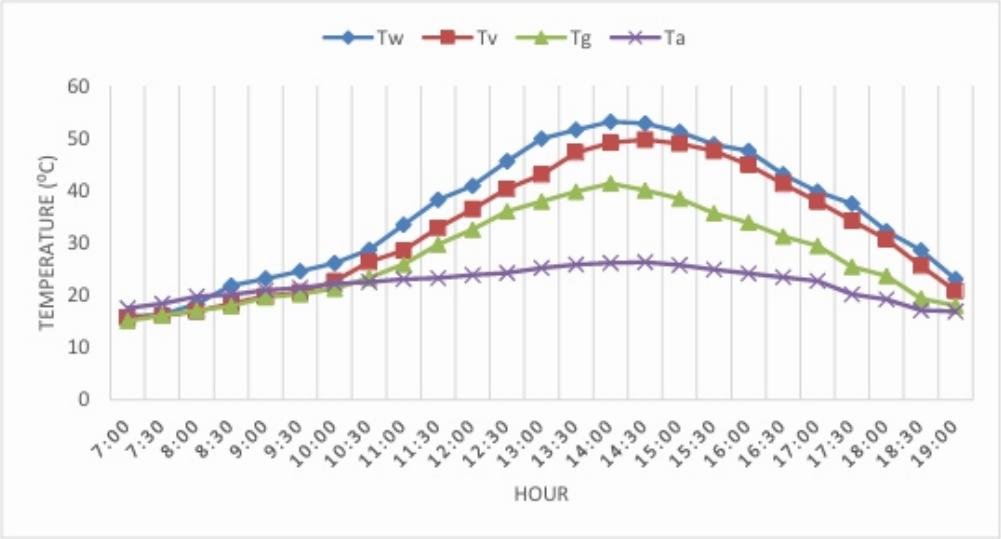

Figure 8. The temperature trend of the conventional solar still.

Figure 9 depicts the yields of water distillates of both solar stills. As can be observed from the graph, the water yield from the developed still started early, at 8:30, while the conventional still produced water at 10:30. The highest amounts of distillate for the developed and conventional stills were collected at 14:30 and 15:00, respectively. The incident solar radiation was 660 W/m2. The accumulated water distillate at the end of the experiment was 2180 mL (4.4 L/m2) for the developed still, while the conventional still produced 1050 mL (2.1 L/m2).

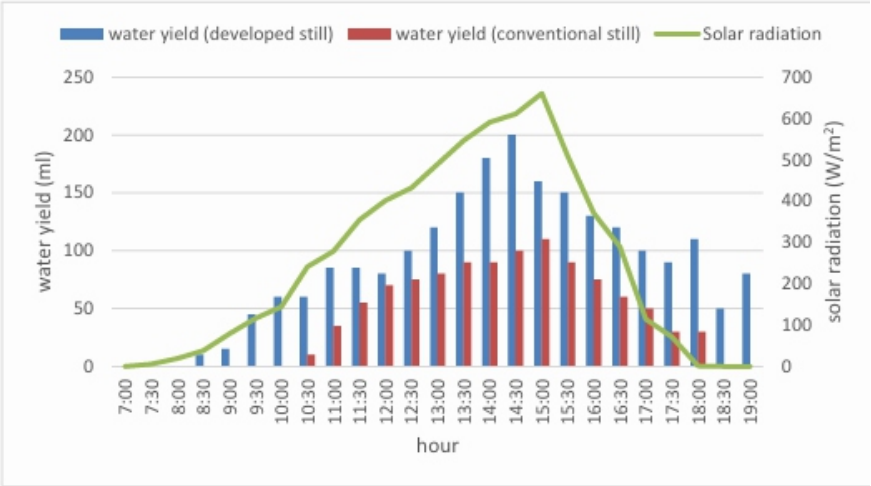

Figure 9. The accumulated water yields from solar stills in May 2021.

The performance of the developed solar still in September 2021 is presented in Figure 10. As is noticeable in the graph, the condensation surface temperature increased gradually after 12:00, due to the fact that the thermoelectric pump was off until 15:30, since the water basin temperature stayed above 52

°C. The maximum water basin temperature recorded was 54.8 °C at 14:00, and maximum ambient temperature was about 17.7 °C at midday. The average temperature difference between the water basin and the condensation surfaces was 24 °C.

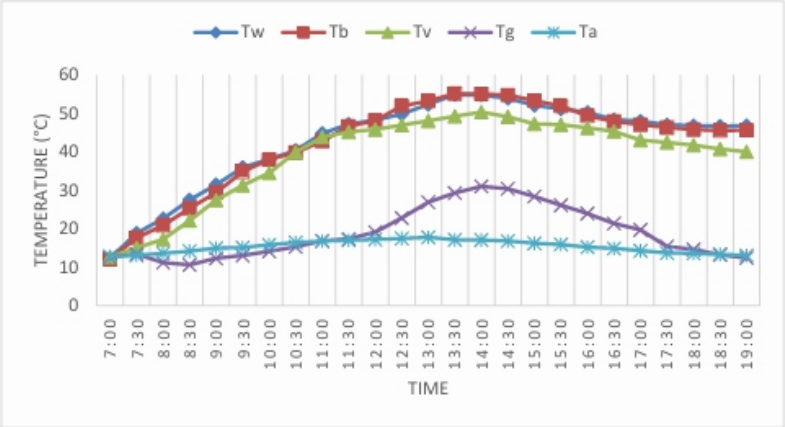

Figure 10. The temperature trend of the developed solar still in September 2021.

Figure 11 depicts the temperature trends in the conventional solar still components. The highest temperature of the water basin, recorded at 13:30, was 45.8 °C. Because of the low intensity of solar radiation, the water basin temperature remained relatively low throughout the day. The average of the temperature difference between the water basin and the condensation surfaces was 11 °C

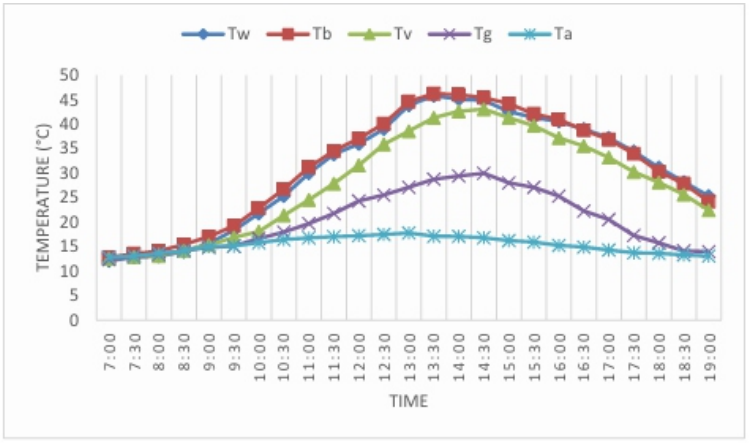

Figure 11. The temperature trend of the developed solar still on September 2021.

Figure 12 depicts the accumulated distillate water of both solar stills. As can be observed from the graph, the water yield from the developed still started early, at 9:30, while the conventional still produced water at 11:00. The highest amounts of distillate for the developed and conventional stills were collected at 14:30 and between 13:30 and 14:30, respectively. The incident solar radiation was 530 W/m2. The ambient temperature was relatively low, and the highest value recorded at 13:00 was 17.8 °C. The accumulated distillate water at the end of the experiment was 4.6 L/m2 for the developed still, while the conventional still produced 1.3 L/m2.

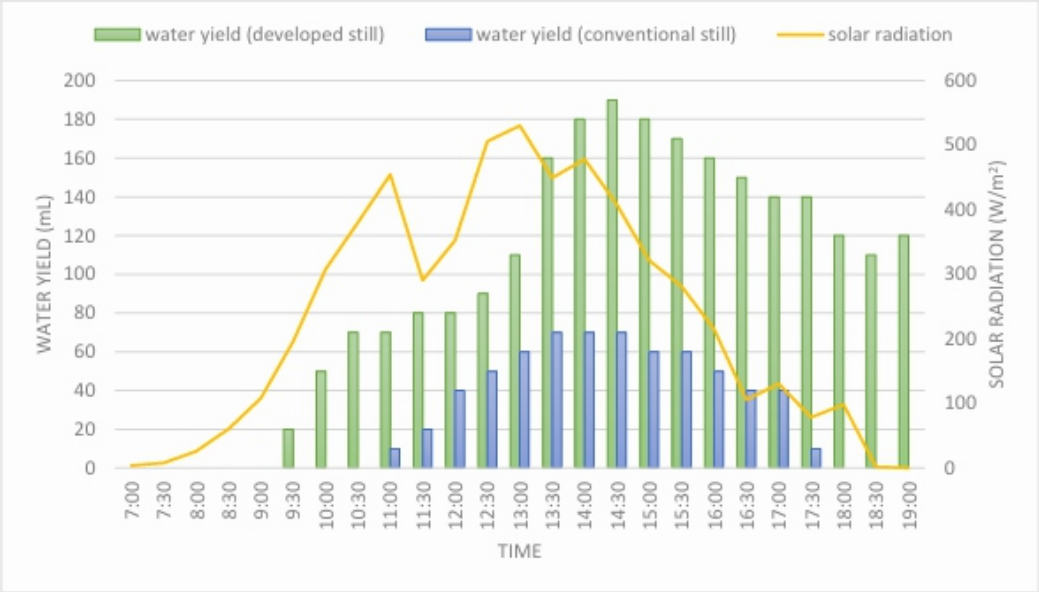

Figure 12. The accumulated water yields from solar stills in September 2021.

The performance of the developed still during a relatively cold night in September 2021 is shown in Figure 13. The water basin temperature (Tw) reached 43 °C at 23:00. The highest value recorded was 50.4 °C. The thermoelectric heat pump system was able to maintain the temperature at around 49 °C until the end of the experiment. The ambient temperature varied between 11.4 and 16.4 °C. The average temperature difference between the water basin and the condensation surfaces was 27 °C. As observed from the graph, the condensation (water yield) began at 22:00. The accumulated water yield at the end of the test was 1180 mL (2.360 L/m2).

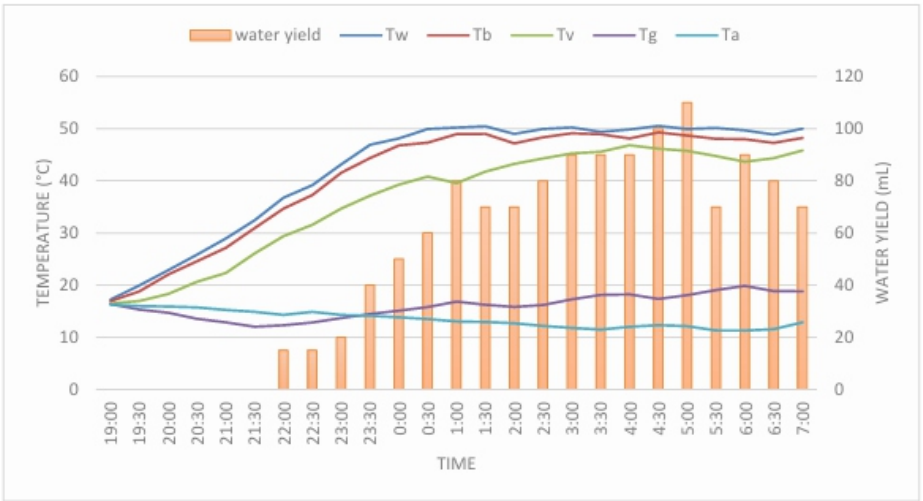

Figure 13. The developed solar still performance at night (September 2021).

Figure 14 shows the variation of the coefficient of performance of the heat pump system at the input current of 5 A. It is noticeable that the COP declines with the increase of the cold side temperature of the

thermoelectric modules (Tc). At 8:00, the temperature of the cold side of the thermoelectric module was 10 °C, the hot side was 28 °C, and the value of the COP was 1.9. At 14:00, the temperature of the cold side increased to 29 °C, and the value of the COP decreased to 0.4 due to the increase in the cooling capacity (Qc). At the end of the experiment (19:00), the value of the COP increased again due to the decrease of TC, which was 13 °C. These findings are in agreement with the results found by [37].

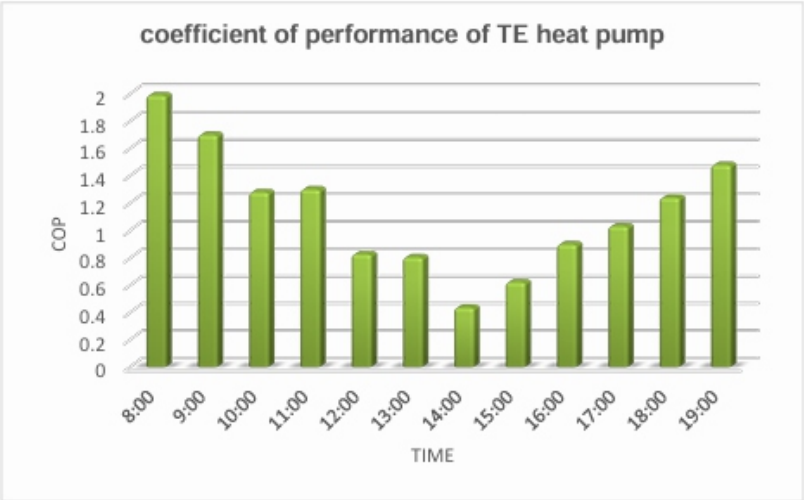

Figure 14. The variation of the coefficient of performance of the TE heat pump system.

5. Conclusions

This research work investigated the performance of a thermoelectric water-to-water heat pump system integrated into a conventional solar distillation unit. A typical solar photovoltaic system was designed to power the thermoelectric heat pump components. The main benefit of the integrated thermoelectric heat pump is that it increased the daily yield of fresh water by means of heating up the saline/brackish water and cooling down the condensation surface, thus increasing the temperature difference between the water basin and the condensation surfaces. This is considered the key factor of the solar still operation. Summer and winter outdoor experiments were conducted to the performance of the solar still under different weather conditions. The obtained results are summarized as follows:

1 The results of the summer outdoor experiments showed that at an incident solar radiation of 660 W/m2 and an ambient temperature of 26 °C, the maximum water basin temperature of the developed solar still was 60 °C, and the daily distillate yield was 2180 mL (4.4 L/m2). Meanwhile, the maximum basin water temperature recorded for the conventional solar still was 53 °C, and the water yield was 1050 mL (2.1 L/m2).

2 On a moderate winter day, the accumulated water yield was 2300 mL (4.6 L/m2), and the maximum water temperature was 54 °C. Despite the low average of the incident solar radiation and low ambient temperature, the daily yield was satisfactory due to the higher temperature difference between the water and the condensation surfaces, which was evaluated as 35 °C. Meanwhile, the accumulated water yield

from the conventional still was 650 mL (1.3 L/m2). The maximum basin water temperature achieved was 46 °C.

3 The results for the developed still during a moderate night in the month of September 2021 showed that the highest water basin temperature was 50 °C, and the accumulated distillate yield was 1180 mL (2.36 L/m2).

4 The maximum value of COP of the thermoelectric heat pump according to energy balance equations and the principles of thermodynamics for a single-stage heat pump was about 1.9.

Based on this work, the integration of the thermoelectric heat pump system into a conventional solar still has shown significant improvement of the daily fresh water productivity. The thermoelectric heat pump system can be integrated into different types of passive solar stills. Herein, simple modifications may be required for the thermoelectric heat pump layout to match the different designs of the solar stills.

For future work, more investigations are needed to improve the thermoelectric heat pump performance. Therefore, the authors recommend further exploration of the use of other types of thermoelectric modules. Moreover, cascades or multi-stage cycles can be addressed in further studies.

Conflict of interest

There is no conflict of interest. This research did not receive any specific grant from funding agencies in the public, commercial or not-for-profit sectors.

Author contributions

Fouad M Alkilani performed Conceptualization, Methodology, Writing, Original draft preparation and editing.

Dr. Ouassini Nemraoui performed Supervision and Reviewing.

Dr. Fareed Ismail performed Supervision and Reviewing.

References

1.Liang R, Hu A, Hatat-Fraile M, et al. (2014) Fundamentals on adsorption, membrane filtration, and advanced oxidation processes for water treatment. In: Nanotechnology for Water Treatment and Purification, Knoxville, Springer, 1–45. https://doi.org/10.1007/978-3-319-06578-6_1

2.Cheremisinoff NP (2002) Handbook of Water and Wastewater Treatment Technologies, 1st ed., Woburn—USA: Butterworth-Heinemann, 2002. https://doi.org/10.1016/B978-0750674980/50004-8

3.Bundschuh J, Kaczmarczyk M, Ghaffour N, et al. (2021) State-of-the-art of renewable energy sources used in water desalination: Present and future prospects. Desalination 508: 115035. https://doi.org/10.1016/j.desal.2021.115035

4.Misdan N, Lau WJ, Ismail AF (2012) Seawater Reverse Osmosis (SWRO) desalination by thinfilm composite membrane—Current development, challenges and future prospects. Desalination: 228–237. https://doi.org/10.1016/j.desal.2011.11.001

5.Darre NC, Toor GS (2018) Desalination of water: A review. Curr Pollut Rep 4: 104–111. https://doi.org/10.1007/s40726-018-0085-9

6.Elsaid K, Kamil M, Sayed ET, et al. (2020) Environmental impact of desalination technologies: A review. Sci Total Environ 748: 141528. https://doi.org/10.1016/j.scitotenv.2020.141528

7.Jones E, Qadir M, van Vliet, et al. (2019) The state of desalination and brine production: A global outlook. Sci Total Environ 657: 1343–1356. https://doi.org/10.1016/j.scitotenv.2018.12.076

8.Shahabi MP, McHugh A, Anda M, et al. (2017) A framework for planning sustainable seawater desalination water supply. Sci Total Environ 575: 826–835. https://doi.org/10.1016/j.scitotenv.2016.09.136

9.Lattemann S, Höpner T (2008) Environmental impact and impact assessment of seawater desalination. Desalination 220: 1–15. https://doi.org/10.1016/j.desal.2007.03.009

10. Zhang Y, Sivakumar M, Yang S, et al. (2018) Application of solar energy in water treatment processes: A review. Desalination 428: 116–145. https://doi.org/10.1016/j.desal.2017.11.020

11. Huang W, Su P, Cao Y, et al. (2020) Three-dimensional hierarchical CuxS-based evaporator for high-efficiency multifunctional solar https://doi.org/10.1016/j.nanoen.2020.104465 distillation. Nano Energy 69: 104465.

12. Tiwari GN, Sahota L (2017) Advanced solar-distillation systems: basic principles, thermal modeling, and its application. Springer. Available from: https://www.amazon.com/AdvancedSolar-Distillation-Systems-Principles-Application/dp/9811046719.

13. Peng G, Sharshir SW, Hu Z, et al. (2021) A compact flat solar still with high performance. Int J Heat Mass Transfer 179: 121657. https://doi.org/10.1016/j.ijheatmasstransfer.2021.121657

14. Bhardwaj R, Ten Kortenaar MV, Mudde RF (2015) Maximized production of water by increasing area of condensation surface for solar distillation. Appl Energy 154: 480–490. https://doi.org/10.1016/j.apenergy.2015.05.060

15. Mohamed AF, Hegazi AA, Sultan GI, et al. (2019) Augmented heat and mass transfer effect on performance of a solar still using porous absorber: Experimental investigation and exergetic analysis. Appl Therm https://doi.org/10.1016/j.applthermaleng.2019.01.070 Eng 150: 1206–1215.

16. Bataineh KM, Abbas MA (2020) Performance analysis of solar still integrated with internal reflectors and fins. Sol Energy 205: 22–36. https://doi.org/10.1016/j.solener.2020.04.059

17. Porta-Gándara MA, Fernández-Zayas JL, Chargoy-del-Valle N (2020) Solar still distillation enhancement through water surface perturbation. Sol Energy 196: 312–318. https://doi.org/10.1016/j.solener.2019.12.028

18. Jani HK, Modi KV (2019) Experimental performance evaluation of single basin dual slope solar still with circular and square cross-sectional hollow fins. Sol Energy 179: 186–194. https://doi.org/10.1016/j.solener.2018.12.054

19. Kabeel AE, Abdelgaied M (2020) Enhancement of pyramid-shaped solar stills performance using a high thermal conductivity absorber plate and cooling the glass cover. Renewable Energy 146: 769–775. https://doi.org/10.1016/j.renene.2019.07.020

20. Esfe MH, Esfandeh S, Toghraie D (2021) Optimization of influential geometrical parameters of single slope solar still equipped with thermoelectric system to achieve maximum desalinated water. Energy Rep 7: 5257–5268. https://doi.org/10.1016/j.egyr.2021.08.106

21. Esfe MH, Toghraie D (2022) Numerical study on the effect of solar radiation intensity on the fresh water productivity of solar still equipped with Thermoelectric Cooling System (TEC) for hot and dry areas of Semnan. Case Stud Therm Eng 32: 101848. https://doi.org/10.1016/j.csite.2022.101848

22. Sheikholeslami M, Said Z, Jafaryar M (2022) Hydrothermal analysis for a parabolic solar unit with wavy absorber pipe and nanofluid. Renewable Energy 188: 922–932. https://doi.org/10.1016/j.renene.2022.02.086

23. Abd Al-wahid WA, Saad HA, Hasan ZH, et al. (2022) Experimental study of the performance of hemispherical solar still with optimum value of rocks as heat transfer enhancers. AIMS Energy 10: 885–899. https://doi.org/10.3934/energy.2022040

24. Kabeel AE, Abdelgaied M, Mahmoud GM (2021) Performance evaluation of continuous solar still water desalination system. J https://doi.org/10.1007/s10973-020-09547-5 Therm Anal Calorim 144: 907–916.

25. Park CD, Lim BJ, Chung KY, et al. (2016) Experimental evaluation of hybrid solar still using waste heat. Desalination 379: 1–9. https://doi.org/10.1016/j.desal.2015.10.004

26. Sohani A, Hoseinzadeh S, Samiezadeh S, et al. (2022) Machine learning prediction approach for dynamic performance modeling of an enhanced solar still desalination system. J Therm Anal Calorim 147: 3919–3930. https://doi.org/10.1007/s10973-021-10744-z

27. Tuly SS, Sarker MRI, Das BK, et al. (2021) Effects of design and operational parameters on the performance of a solar distillation system: A comprehensive review. Groundwater Sustainable Dev 14: 100599. https://doi.org/10.1016/j.gsd.2021.100599

28. Singh AK, Yadav RK, Mishra D, et al. (2020) Active solar distillation technology: A wide overview. Desalination 493: 114652. https://doi.org/10.1016/j.desal.2020.114652

29. Lee HS (2017) Thermoelectrics: Design and Materials, 1st ed., Mishigan: John Wiley & Sons from: https://www.academia.edu/en/73566131/Thermoelectrics_Thermoelectrics_Design_and_Materi als.

30. Riffat SB, Ma X (2003) Thermoelectrics: A review of present and potential applications. ApplTherm Eng 23: 913–935. https://doi.org/10.1016/S1359-4311(03)00012-7

31. Duan M, Sun H, Lin B, et al. (2021) Evaluation on the applicability of thermoelectric air cooling systems for buildings with thermoelectric material optimization. Energy 221: 119723. https://doi.org/10.1016/j.energy.2020.119723

32. Shen ZG, Tian LL, Liu X (2019) Automotive exhaust thermoelectric generators: Current status, challenges future prospects. Energy Convers Manage 195: 1138–1173. https://doi.org/10.1016/j.enconman.2019.05.087

33. Liu Z, Li W, Zhang L, et al. (2019) Experimental study and performance analysis of solar-driven exhaust air thermoelectric heat pump recovery system. Energy Build 186: 46–55. https://doi.org/10.1016/j.enbuild.2019.01.017

34. Siddique ARM, Muresan H, Majid SH, et al. (2019) An adjustable closed-loop liquid-based thermoelectric electronic cooling system for variable load thermal management. Therm Sci Eng Prog 10: 245–252. https://doi.org/10.1016/j.tsep.2019.02.004

35. Liu W, Hu J, Zhang S, et al. (2017) New trends, strategies and opportunities in thermoelectric materials: A perspective. Mater Today Phys 1: 50–60. https://doi.org/10.1016/j.mtphys.2017.06.001

36. Phadatare MK, Verma SK (2007) Influence of water depth on internal heat and mass transfer in a plastic solar still. Desalination 217: 267–275. https://doi.org/10.1016/j.desal.2007.03.006

37. de Garayo SD, Martínez A, Aranguren P, et al. (2021) Prototype of an air to air thermoelectric heat pump integrated with a double flux mechanical ventilation system for passive houses. Appl Therm Eng 190: 116801. https://doi.org/10.1016/j.applthermaleng.2021.116801

Preventive control method for stable operation of proton exchange membrane fuel-cell stacks

Yuto Tsuzuki1,*, Yutaro Akimoto2 and Keiichi Okajima2
1 Graduate School of Science and Technology, University of Tsukuba, SB826,1-1-1, Tennnoudai, Tsukuba, Ibaraki,305-8573, Japan
2 Institute of Systems and Information Engineering, University of Tsukuba, SB826,1-1-1, Tennnoudai, Tsukuba, Ibaraki, 305-8573, Japan

ABSTRACT

Flooding and dry-out are major drawback issues in proton exchange membrane fuel cells (PEMFC), which necessitate adequate prevention control techniques. In a fuel-cell stack, as flooding and dry-out occur on the inlet and outlet sides, respectively, both faults can exist simultaneously. Therefore, the timely detection of these two contradictory faults is crucial for implementing timely control measures. In this study, we propose a preventive control method that detects the fault signs early for more effective prevention. The proposed method uses a curve-fitting method, which uses overpotential as the control index. As the control index can be obtained by measuring the current, voltage, and temperature, the evaluation can be performed quickly, making it easy to implement in a PEMFC system. Under a single fault, the stack output power, hydrogen consumption, and power efficiency of the proposed preventive control method and the previous study on flooding were compared. The results showed that our preventive control method could detect flooding sooner and was superior in stack output power, hydrogen consumption, and power generation compared to the fault control method. Under conditions of mixed flooding and dry-out, both flooding and dry-out were detected using the overpotential as the control index. Thus, because the proposed method initiates control measures before the fault progresses, it is possible to ensure the continued stable operation of the fuel cells.

Keywords: *PEMFC; control; flooding; dry-out; overpotential; curve fitting*

1. Introduction

Proton exchange membrane fuel cells (PEMFCs) have attracted considerable interest due to their ability to exhibit high energy densities at low temperatures, compact size, high efficiency, and minimal carbon emissions. Consequently, they are used in a multitude of applications, such as fuel cell vehicles (FCVs), cogeneration systems, portable electronics, and emergency power sources [1,2]. However, the mass commercialization of PEMFCs has been hindered due to operational issues stemming from water and thermal management, such as flooding or drying out, resulting in reduced power performance and system degradation [3]. Flooding is a fault wherein the water produced during the operation of a PEMFC gets retained, thereby filling up the pores in its gas diffusion layer, which covers the reaction area of the catalyst layer and results in decreased fuel cell performance. The lower the flow rate, the greater the flooding caused by the plugging of the generated water. Correspondingly, the conductivity of the membrane is affected, and the thickness of the electrolyte changes significantly [4]. Dry-out is a fault in which the membrane dries owing to excessive operating temperatures, flow rates, and declining power.

Consequently, the fuel cell membrane degrades more rapidly, causing pinholes and other defects [5].

There are several approaches to identifying the internal conditions, which include investigating the moisture state via X-ray [6], neutron tomography [7], the degree of drying of the membrane by measuring cell resistance using the current interruption method [8], and electrochemical impedance spectroscopy [9,10]. However, it is difficult to implement these methods in PEMFC systems. Fault diagnosis and control are various model-based methods [11] that delve into the reaction process of fuel cell systems and non-model-based methods by utilizing analytical models based on heuristic knowledge and signal processing techniques [12,13]. For model-based applications, Onanena et al. [14] proposed a pattern-recognition-based diagnostic approach based on electrochemical impedance spectroscopy measurements. For non-model-based approaches, Li et al. [15] used a support vector machine, and Steiner et al. [16] used neural networks to facilitate fault diagnosis. However, these methods require prior data collection, which demands time and effort to build the system.

Akimoto et al. [17] proposed a curve-fitting method that uses overpotential as a control index to diagnose and control faults. This method is easy to implement in PEMFC systems, wherein the control index can be calculated using only the initial and measured values of current, voltage, and temperature. Another advantage of this method is that it can respond to sudden faults, allowing evaluations to be performed quickly.

Despite the multiple methods proposed for implementing fault control, they are applicable only for operating conditions that cause a single fault. Each fuel cell in a stack has different internal parameters, such as gas concentration, supply pressure, and temperature. As flooding and dry-out tend to occur on the inlet and outlet side, respectively, two types of faults may coexist in a fuel-cell stack. When these happen simultaneously, purge control is used to drain water from inside the fuel cell. This quickens the drying up of the membranes in the other cells. Therefore, early detection of these two contradictory faults is necessary to control them.

In this study, we propose a preventive control method using a curve-fitting method that uses overpotential as a control index. The remainder of this paper is organized as follows. Section 2 presents the configuration of the PEMFC system used in the experiments, along with an overview of the preventive control method. Section 3 proposes a preventive control method for a single fault and compares it with a previous study. Additionally, a preventive control method was proposed for two mixed types of flooding and dry-out faults. Finally, Section 4 summarizes the conclusions of this study.

2. Experiments and control methods

2.1. Experiments

Figure 1 shows the PEMFC and the control system. A 5-Cell PEMFC stack was used in this study. The flow channel is serpentine, and the reaction area is 37.8 cm2. Figure 2 shows the IV curve of the PEMFC stack. In this PEMFC stack, the maximum output is 38.6 W at 15 A. For each cell voltage at 15 A, cell 1 has the higher voltage, 0.60 V and cell 4 has the lower voltage, 0.54 V. Pure hydrogen was supplied in flow mode from a cylinder, and air through a pump. A fan was installed on the stack for cooling purposes. The cell voltage, stack current, and stack temperature were converted to voltages and recorded on a personal computer (PC).

Table 1 presents the experimental conditions of this study. The faults assumed were flooding and a mixture of flooding and dry-out. Only flooding was reproduced at lower operating temperatures and flow rates. The hydrogen and air flow rates were 0.6 and 3.3 L/min, respectively. The operating temperature of the cooling fan was 45 °C. Mixed flooding and dry-out were reproduced at higher operating temperatures and lower flow rates. The hydrogen and air flow rates were 0.4 and 1.4 L/min, respectively. These parameters for both conditions were adopted from preliminary experiments to cause the respective faults. The voltage drops due to flooding and dry-out were controlled by the flow rate and installed fan, respectively.

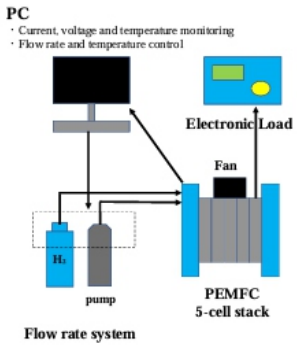

Figure 1. PEMFC and the control system.

Table 1. Experimental conditions.

Fault	Flooding	Mixed flooding and dry-out
Hydrogen [L/min]	0.6	0.4
Air [L/min]	3.3	1.4
Operating temperature [°C]	45	55–75

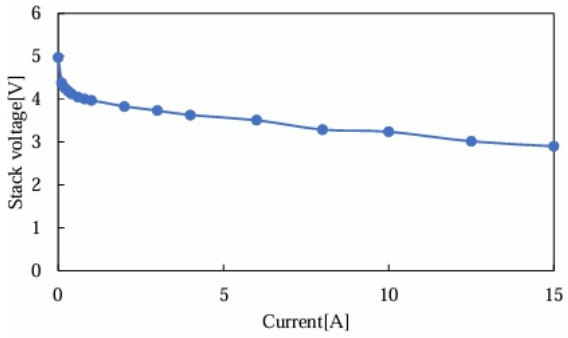

(a) Stack

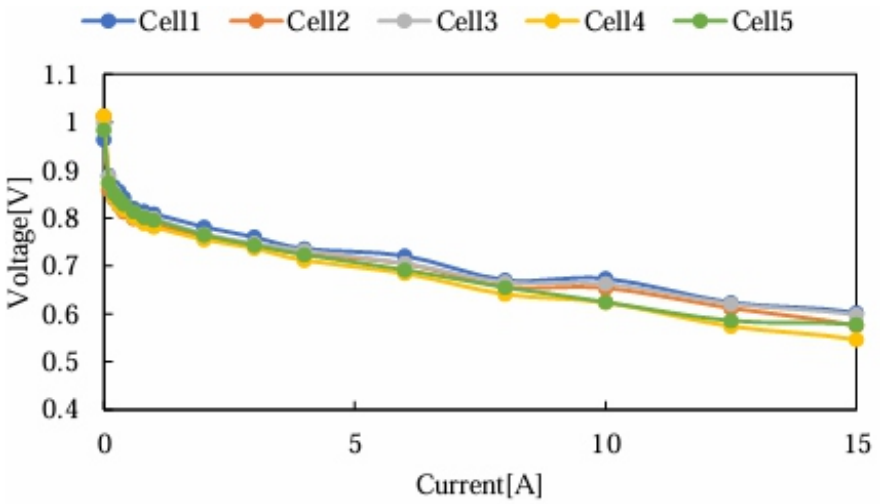

(b) Cells

Figure 2. IV curves of PEMFC stack and cells.

2.2. Control methods

2.2.1. Preventive control

Preventive control is a method to maintain power by detecting signs of faults, such as flooding and dry-out, and controlling them in advance. In this study, we propose a preventive control method that uses overpotential as a control index. Overpotential is the voltage drop associated with an increase in current density. It is classified into three types based on the factors that cause the power to drop: activation, ohmic, and concentration. The voltage drop factor can be evaluated by separating each overpotential type. The activation overpotential is the voltage drop due to the consumption of activation energy and the reaction to become an ion. The ohmic overpotential is the voltage drop arising from the resistance to the transfer of electrons and ions in the electrolyte membrane, electrodes, separator, and other components of the fuel cell. The concentration overpotential is the voltage drop caused by a decrease in oxygen and hydrogen concentrations.

To evaluate the power reduction factor, the overpotential was calculated by fitting the curve model equation with the least-squares method based on the measured values of the cell voltage, stack current, and stack temperature obtained from the PEMFC. In this study, the curve-model equation [18] in Eq (1) was used to calculate the overpotential.

$$V = E_{0(T)} - \eta_{act(T)} - \eta_{ohmic(T)} - \eta_{con(T)} \quad (1)$$

V [V] is the cell voltage, $E_{0(T)}$ [V] is the theoretical voltage, $\eta_{act(T)}$ [V] is the activation overpotential, $\eta_{ohmic(T)}$ [V] is the ohmic overpotential, and $\eta_{con(T)}$ [V] is the concentration overpotential.

The method for calculating overpotential is described below. First, the load is gradually increased to the constant current to be used in the experiment. At that time, the values of cell voltage and stack temperature corresponding to the preset current are recorded. In addition, the cell voltage and stack temperature during constant current operation, which are updated every second, are used for fitting and IV curves are predicted to calculate each overpotential. These overpotentials were calculated by PC in Figure 1 using measuring value of PEMFC stack at every second.

Several equations have been proposed in previous studies on curve models, with the simplest by Kim et al. [19]. Squadrito et al. [20] proposed an equation that used the power of the current density as a factor in the concentration overpotential term to accommodate the steep voltage. However, these assume constant temperature and humidity, while the curve model equation employed herein uses temperature as a variable for all overpotential terms. Thus, it can be considered appropriate for actual system implementation because the temperature of the fuel cells changes during the operation phase.

2.2.2. Control strategy

In Section 3, the method proposed herein is compared with that in a previous study [17] for a single fault. Subsequently, the proposed control method under mixed flooding and dry-out conditions was adopted.

Figure 3 shows the control flow in the preventive and fault-control strategies employed against flooding. After starting the constant-current operation, the overpotential was calculated every second. The concentration overpotential was used as a control index since flooding is caused by it. Control was exercised when the concentration overpotential exceeded the control threshold. In this experiment, the control threshold was set to 15% of the theoretical voltage $E_{0(T)}$. The control method is not a purge as in fault control, but rather the flow rate of hydrogen and air is increased every 2 seconds by 0.2 and 0.6 L/min, respectively, and when concentration overpotential is no longer calculated (0.001 V), the control is finished and the flow rate returns to the initial flow conditions.

The fault control method used for comparison was adopted from a previous study [17]. The control method involved a second hydrogen and air purge (20 L/min) when the threshold value was lowered. The experiment was conducted at a constant-current operation for 30 min, and four parameters were compared: the control frequency, stack output, hydrogen consumption, and power efficiency. The calculation of efficiency is described in Eq (2).

$$\eta_{LHV} = \frac{W}{C \times \Delta H^0} \times 100 \quad (2)$$

where η_{LHV} [%] represents the power efficiency (Lower Heating Value), W [W] is the stack power, C [mol/s] represents the fuel consumption, and ΔH^0 [kJ/mol] represents the standard enthalpy of the reaction.

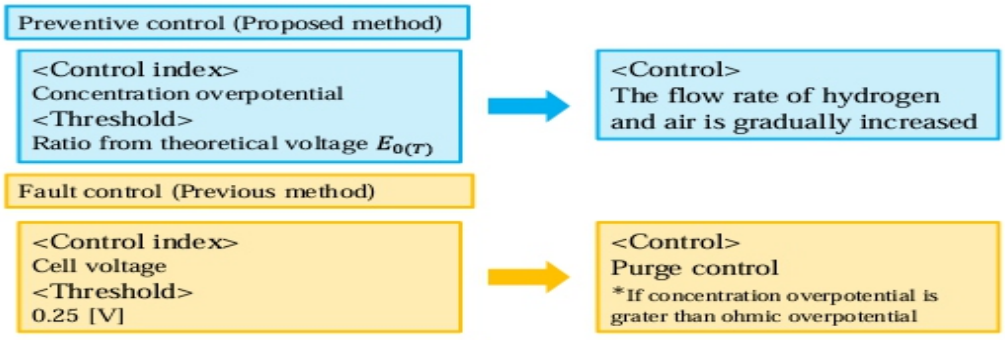

Figure 3. Outline of the proposed and previous method of flooding.

Figure 4 shows the control flow of the preventive control strategy for a mixture of flooding and dry-out. Concentration overpotential was used as the control index to control the flooding. The control threshold 1 in Figure 3 was set at 10% of the theoretical voltage $E_{0(T)}$ to detect dry-out more quickly. The control method would increase the hydrogen and air flow rates by 0.2 and 0.6 L/min, respectively, every 5 seconds until the concentration overpotential fell below the control threshold.

Dry-out is caused by the ohmic overpotential, which is used as the control index. The evaluation method records the initial ohmic overpotential after starting a constant-current operation and calculates the difference from the ohmic overpotential during operation. This difference is used as the control threshold 2 in Figure 3. This is because the ohmic overpotential is proportional to the current value; therefore, its value changes depending on the current during the operational phase. The control threshold of ohmic overpotential in this experiment was set to 0.075 V. When the value exceeded the control threshold, the fan cooled the temperature down to 60 °C, and when it fell below the control threshold, preventive control was suspended.

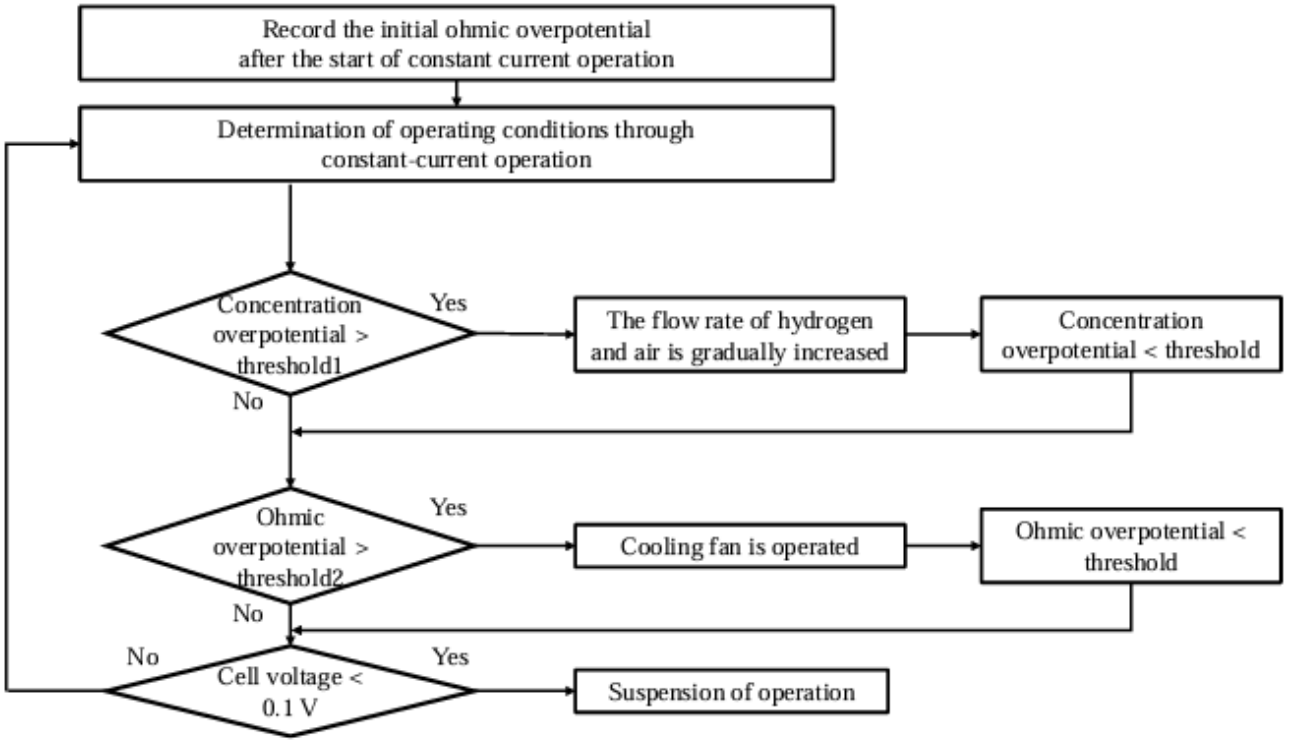

Figure 4. Control flowchart to prevent mixed flooding and dry-out.

3. Results and discussion

3.1. Comparison between the proposed method and previous study for single fault

Figure 5 shows the transition of Cell 4 voltage in preventive and fault control methods. In this stack, flooding was often detected in Cell 4. Flooding is detected at cell voltages around 0.25 V in fault control method, whereas in the preventive control method, it is detected at cell voltages around 0.45 which restrain the cell voltage drop.

Figure 6 compares the hydrogen and air flow rates, Cell 4 voltage and concentration overpotential, in the preventive control method from 1400 to 1500 s. From 1400 s, the concentration overpotential increased

as the cell voltage decreased and reached the control threshold at 1448 s. At 1400 s, the cell voltage and concentration overpotential were 0.556 and 0.029 V, respectively. The control measures were implemented at 1449 and 1457 s. When the cell voltage increased (0.602 V) and the concentration overpotential decreased (5.65 × 10–5 V), the control measures were suspended.

Table 2 shows the efficiency and parameters of each control method during the constant-current operation. The control frequency is higher for the preventive control method at 54 times and the fault control method at 6 times, but the stack output power is higher and the hydrogen consumption is lower than that of the fault control method. The efficiency of the preventive control method was 1.4% higher than that of the fault control method at 26.5%, compared to 25.1% for the fault control method.

Based on these results, the proposed method detects flooding earlier than the fault control method using the concentration overpotential as a control index. Therefore, it has the advantage of average output power. Additionally, the operation could be performed while increasing the power efficiency as hydrogen consumption was suppressed by gradually increasing the flow rate unlike the purge control method used in the previous study.

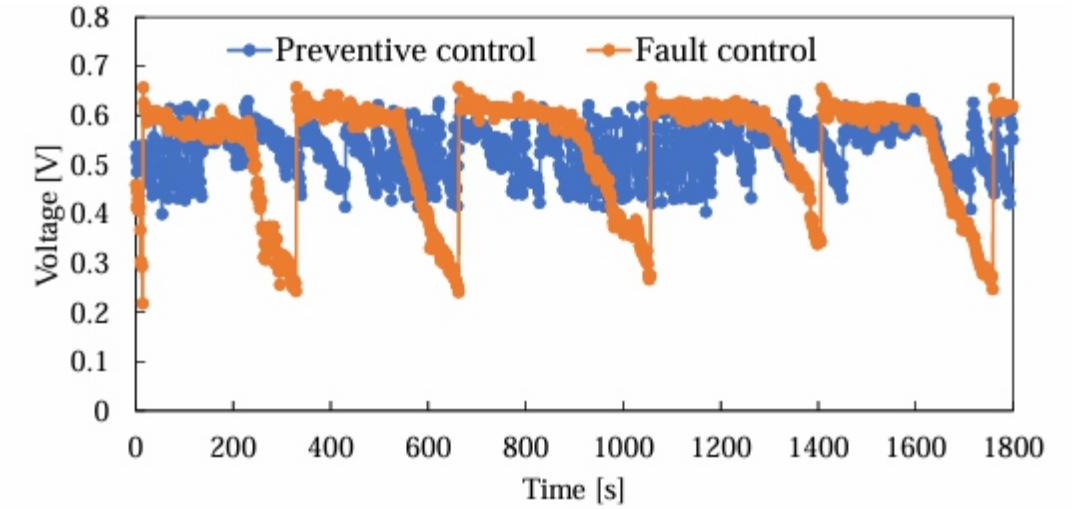

Figure 5. Comparison of Cell 4 voltage in preventive and fault control.

Table 2. Comparison of proposed and previous study method.

Method	Preventive control	Fault control
Control frequency [Times]	54	6
Average power output [W]	30.7	30.1
Hydrogen consumption [L]	19.4	19.9
Efficiency [%]	26.5	25.1

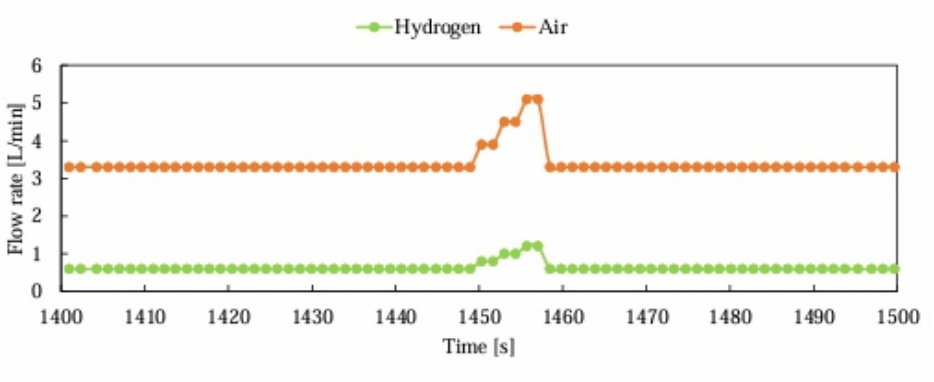

(a) Hydrogen and air flow rates.

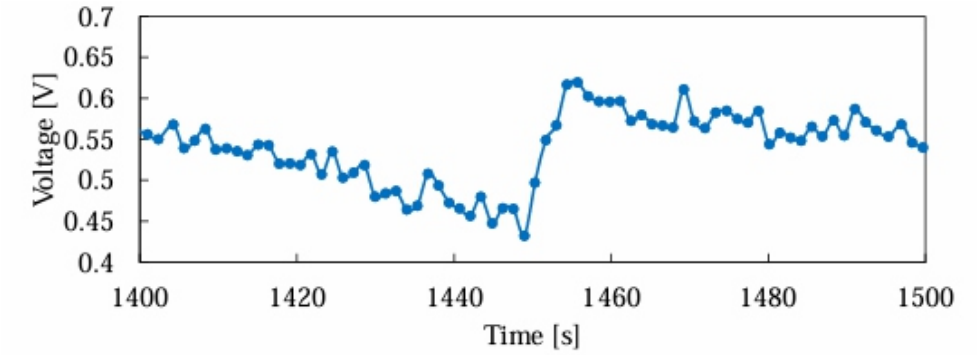

(b) Cell voltage.

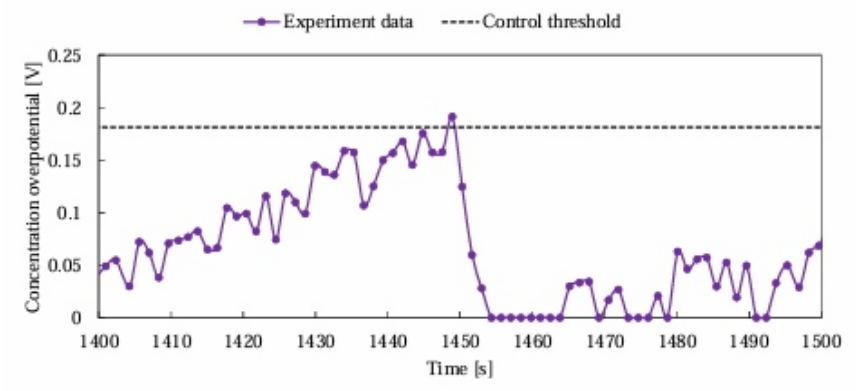

(c) Concentration overpotential.

Figure 6. Hydrogen, air flow rate, Cell 4 voltage, and concentration overpotential in the preventive control method from 1400 to 1500 seconds.

3.2. Preventive control of mixed faults in the proposed method

Figure 7 shows the voltage and temperature transitions for all the cells under the preventive control method. All cells were maintained at the voltage of 0.35 V until 1100 seconds. Table 3 shows number of control frequency for the proposed method. In this experiment, dry-out was detected 7 times and flooding was detected 3 times. Figure 8 shows the voltage and ohmic overpotential of Cell 2 with temperature and dry-out control from 400 to 1000 s. The dry-out was detected three times: from 539 to 650 s, from 758 to 816 s, and from 860 to 927 s. The initial ohmic overpotential of Cell 2 in this experiment was 0.137 V. As the temperature increased from 400 to 539 s, the cell voltage decreased from 0.438 to 0.372 V, and the ohmic overpotential increased from 0.164 to 0.220 V. From 539 to 650 s, the fan was controlled to suppress the decrease in cell voltage. This behavior is evident from 813 to 927 s: from 813 to 860 s, the temperature increases from 62.2 ℃ to 67.7 ℃, the Cell voltage decreases from 0.425 to 0.392 V, and the ohmic overpotential increases from 0.194 to 0.210 V. From 860 to 927 s,fan control increased the cell voltage to 0.440 V and decreased the ohmic overpotential to 0.183 V.

Because stable operation was possible with the cooling fan during all periods, it is considered that the membrane got dried when operating at a high temperature. The difference in the internal condition of the stack before control was considered to be the cause of the output increase due to the cooling fan during the third control at 860–927 s. In this experiment, dry-out was detected for the first time at 539–650 s. Moreover, the fan control involves temporary cooling. Therefore, from the second detection onwards, residual heat remained in the stack compared to the first control at 539–650 s, so the membrane was more likely to dry. Furthermore, the fact that the stack temperature rises earlier after the second control at 758–816 s also indicates that the latter is drying the membrane. Consequently, the control frequency of the cooling fan also increased, prompting an increase in the cell voltage during the third control at 860–927 s. Furthermore, the voltage of Cell 5 was 0.477 V at 758 s, but increased to 0.512 V at 927 s due to the cooling fan control.

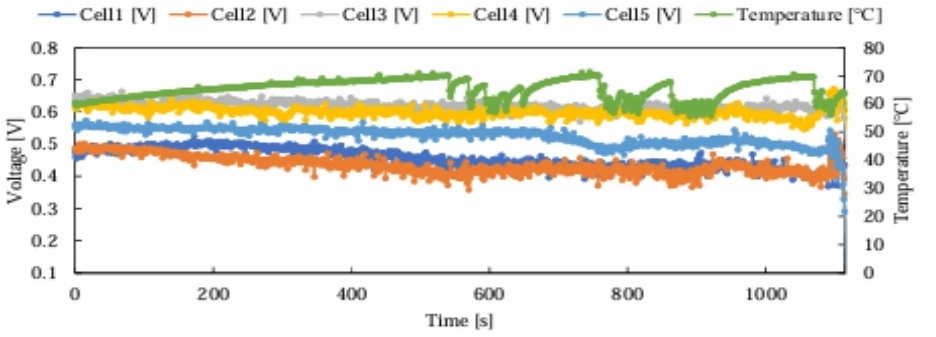

Figure 7. Comparison of each cell voltage and stack temperature.

Table 3. Comparison of each failure control frequency in proposed method.

Method	Preventive control
Control frequency of dry-out [Times]	7
Control frequency of flooding [Times]	3

Figure 9 shows the voltage and concentration overpotential of Cell 1 with hydrogen, airflow, and flooding control from 950 to 1115 s. At 1091 s, the concentration overpotential exceeds the control threshold for the first time. The cell voltage and concentration overpotential in Cell 1 were 0.369 and 0.152 V, respectively. The cell voltage increased at 0.511 V, and the concentration overpotential at 3.68 × 10–5 V decreased via flow rate control. The cell voltage is increased by controlling the flow rate. However, at the third control time, despite the increase in cell voltage, the flow control continued, and the voltage dropped. This was because flooding was detected in other cells. Figure 10 shows the voltage and concentration overpotentials of cell 5 from 1090 to 1115 s. The concentration overpotential exceeded the control threshold of 1104 second. Control was initiated, and the cell voltage increased at 1105 s, but then gradually decreased. It is thought that the cell membrane accelerated drying via the continued flow rate control.

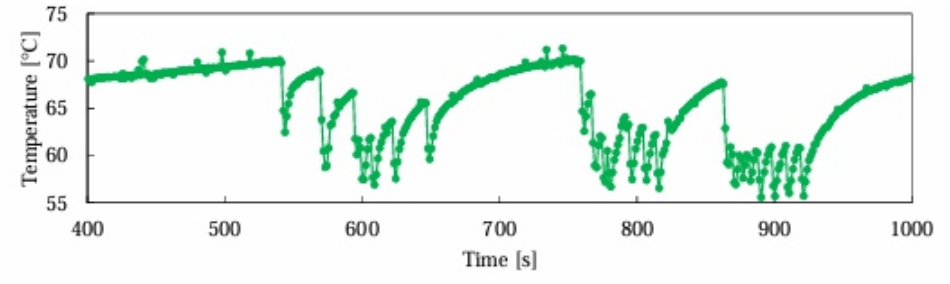

(a) Temperature.

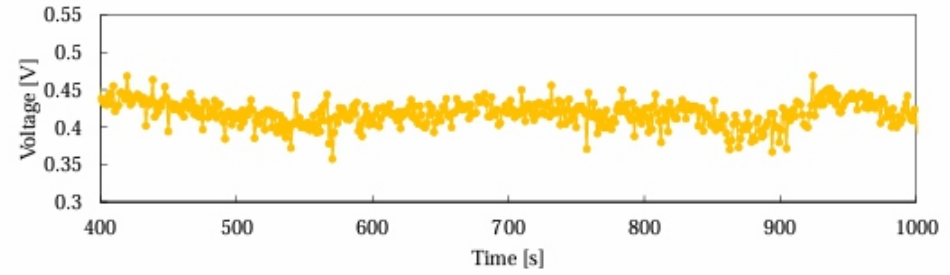

(b) Cell voltage.

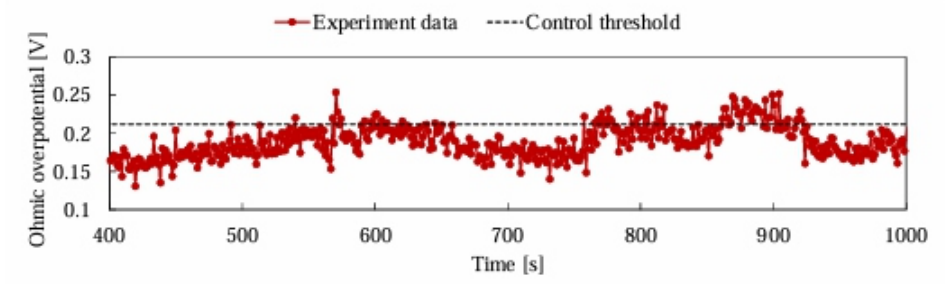

(c) Ohmic overpotential.

Figure 8. Stack temperature, Cell 2 voltage, ohmic overpotential from 400 to 1000 s

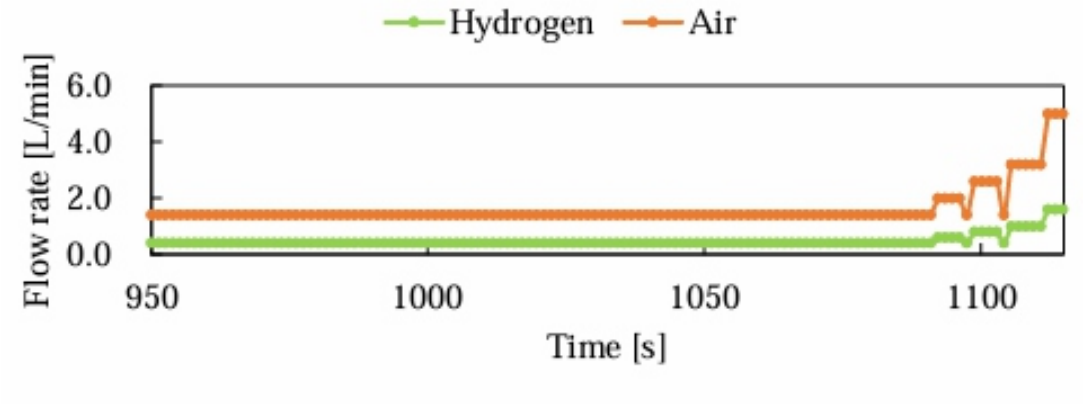

(a) Hydrogen and air flow rates.

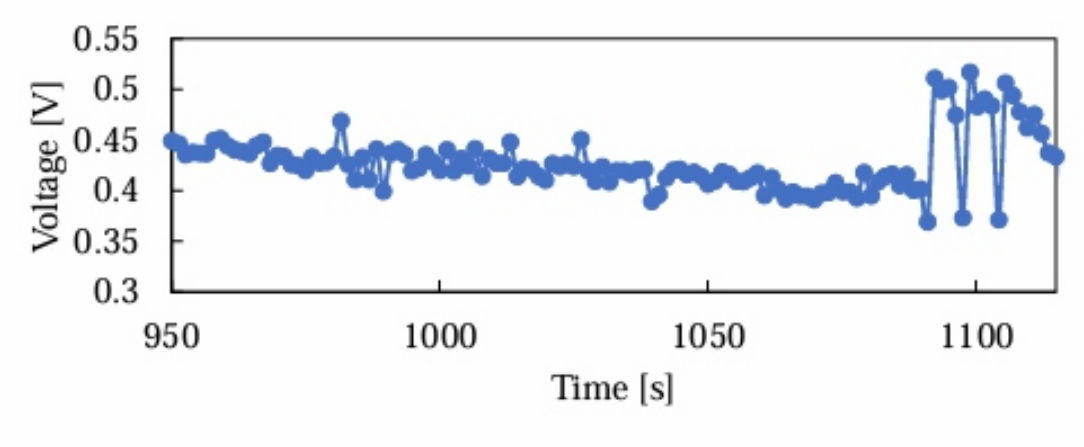

(b) Cell voltage.

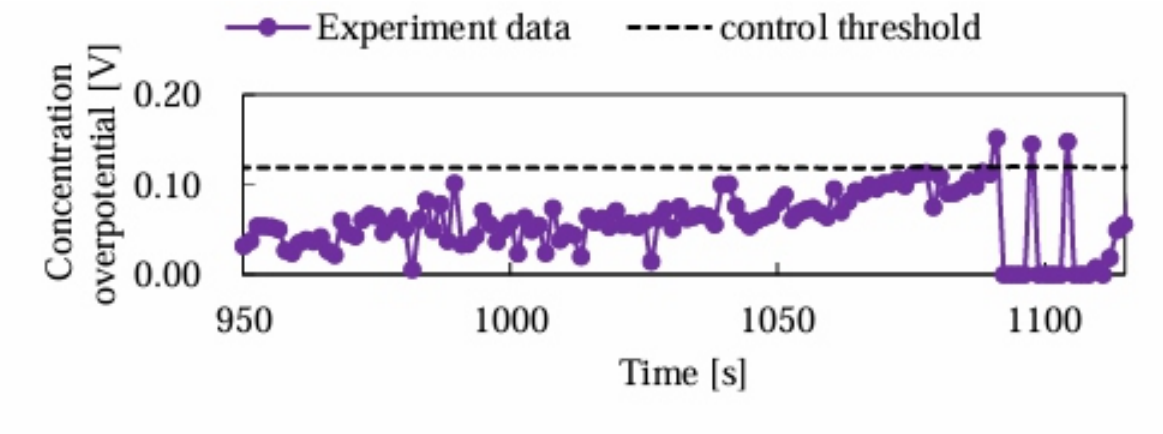

(c) Concentration overpotential.

Figure 9. Hydrogen, air flow rate, Cell 1 voltage, and concentration overpotential from 950 to 1115 s.

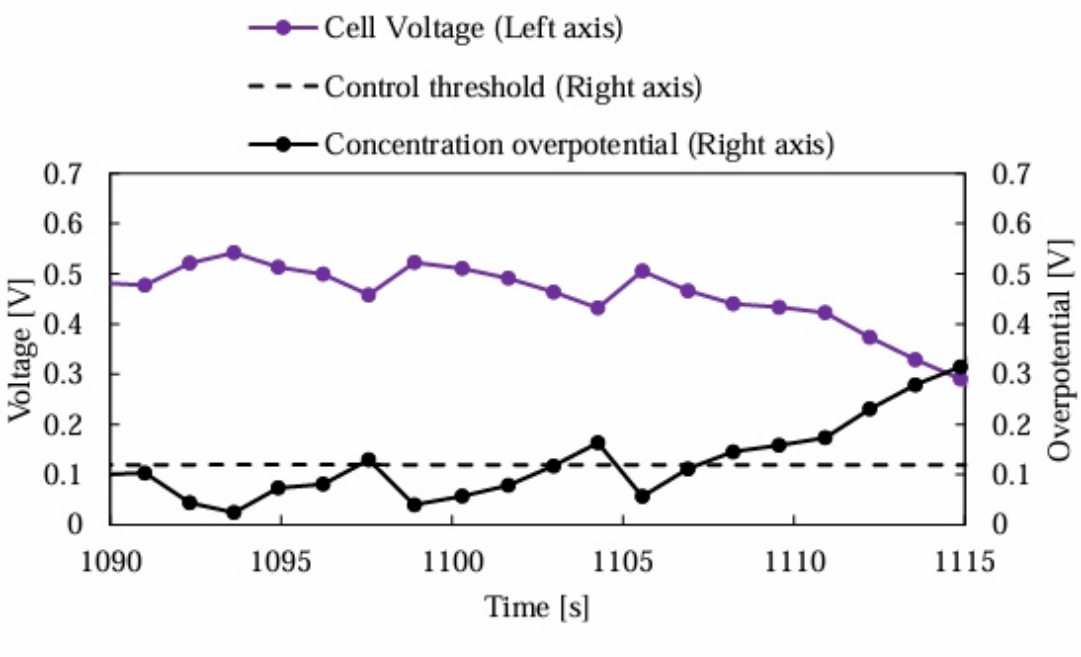

Figure 10. Cell 5 voltage and concentration overpotential from 1090 to 1115 s.

4. Conclusions

In this study, a preventive control method using overpotential as a control index was proposed that can diagnose and avoid contradictory faults in the stack to ensure stable operation of the fuel cell systems. The proposed method is easy to implement in a PEMFC system because the control index can be calculated by measuring the current, voltage, and temperature and can be evaluated quickly.

For a single fault, we compared the method proposed in this study with a previous study on flooding. The preventive control method detected flooding earlier than the fault control method by using the concentration overpotential as the control index and improved the voltage of Cell 4. Additionally, although the control frequency increased, hydrogen consumption was suppressed by gradually increasing the flow rate unlike the purging control method. Furthermore, the system was superior in terms of the stack power output and power efficiency. This showed that not only could faults be avoided in advance, but the system could also be operated while improving the power efficiency.

Under conditions of mixed flooding and dry-out, both flooding and dry-out were detected using the concentration overpotential for flooding and the difference between the ohmic overpotential after the start and during operation, as the control index for dry-out. The voltage of Cell 1 was improved for flooding, and that of Cell 2 was improved for dry-out. As a result, we were able to maintain more than 0.35 V in all cells until 1100 seconds.

From these results, because the proposed method initiates control measures before the fault progresses, stable operation is possible. Furthermore, it can be integrated with other control systems, increasing the

reliability of the fuel cell system.

Acknowledgments

This research was supported by the Iwatani Naoji Foundation, TEPCO Memorial Foundation research grant and the Mazda Foundation research grant.

Conflict of interest

The authors declare no conflict of interest.

References

1.Ritzberger D, Hametner C, Jakubek S (2020) A real-time dynamic fuel cell system simulation for model-based diagnostics and control: Validation on real driving data. Energies 13: 3148. https://doi.org/10.3390/en13123148

2.Bizon N, Mazare G, Ionescu M, et al. (2018) Optimization of the proton exchange membrane fuel cell hybrid power system for residential buildings. Energy Convers Manage 163: 22–37. https://doi.org/10.1016/j.enconman.2018.02.025

3.Yang B, Wang J, Yu L, et al. (2020) A critical survey on proton exchange membrane fuel cell parameter estimation using meta-heuristic algorithms. J Cleaner Prod 265: 121660. https://doi.org/10.1016/j.jclepro.2020.121660

4.Mason T, Millichamp J, Neville T, et al. (2013) A study of the effect of water management and electrode flooding on the dimensional change of polymer electrolyte fuel cells. J Power Sour 242: 70–77. https://doi.org/10.1016/j.jpowsour.2013.05.045

5.Barbir F, Gorgun H, Wang X (2005) Relationship between pressure drop and cell resistance as a diagnostic for PEM fuel https://doi.org/10.1016/j.jpowsour.2004.08.055

6. J Power Sour 141: 96–101. Chevalier S, Ge N, George M, et al. (2017) Synchrotron X-ray radiography as a highly precise and accurate method for measuring the spatial distribution of liquid water in operating polymer electrolyte membrane fuel cells. J Electrochem Soc 164: F107–F114. Available from: https://iopscience.iop.org/article/10.1149/2.0041702jes.

7. Alrwashdeh S, Alsaraireh F, Saraireh M, et al. (2018) In-situ investigation of water distribution in polymer electrolyte membrane fuel cells using high-resolution neutron tomography with 6.5 μm pixel size. AIMS Energy 6: 607-614. https://doi.org/10.3934/energy.2018.4.607

8.Rubio M, Urquia A, Dormido S (2007) Diagnosis of PEM fuel cells through current interruption. J Power Sour 171:670–677. https://doi.org/10.1016/j.jpowsour.2007.06.072

9.Jullian G, Cadet C, Rosini S, et al. (2020) Fault detection and isolation for proton exchange membrane

fuel cell using impedance measurements and Multiphysics modeling. Fuel Cells 20: 558–569. https://doi.org/10.1002/fuce.202000022

10. Canut J, Abouatallah R, Harrington D. (2006) Detection of membrane drying, fuel cell flooding, and anode catalyst poisoning on PEMFC stacks by electrochemical impedance spectroscopy. J Electrochem Soc153: A857–A864. https://iopscience.iop.org/article/10.1149/1.2179200.

11. Saygili Y, Eroglu I, Kincal S (2015) Model based temperature controller development for water cooled PEM fuel cell systems. Int J Hydrogen Energy 40: 615–622. https://doi.org/10.1016/j.ijhydene.2014.10.047

12. Cadet C, Jemeï S, Druart F, et al. (2014) Diagnostic tools for PEMFCs: From conception to implementation. Int J Hydrogen Energy 39: 10613–10626. https://doi.org/10.1016/j.ijhydene.2014.04.163

13. Wang J, Yang B, Zeng C, et al. (2021) Recent advances and summarization of fault diagnosis techniques for proton exchange membrane fuel cell systems: A critical overview. J Power Sour 500: 229932. https://doi.org/10.1016/j.jpowsour.2021.229932

14. Onanena R, Oukhellou L, Côme E, et al. (2012) Fault-diagnosis of PEM fuel cells using electrochemical spectroscopy impedance. IFAC Proc 45: 651–656. Available from: https://hal.archives-ouvertes.fr/hal-03223601.

15. Li Z, Outbib R, Giurgea S, et al. (2019) Fault diagnosis for fuel cell systems: A data-driven approach using high-precise voltage sensors. Renewable Energy 135: 1435–1444. https://doi.org/10.1016/j.renene.2018.09.077

16. Steiner Y, Hissel D, Moçotéguy P (2011) Diagnosis of polymer electrolyte fuel cells failure modes (flooding & drying out) by neural networks modeling. Int J Hydrogen Energy 36: 3067–3075. https://doi.org/10.1016/j.ijhydene.2010.10.077

17. Akimoto Y, Okajima K (2021) Simple on-board fault-detection method for proton exchange membrane fuel cell stacks using by semi-empirical curve fitting. Appl Energy 303: 17654. https://doi.org/10.1016/j.apenergy.2021.117654

18. Akimoto Y, Okajima K (2014) Semi-empirical equation of PEMFC considering operation temperature. Energy Technol Policy 1: 91–96. https://doi.org/10.1080/23317000.2014.972480

19. Kim J, Lee M, Srinivasan S, et al. (1995) Modeling of proton exchange membrane fuel cell performance with an empirical equation. J Electrochem Soc 142: 2670–2674. https://doi.org/10.1149/1.2050072

20. Squadrito G, Maggio G, Passalacqua E, et al. (1999) An empirical equation for polymer electrolyte fuel cell (PEFC) behaviour. J Appl Electrochem 29: 1449–1455. Available from: https://link.springer.com/article/10.1023/A:1003890219394.

Instructions for Authors

Essentials for Publishing in this Journal

1 Submitted articles should not have been previously published or be currently under consideration for publication elsewhere.

2 Conference papers may only be submitted if the paper has been completely re-written (taken to mean more than 50%) and the author has cleared any necessary permission with the copyright owner if it has been previously copyrighted.

3 All our articles are refereed through a double-blind process.

4 All authors must declare they have read and agreed to the content of the submitted article and must sign a declaration correspond to the originality of the article.

Submission Process

All articles for this journal must be submitted using our online submissions system. http://enrichedpub.com/ . Please use the Submit Your Article link in the Author Service area.

Manuscript Guidelines

The instructions to authors about the article preparation for publication in the Manuscripts are submitted online, through the e-Ur (Electronic editing) system, developed by **Enriched Publications Pvt. Ltd**. The article should contain the abstract with keywords, introduction, body, conclusion, references and the summary in English language (without heading and subheading enumeration). The article length should not exceed 16 pages of A4 paper format.

Title

The title should be informative. It is in both Journal's and author's best interest to use terms suitable. For indexing and word search. If there are no such terms in the title, the author is strongly advised to add a subtitle. The title should be given in English as well. The titles precede the abstract and the summary in an appropriate language.

Letterhead Title

The letterhead title is given at a top of each page for easier identification of article copies in an Electronic form in particular. It contains the author's surname and first name initial .article title, journal title and collation (year, volume, and issue, first and last page). The journal and article titles can be given in a shortened form.

Author's Name

Full name(s) of author(s) should be used. It is advisable to give the middle initial. Names are given in their original form.

Contact Details

The postal address or the e-mail address of the author (usually of the first one if there are more Authors) is given in the footnote at the bottom of the first page.

Type of Articles

Classification of articles is a duty of the editorial staff and is of special importance. Referees and the members of the editorial staff, or section editors, can propose a category, but the editor-in-chief has the sole responsibility for their classification. Journal articles are classified as follows:

Scientific articles:

1. Original scientific paper (giving the previously unpublished results of the author's own research based on management methods).

2. Survey paper (giving an original, detailed and critical view of a research problem or an area to which the author has made a contribution visible through his self-citation);

3. Short or preliminary communication (original management paper of full format but of a smaller extent or of a preliminary character);

4. Scientific critique or forum (discussion on a particular scientific topic, based exclusively on management argumentation) and commentaries. Exceptionally, in particular areas, a scientific paper in the Journal can be in a form of a monograph or a critical edition of scientific data (historical, archival, lexicographic, bibliographic, data survey, etc.) which were unknown or hardly accessible for scientific research.

Professional articles:

1. Professional paper (contribution offering experience useful for improvement of professional practice but not necessarily based on scientific methods);
2. Informative contribution (editorial, commentary, etc.);
3. Review (of a book, software, case study, scientific event, etc.)

Language

The article should be in English. The grammar and style of the article should be of good quality. The systematized text should be without abbreviations (except standard ones). All measurements must be in SI units. The sequence of formulae is denoted in Arabic numerals in parentheses on the right-hand side.

Abstract and Summary

An abstract is a concise informative presentation of the article content for fast and accurate Evaluation of its relevance. It is both in the Editorial Office's and the author's best interest for an abstract to contain terms often used for indexing and article search. The abstract describes the purpose of the study and the methods, outlines the findings and state the conclusions. A 100- to 250-Word abstract should be placed between the title and the keywords with the body text to follow. Besides an abstract are advised to have a summary in English, at the end of the article, after the Reference list. The summary should be structured and long up to 1/10 of the article length (it is more extensive than the abstract).

Keywords

Keywords are terms or phrases showing adequately the article content for indexing and search purposes. They should be allocated heaving in mind widely accepted international sources (index, dictionary or thesaurus), such as the Web of Science keyword list for science in general. The higher their usage frequency is the better. Up to 10 keywords immediately follow the abstract and the summary, in respective languages.

Acknowledgements

The name and the number of the project or programmed within which the article was realized is given in a separate note at the bottom of the first page together with the name of the institution which financially supported the project or programmed.

Tables and Illustrations

All the captions should be in the original language as well as in English, together with the texts in illustrations if possible. Tables are typed in the same style as the text and are denoted by numerals at the top. Photographs and drawings, placed appropriately in the text, should be clear, precise and suitable for reproduction. Drawings should be created in Word or Corel.

Citation in the Text

Citation in the text must be uniform. When citing references in the text, use the reference number set in square brackets from the Reference list at the end of the article.

Footnotes

Footnotes are given at the bottom of the page with the text they refer to. They can contain less relevant details, additional explanations or used sources (e.g. scientific material, manuals). They cannot replace the cited literature.
The article should be accompanied with a cover letter with the information about the author(s): surname, middle initial, first name, and citizen personal number, rank, title, e-mail address, and affiliation address, home address including municipality, phone number in the office and at home (or a mobile phone number). The cover letter should state the type of the article and tell which illustrations are original and which are not.

Address of the Editorial Office:

Enriched Publications Pvt. Ltd.
S-9,IInd FLOOR, MLU POCKET,
MANISH ABHINAV PLAZA-II, ABOVE FEDERAL BANK,
PLOT NO-5, SECTOR -5, DWARKA, NEW DELHI, INDIA-110075,
PHONE: - + (91)-(11)-45525005

Note